2007

Agricultural vulnerability to drought in southern Alberta : a quantitative assessment

Ren, Xiaomeng

AGRICULTURAL VULNERABILITY TO DROUGHT IN

SOUTHERN ALBERTA:

A QUANTITATIVE ASSESSMENT

Xiaomeng Ren

B. Eng. Wu Han University

A Thesis Submitted to the School of Graduate Studies of the University of

Lethbridge

In Partial Fulfillment of the Requirements for the Degree

MASTER OF SCIENCE

Department of Geography

University of Lethbridge

Lethbridge, Alberta, Canada

Dedication

This research is dedicated to my mom and dad, and my Canadian parents, Walter and Maureen. Without their love and support, this research would not be possible. It is also dedicated to my extended families back in China, whose encouragement was always being the greatest motivation for me. At the mean while, this thesis is dedicated to my extended Canadian family who had provided me a cozy home away from home. This is also dedicated to all my wonderful friends, especially Chien and Erwin who helped me a lot in these two years.

I'm so lucky to be loved by all of you! Much appreciation and love to you all!

Abstract

Agricultural vulnerability is generally referred to as the degree to which agricultural systems are likely to experience harm due to a stress. In this study, an existing analytical method to quantify vulnerability was adopted to assess the magnitude as well as the spatial pattern of agricultural vulnerability to varying drought conditions in Southern Alberta. Based on the farm reported data and remote sensing imagery, two empirical approaches were developed to implement vulnerability assessment in Southern Alberta at the quarter-section and 30 meter by 30 meter pixel levels. Cereal crop yield and the Standardized Precipitation Index (SPI) were specified as the agricultural wellbeing and stress pair in the study. Remote sensing data were used to generate cereal crop yield estimations, which were then implemented in vulnerability quantification. The utility of the remote sensing data source for vulnerability assessment were proved. The spatial pattern of agricultural vulnerability to different severity and duration of drought were mapped.

Acknowledgement

First of all, I want to thank my supervisor Dr. Wei Xu, for his continuous support in my Master program. Wei was always there to listen and give advice. Through these two years of study he taught me how to be confident to express my ideas. He also helped me tremendously on my speaking and writing English, especially at the thesis writing stage. Without his help this thesis would not be possible. I also want to thank Dr. Anne Smith, as my committee member, who provided me remote sensing data, software facilities and working space for remote sensing related work. Anne also shared her agrological knowledge with me and gave me valuable help on some problem I had related to image pre-processing. Thanks also to Dr. Tom Johnston, who is also my committee member. He was always there to insure that my study was in good progress and was willing to help me whenever. A special thank goes to my another committee member, Dr. Kurt Klein, who was the first person I contacted at the University of Lethbridge, and was responsible for introducing me to Wei. The financial support from Kurt for the first year of my study is much appreciated.

Table of Contents

List of Figures

List of Tables

CHAPTER 1 INTRODUCTION

1.1   Introduction

Over the last two decades, there has been an increasing concern worldwide over the long term sustainability of agricultural sectors (Reilly and Schimmelpfennig, 1999; Humphreys et al., 2006). At the global scale, a sustainable and sufficient food supply is demanded to meet the long term need of a growing world population (IFPRI, 2002). At the national scale, a stable and reliable agricultural system is an important basis to ensure the national competitiveness in the global economy. Therefore, local and regional agricultural systems need to be understood, closely monitored, and efficiently managed in order to achieve the national and international goal of sustainable agriculture.

As the global industrial economy expands further, its impacts on the environment have increased tremendously, and the global environmental conditions have been aggravated noticeably. Consequently, the world is faced with increasing risks from a degrading environment including global warming and climate change. Traditionally, agricultural systems are very much dependent on environmental conditions such as soil, rainfall, and temperature. Although the modern commercial agricultural systems based on fossil fuel inputs are less dependent on the favorable environmental supports, climate condition remains an important shaper of agricultural production (De Sherbinin, 2000; Thomson et al., 2005a; Thomson et al., 2005b). With the increasingly variable climate conditions, the viability of farming practices is increasingly threatened. Climate related natural hazards are still one of the biggest challenge faced by the agricultural industry (Moore, 1998; De Sherbinin, 2000; Johnston and Chiotti, 2000). One of the most damaging climate hazards for agricultural systems is drought (Baethgen, 1997).

As an important agricultural region in Canada, Southern Alberta is a semi-arid area. The agricultural industry of Southern Alberta has been historically and is currently impacted by droughts. Meteorological drought during the growing season occurred in 15 of the last 74 years. Several of these droughts happened in two or three consecutive years. In the last 74 years, the most significant drought occurred in 2001 (AAFRD, 2002). The drought was so widespread that it even caused a serious shortage in the water supply throughout most of the irrigation areas of Southern Alberta (AAFRD, 2002). As a result of global warming, it has been predicted that the Canadian Prairies will possibly face an increase in drought frequency in the future (IPCC, 2001)

Given the current and expected situation of drought occurrence, it is imperative to understand the interacting relationship between agricultural systems and drought-related water shortage in order to design drought-proofing measures for alleviating possible damage. Vulnerability assessment is now widely used as an effective way to facilitate the understanding of the interaction between hazards or disturbances and the exposed systems. Numerous studies have been done in many different scholarly fields including geography, agricultural science, water resource analysis, climate research, and social sciences (e.g., Baethgen, 1997; Eakin and Conley, 2002; Wilhelmi and Wilhite, 2002; Descroix et al., 2003). Some analysts have conceptualized the nature of vulnerability from various theoretical perspectives (e.g., Cutter, 1996; Villa and McLeod, 2002; Turner et al., 2003a) while others have attempted to develop some quantitative measures of vulnerability (e.g., Gogu and Dassargues, 2000; Cutter et al., 2003). Because of the complexity of the systems under analysis and the fact that vulnerability is not a directly observable phenomenon, it has been proved difficult to develop measures for quantifying

2

vulnerability (Downing et al., 2001; Luers et al., 2003). This research employs a quantitative approach to assess agricultural vulnerability to varying drought conditions in Southern Alberta. Different data sources were used in this research to assess agricultural vulnerability at two different spatial scales and resolutions. It is hoped that the findings from this research will help improve agricultural management in Alberta.

In more recent years, with increasing availability, remote sensing imagery has become a new information source for researchers. By analyzing the spectral signals recorded on the remote sensing imagery, researchers can get useful information on many aspects of their targets of interest on the ground. Agriculture is one of the major users of the remotely sensed data (Moulin et al., 1998). It has been demonstrated that remotely sensed signals in various wavelengths can provide information about vegetation conditions (Smith et al., 1995). Remote sensing technology makes it possible to monitor crop growth conditions over a very large area. It facilitates the mapping and investigation of the spatial variability in vegetation characteristics. A number of studies indicate that it is possible to predict (or estimate) crop yields using remote sensing images at a relatively high resolution (e.g., Hochheim and Barber, 1998; Doraiswamy et al., 2003; Ferencz et al., 2004). Few studies, however, have employed the remote sensing estimated yield as an indicator of agricultural vulnerability assessment. This research will test the utility of remote sensing data in agriculture vulnerability assessment.

1.2   Research Objectives

Agricultural systems constitute a pivotal economic sector in rural Canada and worldwide. Sustainable rural systems are very much dependent upon the healthy development of agriculture. As a multi-faceted biophysical and socio-economic system,

the agricultural system is heavily affected by variations and changes in climate conditions. Extreme climatic events such as severe drought can often cause devastating damage to agriculture and consequently to rural communities.

The overall goal of this research is to investigate the relationship between agricultural production and the occurrence of meteorological droughts over time, and consequently to examine how sensitive and vulnerable agricultural production is, given the variability in climate conditions in Southern Alberta.

The empirical research objectives of this study are:

1) To estimate the yields of cereal crops in selected years based on remotely sensed data in Southern Alberta. A remote sensing approach will be developed. The yield estimates based on the remote sensing approach will provide a primary data source to measure agricultural well-being and quantify agricultural vulnerability to drought;

2) To assess the magnitude and spatial pattern of agricultural vulnerability to varying drought conditions in Southern Alberta using the farm reported crop yield data at a quarter-section level. The drought condition as the stressor to agricultural production systems will be characterized using the standard precipitation index (SPI). The SPI will be estimated based on precipitation data between 1965 and 2004. The estimated SPI data will be used in estimating the sensitivity of agricultural systems as well as the system's exposure to drought; and

3) To assess the magnitude and spatial pattern of agricultural vulnerability to varying drought conditions in Southern Alberta using the yield estimates derived from the remote sensing approach. The estimated SPI data will also be employed in this part of the empirical research. The findings will be compared with those using the farm reported

yield data to assess the utility of the remote sensing based approach in assessing agricultural vulnerability.

1.3   Organization of Thesis

This thesis is organized into six chapters. Following the introduction, the second chapter presents a literature review. The conceptual and analytical development of vulnerability assessment is reviewed with respect to its definitions, theoretical assessment frameworks and quantitative assessment methods. The yield estimation methods using remote sensing techniques are discussed and drought indices are introduced and commented. The discussion focuses on their relevance to the measurement of vulnerability indicators of this study.

In the third chapter, an empirical research methodology is presented. The chapter begins with an introduction of two proposed empirical approaches and study areas. The detailed quantitative methods for vulnerability measurement are introduced. Data collection and preparation for each empirical approach are detailed.

In the following two chapters, the empirical results of the study are presented. Chapter four presents the procedures tested and the results of the land use classification using the remote sensing data. Based on the classification results, the yield estimation regression models are built mainly based on the remote sensing data. The most effective models are presented and the yield estimation results are mapped. In the fifth chapter, the magnitude and spatial pattern of the quantitatively assessed agriculture vulnerability to drought are presented and described.

In the concluding chapter, the study is summarized, and the findings of the study are discussed. The contribution of this thesis is outlined and related future research is

suggested.

CHAPTER 2 LITERATURE REVIEW

2.1   Introduction

This chapter presents a review of the literature in three main fields that are relevant to this study. The literature on vulnerability assessment is reviewed with respect to its definitions, theoretical frameworks and quantitative assessment methods. Different yield estimation methods using the remote sensing techniques are summarized and discussed. The drought indices used for measuring and monitoring drought events are reviewed.

2.2   Vulnerability Assessment

2.2.1   Defining vulnerability

Vulnerability is a concept used in various disciplines, including biology, psychology, sociology and environmental science (Adger, 2006). It is defined differently depending upon different research orientations and perspectives (Dow, 1992; Cutter, 1996; Boruff et al., 2005). Without considering any specific context, vulnerability may be generally defined as "the quality or state of being vulnerable" (Gove, 1981, p. 2566). Under a broad context of social and environmental sciences, the vulnerability often refers to as "a potential of loss" (Cutter, 1996; Cutter et al., 2003). This "potential of loss" is considered either as a characteristic that inherently exists in an individual (a group or a system), or a function combining the sensitive individual and the force (stress) that the individual is sensitive to. Two main types of vulnerability definitions are consequently derived from the above considerations. Some scholars define vulnerability as the inherent capacity of an individual of suffering from or reacting to disturbing factors. For example, Kates (1985) identified vulnerability as the "capacity to suffer harm and react adversely"

(cited from Cutter, 1996, p. 531), while Blaikie et al. (1994) stated "By vulnerability we mean the characteristics of a person or a group in terms of their capacity to anticipate, cope with, resist and recover from the impact of a natural hazard" (cited from Cutter, 1996, p. 532).

Others view vulnerability as the interaction between the stresses or disturbances, which arise outside and/or inside the system, and the system's inherent capacity to respond. For example, Chen et al. (2001) defined the vulnerability to earthquakes as "the expected degree of losses within a defined area resulting from the occurrence of earthquakes (p. 349)". Cutter et al. (2003), on the other hand, argued that vulnerability should be the likelihood that an individual or group would be exposed and adversely affected by a hazard. The focus of this definition is on the interaction of the hazards of place (risk and mitigation) with the social profile of communities. This type of definition can often be used to capture the variation in vulnerability among different individuals or systems (Chambers, 1989; Cutter, 1996; IPCC, 2001; Cutter et al., 2003).

Recently, it is widely agreed and accepted that vulnerability is a function of three components: sensitivity, adaptive capacity and exposure (IPCC, 2001; Turner et al., 2003a; Brooks et al., 2005; Alberini et al., 2006). In general, sensitivity refers to the degree to which a system responds to a fluctuation in force (stress). It includes both the potential of being harmed or benefited (Lowry et al., 1995; IPCC, 2001; Tao et al., 2002; Dixon, 2005). Adaptive capacity, also referred to as resilience (Turner et al., 2003a) or coping capacity (Gallopin, 2006), refers to the capacity of a system to moderate or offset the potential for damage or take advantage of the change in force. This capacity is often associated with management strategies, practices and/or processes (Burton, 1997; IPCC,

2001; Luers et al., 2003; Brooks et al., 2005; Gallopin, 2006; Smit and Wandel, 2006). Exposure is often defined as the possibility of a system being exposed to the concerned change in stress or force (IPCC, 2001; Luers et al., 2003; Turner et al., 2003a). Because the three components of vulnerability vary geographically, fluctuate over time, and differ across different systems (or different sectors of a system), vulnerability outcomes are spatially and temporarily distinct, and they also largely depend upon how the scope of the system is defined

2.2.2   Vulnerability assessment: theories and methods

2.2.2.1 Theoretical frameworks and qualitative vulnerability assessment

Different from the traditional impact assessment, vulnerability assessment not only addresses the effects on the system under concern, but also seeks to understand why. Many theoretical frameworks have been proposed from different perspectives to conceptualize the relationship between the systems' stressors or disturbances and responses (Currens and Busack, 1995; Cutter, 1996; Boughton et al., 1999; Murray, 2003; Turner et al., 2003a).

Cutter (1996) developed a conceptual framework for vulnerability assessment (see Figure 2-1). This framework illustrated various elements that constituted the vulnerability of a specific place to environmental hazard and how their interactions bring out the vulnerability. She also stated that this vulnerability would change over time in relation to changes of risk exposed by the place. This framework emphasizes that the vulnerability of a specific place needs to be integrated with the vulnerability of biophysical and social extents of the place. But it does not provide the detailed context in which each major component of a system's vulnerability may exist. The above

framework was later modified by presenting a few detailed structures in relation to the characteristic of the geographic context and social fabric of a place (see Cutter et al., 2003).
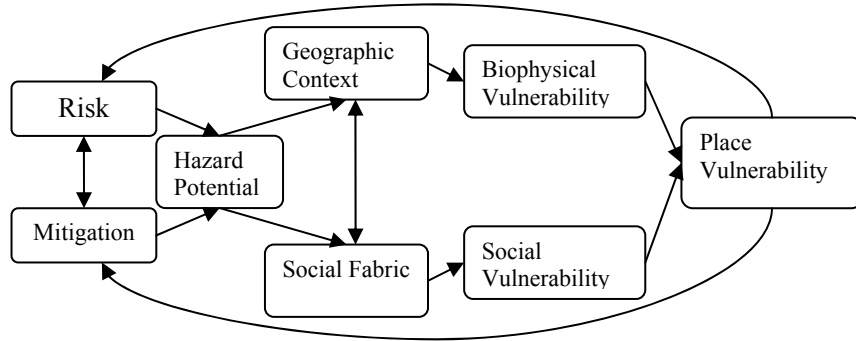
Figure 2-1 The Hazard of place model of vulnerability *Source:* Cutter (1996)

Turner et al. (2003a) proposed a comprehensive framework for vulnerability assessment. The framework was considered by Adger (2006) as one of the important successes in vulnerability research in recent years. Focusing on the human-environment coupled system at a particular spatial scale, the framework portrays the interactions among each vulnerability component (exposure, sensitivity and resilience) within, beyond, and across the spatial scale (see Figure 2-2). It also illustrates the detailed structure of each component, which facilitates the development of possible indicators for quantifying vulnerability (Figure 2-2). In a review article of vulnerability assessment, Adger (2006) stated that due to the interdisciplinary and integrative nature of this framework, this framework should also be applicable for vulnerability assessment of different orientations.
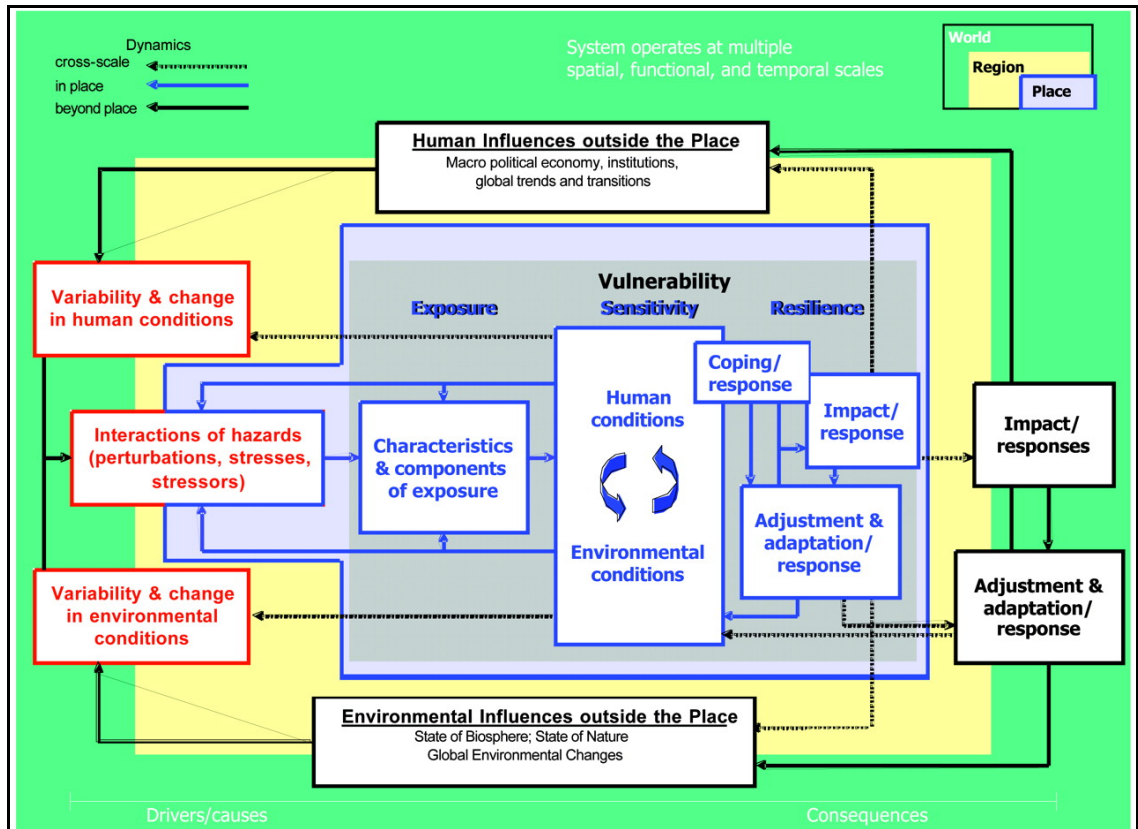
Figure 2-2 Vulnerability framework: Components of vulnerability identified and linked to factors beyond the system of study and operating at various scales. Source: Turner et al. (2003a).

The conceptual frameworks reviewed above provide an important theoretical basis for analyzing vulnerability issues of any concerned system or place. They also provide conceptual pillars upon which the complexity involves in the vulnerability of a system or a place may be understood. However, qualitative conceptual frameworks focusing on theory building may be hard to justify without sufficient empirical evidence. The development of quantitative indicators for measuring vulnerability will not only make it possible to understand practically how vulnerable a system might be, but also further a theoretical understanding of vulnerability.

2.2.2.2 Quantifying vulnerability

While the theoretical frameworks discussed above help to understand the

relationships between the systems and their stressors, quantitative measures are needed to understand empirically the degree and magnitude of the systems' vulnerability in order to provide meaningful inputs to the policy making processes towards vulnerability management. Quantifying vulnerability can be quite difficult due to the complexity of the system under analysis and the fact vulnerability is not a directly observable phenomenon (Downing et al., 2001; Luers et al., 2003; Gemitzi et al., 2006).

The traditional approach of quantifying vulnerability is primarily based on summing or averaging a set of weighted indicators that are indicative of vulnerability components. The function used for these assessments is similar as Equation 2-1

$$V = \sum_{i=1}^{n} (W_i \times R_i) \quad \text{or} \quad V = \frac{1}{n} \sum_{i=1}^{n} (W_i \times R_i) \tag{2-1}$$

Where, V is the vulnerability index of a system; W_i is the weighting factor for indicator i; R_i is the measured value or the classification of the selected indictor i, n is total number of indicators under concern.

These indicators are always the directly observable or measurable conditions of the systems' elements and/or the characteristics of the disturbances that the system is exposed to. This method has been used to assessing vulnerability of both ecosystems and societies to different disturbances such as natural hazards, environmental changes, and pollution (Lowry et al., 1995; Kellman et al., 1996; Doerfliger et al., 1999; Wilhelmi and Wilhite, 2002; Cutter et al., 2003; Wei et al., 2004; Adger, 2006).

For example, Wilhelmi and Wilhite (2002) used a set of indicators representing climate, soil, land use, and accessibility to irrigation. Together with a numerical weighting scheme, these indicators were employed to evaluate the spatial pattern of

agricultural vulnerability to drought in Nebraska. Brooks et al. (2005) conducted an empirical analysis for assessing the national level social vulnerability to climate change by aggregating a set of weighted indicators that characterize human systems.

These conventional quantitative approaches are valuable for understanding the construction of a place's vulnerability. The results of these assessments are often presented in the form of relative values or scaled degrees of vulnerability, which make the comparison between different places possible. The main drawbacks of this approach are: 1) it often leads to a lack of correspondence between the conceptual definition of vulnerability and the metrics (Luers et al., 2003); and 2) the value of weighting factors depends to a great extent upon arbitrary decisions, and this reduces the confidence of such weighting methods (Wei et al., 2004).

Luers et al. (2003, p. 257) stated that "vulnerability measures can only accurately relate to the specific variables, rather than the generality of a place, because even the simplest system is so complex that it is difficult to fully account for all of the variables, processes and disturbances that characterize it." Based on this thinking they developed a new metric for quantifying vulnerability, which transformed the general definition of vulnerability (i.e. a function of sensitivity, exposure and adaptive capacity) into mathematical functions. Three components of vulnerability are measured as: 1) "sensitivity is represented as the absolute value of the derivative of well-being with respect to the stressor" (Luers et al., 2003, p. 258); 2) exposure refers to "probability of the occurrence of stressor" (Luers et al., 2003, p. 258); 3) adaptive capacity is the "difference in the vulnerability under existing conditions and under the less vulnerable condition to which the system could potentially shift" (Luers et al., 2003, p. 259). The

most general function of this vulnerability quantifying method is presented in Equation 2-2:

$$V = \frac{\text{Sensitivity to stress}}{\text{Wellbeing state relative to threshold}} \times \text{Exposure to stress} \qquad (2\text{-}2)$$

In the case study, they investigated the vulnerability of agriculture system in a sub-tropical irrigated area of Mexico (Luers et al., 2003). Well-being was captured by agricultural yields, while the stress of concern was night time temperature. Although it is suggested by Adger (2006) that this generalized function could also be used to examine the vulnerability of many other systems and/or places in response to many types of stresses, few has conducted empirical investigation that employs this approach to quantify spatial and temporal variations of agricultural vulnerability to varying drought conditions in temperate semi-arid areas.

2.3   Remote Sensing and Crop Yield Estimation

Remote sensing data have been widely applied to many research problems and practical applications, including meteorology, geology, canopy and soil investigations, ocean research, water management, and environmental monitoring (Ferencz et al., 2004). Compared to the traditional data collection methods, the capability of remote sensing techniques of providing timely information over a large spatial extent at a wide range of spatial, temporal, and spectral resolutions is appreciated by numerous users in different application fields (Smith et al., 1994; Moulin et al., 1998; Bastiaanssen et al., 2000).

2.3.1   Yield estimation strategies

Agriculture is one of the major users of remote sensing data (Moulin et al., 1998). Numerous research efforts have been devoted to seeking a quantitative relation between remotely sensed spectral information and crop yields, and consequently obtaining a

robust estimation and forecasting for agricultural productions (e.g., Idso et al., 1977; Hatfield, 1983; Zhang, 1984; Bouman, 1995; Sanchez-Arcilla et al., 1998; Serrano et al., 2000; Shao et al., 2001; Labus et al., 2002; Lobell and Asner, 2003; Lobell et al., 2003; Luers et al., 2003; Lobell et al., 2005; Babar et al., 2006; Badarinath et al., 2006; Prasad et al., 2006).

There are generally two main types of strategies used in the literature for estimating crop yields based on remote sensing data (Moulin et al., 1998; Ferencz et al., 2004). The first one can be classified as the mechanistic yield estimation method, which incorporates remote sensing data into agro-meteorological or bio-physiological models. For example, Doraiswamy et al. (2003) implemented the real-time assessment of the magnitude and variation of crop condition parameters into the crop model called (Erosion Productivity Impact Calculator (EPIC). The EPIC model was used to estimate crop yields at regional and state levels. Abou-Ismail et al. (2004) developed a rice yield estimation model by combining a rice growth simulation model with remote sensing data (for more examples, see Bouman, 1995; Moulin et al., 1998; Babar et al., 2006; Badarinath et al., 2006; Prasad et al., 2006).

This method is considered capable in describing the complexity of plant-physiology, and is suitable at a field scale (Moulin et al., 1998). Ferencz et al. (2004) summarized several main drawbacks of this method: 1) the number of input parameters required for the agro-meteorological or bio-physiological models is always considerably large, 2) it needs sufficient ground reference information which is expensive to collect, and 3) the models can be quite complex.

Another commonly used method is to empirically relate the remote sensing data to crop yields at a local or regional scale. These types of relations are always investigated based on the use of some indices generated from remotely sensed imagery. For example, Dadhwal and Sridhar (1997) investigated the relationship of a near-infrared (NIR)/red radiance ratio with wheat yield using a regression model. The relationship was then used for wheat yield estimation. In a study by Ferencz et al. (2004), a new vegetation index, called the General Yield Unified Reference Index (GYURI)), was proposed which uses a fitted double-Gaussian curve to NOAA AVHRR data during the vegetation growth period. The regression models were established for different crop types to estimate crop yields. Although the relationship found between the remote sensing data and crop yield from these empirical analyses may only have a local or regional value, such an approach is still preferred by many researchers as it is simple and can be achieved without any background physiological knowledge (for more examples, see Hochheim and Barber, 1998; Basnyat et al., 2004; Bullock, 2004).

2.3.2 Remote sensing derived vegetation index

One of the primary variables used in modeling the relationship between remotely sensed information and crop yield is the vegetation index. Various vegetation indices have been generated from optical satellite sensors which can provide quantitative information about vegetation health and biomass (Muldavin et al., 2001; Bullock, 2004; Zarco-Tejada et al., 2005; Beeri and Peled, 2006). One of the most commonly used vegetation indices for yield estimation is the normalized difference vegetation index (NDVI). The NDVI is calculated using Equation 2-3:

$$NDVI = (\ell_2 - \ell_1) / (\ell_2 + \ell_1) \tag{2-3}$$

Where: ℓ_1 and ℓ_2 are the reflectance values in the red and near infrared wavelengths, respectively.

The NDVI is deduced from the physiological fact that "Chlorophyll a and b in the palisade layer of healthy green leaves absorbs most of the incident red radiant flux while the spongy mesophyll leaf layer reflects much of the near-infra-red radiant flux" (Jensen, 2005, p. 7). The NDVI reflects the relationship between the amount of healthy green vegetation and the spectral reflectance of near-infrared and red wavelengths, and therefore can be used as a measure of ground green vegetation health and volume.

In the literature, through the use of simple regression or multiple regression analysis, correlations between NDVI and crop yield can be derived and used in yield estimation models for different vegetation types (corn, wheat, sugar beets, cotton, canola and grass) in various regions (e.g., Ray et al., 1999; Plant et al., 2000; Seaquist et al., 2003; Basnyat et al., 2004; Hoffmann and Blomberg, 2004). It is found the suitability of NDVI for yield estimation varies depending upon the acquisition time of the remote sensing images (Hochheim and Barber, 1998; Basnyat et al., 2004; Vicente-Serrano et al., 2006). Several studies have discovered that the optimal image acquisition time for the best correlation between NDVI and crop yield is late July, particularly in western Canada (Hochheim and Barber, 1998; Basnyat et al., 2004).

2.4   Drought Indices

"Drought" is a simple term that refers to a complex natural hazard. It is noted that defining the severity and duration of drought events can be difficult (Steinemann, 2003). A number of drought indices are available to measure quantitatively the drought severity and duration. Each of them stems from a different concern. As one of the most widely

known drought indices, the Palmer Drought Severity Index (PDSI) was developed in 1965 and has been used for about 30 years as a primary means of measuring meteorological drought severity (Guttman, 1999). It is designed to describe wet and dry conditions from a water balance viewpoint, and is hence widely viewed as a measure of hydrological drought (Alley, 1985), or an index of soil moisture (Mika et al., 2005). The index was used for assessing moisture availability in a study by Jones et al. (1996), and for characterizing the stochastic behaviour of drought (Lohani and Loganathan, 1997). Many U.S. government agencies and states have been relied on the PDSI to trigger drought relief programs (Hayes, 2005).

A newer drought index, the Standardized Precipitation Index (SPI), was developed to improve the capability for drought detection and monitoring (McKee et al., 1993; 1995). Based on a comparative study (Guttman, 1998), it is concluded that the SPI should be used as a meteorological drought index for risk and decision making analysis rather than the PDSI. This is because the SPI is "simple, spatially invariant in its interpretation, and probabilistic (Guttman, 1998, P. 119)" and it "can be tailored to time periods of concern to a user" (Guttman, 1998, P. 119). In contrast, the PDSI is found to be "very complex, spatially variant, difficult to interpret, and has inherent a fixed time scale of about 9-12 months" (Guttman, 1999, P. 311). This point of view has been widely accepted by many analysts in recent studies in which the SPI is used as the means of measuring and representing the geographical variations of drought severity and duration (e.g., Hayes et al., 1999; Dupigny-Giroux, 2001; Wu and Wilhite, 2004; Sonmez et al., 2005; Vicente-Serrano and Lopez-Moreno, 2005). The SPI can also be used for drought monitoring and prediction (Hayes, 2005).

The calculation of the SPI first requires fitting the long-term precipitation record for the interested location into an appropriate probability density function. This function is then transformed into a normal distribution, so that the mean of the distribution is zero (Edwards and McKee, 1997). SPI values above zero indicate wetter periods and values less than 0 indicate drier periods. The classification of SPI value is presented in Table 2-1.

Table 2-1 SPI value classification

SPI Values	Drought condition
2.0+	Extremely wet
1.5 to 1.99	Very wet
1.0 to 1.49	Moderately wet
-.99 to .99	Near normal
-1.0 to -1.49	Moderately dry
-1.5 to -1.99	Severely dry
-2 and less	Extremely dry

Source: (Hayes, 2005)

2.5   Chapter Summary

This chapter presented a literature review from the perspective of the proposed study. The conceptual frameworks and analytical methods of vulnerability assessment are presented and criticized. The yield estimation method based on remote sensing techniques is introduced and discussed. In addition, the indices developed for drought measurement are reviewed by highlighting the utility of a newly proposed drought index, the SPI.

Based on the review and discussion, it is concluded that although a comprehensive quantitative vulnerability assessment is difficult, if not impossible, vulnerability of a system or a place can be quantified by simplifying a complex system as a pair or pairs of interacting well-being and stresses. The reviewed works suggest that the empirical regression relationship between NDVI and crop yield is valuable for yield

estimation modeling at a local scale. Although drought is a natural hazard involving complex behaviors and impacts, the SPI is recognized as a good measure of the severity and spatial variation of meteorological drought, and consequently can be used in risk analysis.

CHAPTER 3 METHODOLOGY

3.1   Introduction

In this chapter, the analytical methods and procedures are developed to empirically assess agricultural vulnerability to drought. The quantitative measures for assessing vulnerability are adopted and implemented in a case study to assess agricultural vulnerability to different drought conditions in Southern Alberta. The empirical approaches and procedures are designed to deal with various datasets, including precipitation data, remotely sensed images and the farm reported yield data, in order to measure individual components of the vulnerability functions.

The chapter first presents the empirical approaches and study area. The detailed data preprocessing procedures are then presented. The vulnerability measure and its components used in this study are specified and explained.

3.2   Empirical Approaches and Study Area

3.2.1   Empirical objectives

This study is aims to achieve an understanding of the Southern Alberta agricultural system's vulnerability to various severities of drought conditions. Due to the complex nature of the agricultural systems, it is difficult, if not impossible, to derive a complete understanding of a particular system's vulnerability in one study. The empirical part of this study attempts to achieve the following objectives:

1) To estimate the yields of cereal crops in selected years based on remotely sensed data for Southern Alberta so that agricultural vulnerability to drought can be assessed at a high spatial resolution;

2) To assess the magnitude and spatial pattern of agricultural vulnerability to varying drought conditions in Southern Alberta using the farm reported crop yield data at a quarter-section level; and

3) To assess the magnitude and spatial pattern of agricultural vulnerability to varying drought conditions in Southern Alberta using the yield estimates derived from the remote sensing approach.

3.2.2   Study area

This study is concerned with agricultural production in Southern Alberta. Two spatial extents within Southern Alberta are defined to achieve the proposed empirical objectives, largely as a result of data availability. Since the spatial coverage of the farm reported yield data is within the provincial boundary, the selected study area approximately covers the census divisions one to six (see Figure 3-1a). The study area includes townships 1 to 35 from range 2 in meridian 4 to range 4 in meridian 5. There are about 156,000 quarter-sections in the study area. Some non-agricultural area is included in the selected study area (see Figure 3-1): 1) the southwest corner of the study area is within the high elevation area that is mainly covered with forestry; and 2) a large area north of Medicine Hat is of military use. The vulnerability assessed at the non-agriculture areas is only hypercritical.

The spatial extent of the Landsat TM scenes defines the boundary of the second study area within which agricultural vulnerability assessment is conducted using remotely sensed data. This area represents the majority of agricultural regions in Southern Alberta (see Figure 3-1b).
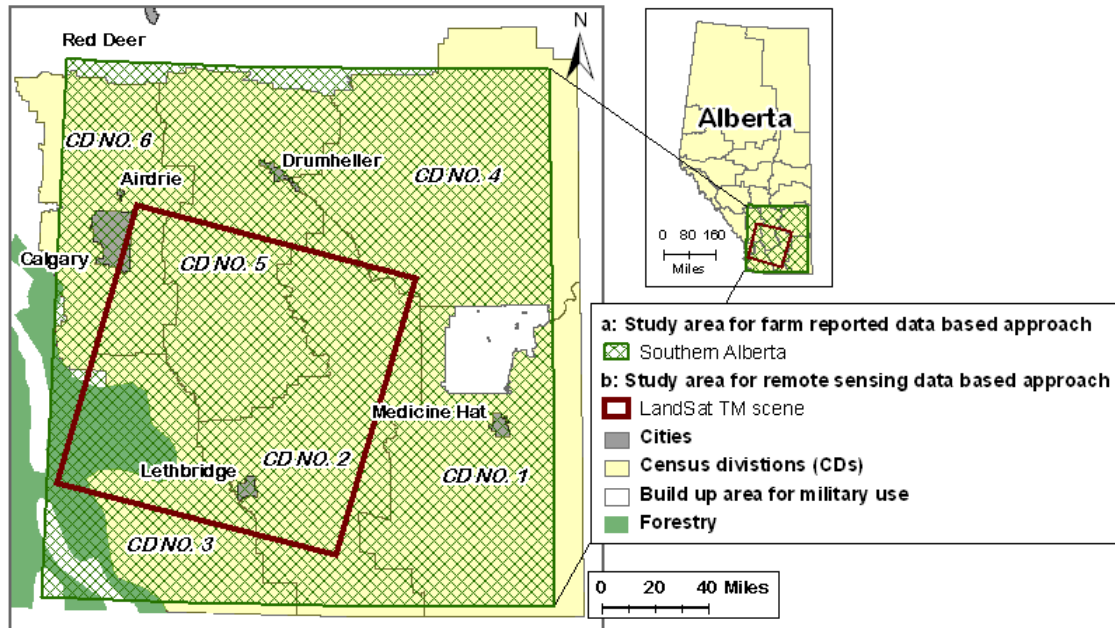
Figure 3-1 Study areas for the two empirical approaches: a: southern Alberta; b: Landsat TM scene

3.2.3   Characteristics of Alberta agricultural system

As Canada's second largest agricultural producer and exporter, Alberta accounted for 21.3 percent of Canadian farm cash receipts from agriculture, and the farm cash receipts totaled $7.9 billion in 2005 (AAFRD, 2006). In total, Alberta's agri-food exports were $5.0 billion in 2005. Crop production and livestock are the two dominant sectors in Alberta agriculture. Livestock and livestock products accounted for 56.4% of the farm cash receipts, while 29.4% was derived from crop production (AAFRD, 2006). According to the agricultural census of 2001, there were 53,652 farms in Alberta, with approximately 149 thousand people living in rural farm households. The healthy development of agricultural systems is of pivotal importance to Canada's economy as well as the well-being of rural communities in Alberta.

Total Alberta farmland area was 52.1 million acres, with an average farm size of 970 acres. The dominant crops in the study area are cereal crops including wheat, barley,

oats and rye. During the past decade, Alberta produced 28% of the nation's wheat crop, 44% of the barley, and 23% of the oats (AAFRD, 2006).

Because of the importance of cereal crops in Alberta agriculture and rural community, this empirical research focuses on cereal crop production as a measure of agricultural well-being in Alberta. In addition to the cereal crop yields as agricultural well-being measure in the vulnerability assessment function, the stress of the system under concern is the insufficiency of precipitation, or meteorological drought, which is measured by the Standard Precipitation Index (SPI) during the growing season between May to August. The coping capacity of the agricultural system is assessed by describing the effects of drought mitigation measures such as irrigation systems

3.3   Quantitative Measure for Vulnerability Assessment

The quantitative method for assessing vulnerability developed by Luers et al. (2003) is adopted to assess the agricultural vulnerability to different drought conditions in Southern Alberta. Vulnerability is defined as a function of three components: sensitivity, well-being state relative to its damage threshold, and exposure. Equations 3-1, 3-2 and 3-3 list three individual quantitative vulnerability measures used in the study:

$$V_{NEXPi} = SEN \times W_i \, / \, W_0 \tag{3-1}$$

$$V_{NEXP} = \overline{V}_{NEXPi} \tag{3-2}$$

$$V_{EXP} = V_{NEXP} \times EXP \tag{3-3}$$

Where:

V_{NEXPi} is the vulnerability value without considering the occurrence frequency of the
        concerned level of a stressor for a specific year. It represents the system's

vulnerability to a small change in the stress condition (Luers et al., 2003; Turner et al., 2003a; Turner et al., 2003b).

SEN is the system's sensitivity. It is defined as the change in the system's well-being corresponding to a small change in stress. Different from that described by Luers et al. (2003), the value of sensitivity can be negative or positive instead of an absolute value. A negative sensitivity value indicates that the concerned stress is beneficial to the studied system, while a positive value indicates that the concerned stress is harmful to the system.

W_i/W_0 is defined as the relative proximity of the system well-being to its damage threshold;

V_{NEXP} is calculated as the average of the V_{NEXPi} of several selected years that are representative of the general stress level to which a system is exposed.

V_{EXP} is the vulnerability value considering the occurrence frequency of the concerned level of stress. This vulnerability value can be used to capture the differences among the systems facing different occurrence frequencies of a concerned level of stressors.

EXP is the value of exposure defined as the occurrence frequency of the concerned level of stressors.

In this study, three components of the quantitative vulnerability function described above are calculated using the Equations 3-4, 3-5, and 3-6.

$$SEN = SLOPE_{Y/SPI} = \frac{n\sum SPI \times Y - \left(\sum SPI\right)\left(\sum Y\right)}{n\sum (SPI)^2 - \left(\sum SPI\right)^2} \qquad (3\text{-}4)$$

Where: $SLOPE_{Y/SPI}$ is the slope value of the simulated trend line (regression line) of yield (dependent variable) to SPI (independent variable); n is the total number of the years used for sensitivity calculation; and Y is yield.

$$W_i / W_0 = Y_i / Y_0 \qquad (3\text{-}5)$$

Where: Y_i is the yield of a specific year; Y_0 is the average yield over the selected years, and is assumed to be the relative damage threshold. This value varies from location to location. Here, we are aware that average yield over years may not be the threshold under which the system is considered to be damaged (such as breakeven yield). We assume the difference between the average yield and the damage threshold is fairly stable for each location.

$$EXP = N_x / N_T \qquad (3\text{-}6)$$

Where: N_x is the number of years that have a SPI value under the specified level, within the concerned period; N_T is the total number of years of the concerned period. In this study, three exposure values are calculated respecting the occurrence frequency of two different levels of SPI value, and within two different concerned periods:

1) EXP_L is the occurrence frequency of severe drought from 1965 to 2004. It is calculated as the proportion of years having SPI under −1.5 in these 40 years.

2) EXP_S is the occurrence frequency of severe drought from 1991 to 2004. It is calculated as the proportion of years having SPI under −1.5 in these 14 years.

3) EXP_L' is the occurrence frequency of moderate drought from 1965 to 2004. It is calculated as the proportion of years having SPI under −1 in these 40 years.

V_{EXP} values calculated using Equation 3-3 based on EXP_L EXP_S and EXP_L' are denoted as V_{EXPL}, V_{EXPS} and V_{EXPL}', respectively.

Several studies forecasted the possibility of increasing drought frequency on the Canadian prairies (IPCC, 2001; Weber and Hauer, 2003). In this study, we capture the possibility of increasing drought frequency by describing the exposure trend (T_{EXP}), as presented in Equation 3-7.

$$T_{EXP} = EXP_S / EXP_L \qquad (3\text{-}7)$$

Where, T_{EXP} is the trend of exposure. It presents the increasing or decreasing propensity of severe drought over the recent time.

The expected occurrence frequency of severe drought is calculated using Equation 3-8.

$$EEXP = EXP_S \times T_{EXP} \qquad (3\text{-}8)$$

Where, $EEXP$ is the expected exposure. It takes into account the recent exposure and possible change of exposure.

Considering the expected change in exposure, the expected vulnerability is assessed using Equation 3-9.

$$EV_{EXP} = V_{NEXP} \times EEXP \qquad (3\text{-}9)$$

Where, EV_{EXP} is the expected vulnerability considering the expected frequency of drought.

The unit of the estimated vulnerability value is the same as that described by Luers et al. (2003), which is the unit of well-being factor divided by the unit of the stress measure indicator. Therefore, in our empirical study, the unit of vulnerability is the unit of yield, because SPI being a normalized index does not have unit.

For each empirical approach, the vulnerability is quantified using the methods introduced above. The data sources and their processing methods are described in the following sections. The vulnerability assessment results will be presented in Chapter 5.

3.4   Methods for Vulnerability Assessment Based on the Farm Reported Data

3.4.1   Data source

A confidential dataset on crop production was provided by Alberta Financial Services Corporation (AFSC). The crop data are reported by individual farms on a quarter-section level. The dataset includes variables of seeded crop type, seeded acreage, farming practice, and crop yield. These variables are recorded for 14 years between 1991 and 2004. The spatial coverage of the requested dataset is within the census divisions one to six. Three types of farming practices are reported: 1) "fallow" means to plant the crop in a field in which no crop was planted in the previous year; 2) "stubble" means to plant crop in the field where crop stubble is left from the previous harvest; 3) "irrigated" means the field has access to irrigation systems and is irrigated. The yield is measured based on grain weight. Dockage is applied to reduce the possible error caused by the presence of harvested straw or weed seeds. The yield is reported and recorded in kg/acre. This unit is used for the following analysis, because kilogram and acre are the units that farmers are most familiar with and are widely used in agricultural industry.

Several confusing problems are found in this dataset, and the data are manipulated to solve some of the problems using the procedures described below.

1) A large number of data records in the earlier years are reported at the whole section level rather than the quarter-section level. In order to conduct vulnerability assessment at a quarter-section level and to keep spatial resolution of data consistent over

time, these section level records are divided evenly into quarter-section records, assuming the whole section was planted with the same crop and their yield is the same.

2) For some quarter-sections, one quarter-section was associated with more than one record which recording different crop types seeded or same crop type farmed with different farming practices. Since most of these quarter-sections have a total acreage much bigger than 160 acres (the total area of a quarter-section), it is recognized that there are possible errors associated with these duplicated quarter-sections. Therefore all the duplicated quarter-section records are eliminated in the following analysis.

3) The identification of quarter-section locations is recorded in five individual columns indicating meridian, township, range, section and quarter-section, respectively. Since a unique identifier is required to link this dataset with the existing quarter-section boundary coverage in GIS, an eight digit ID is created using Equation 3-10

$$LANDID = M \times 10^7 + T \times 10^5 + R \times 10^3 + S \times 10 + Q \qquad (3\text{-}10)$$

Where: *LANDID* is the unique ID for each quarter-section. *M, T, R* and *S* indicate meridian, township, range and section respectively. *Q* is the numerical number 1, 2, 3 and 4 assigned to the northwest, northeast, southwest and southeast quarter of a section respectively. The created eight digit IDs are in *MTTRRSSQ* Format.

The AFSC dataset which is imported into ArcGIS software and linked to the quarter-section boundary coverage using the LANDID is used in following analysis in the study.

3.4.2   Specifying the factors for vulnerability quantifying functions

Based on Equation 3-4, the sensitivity component of the vulnerability measure is calculated using the farm reported cereal crop yield and the SPI value for the growing

season. It is estimated as the slope value of the regression trend line. Using the farmer reported cereal crop yield as the dependent variable and SPI as the independent variable, the slope is estimated using the least square approach. In order to document the detailed spatial variation of vulnerability in the study area, sensitivity is calculated for each single quarter-section where the cereal crop yield and SPI value are available for 14 years (n in Equation 3-4). The reported yield for each representative year is used as the well-being state (Y_i in Equation 3-5). In this study, we use 1998, 1999 and 2001 as three representative years, because these three years provide a relatively representative variation of precipitation conditions. The year of 2001 was known as an extremely dry year (AAFRD, 2002), while according to the precipitation records 1998 and 1999 can be considered as normal year and wet year, respectively. The average yield over 14 years is used as the relative damage threshold (Y_0 in Equation 3-5). V_{NEXP} is the average V_{NEXPi} over 1998, 1999 and 2001 (see Equation 3-1).

The data preparations for quantifying vulnerability are presented in detail in the following subsections.

3.4.3 Moving window approach for yield estimation

In the AFSC dataset, there are only 33 quarter-sections in which cereal crop yields are available for all 14 years. This is because farmers seldom grow the same crop in the same field for such a long period. Because 33 quarter-sections are not enough to represent the spatial pattern of sensitivity for the study area, a moving window approach is developed to estimate the cereal crop yields for those quarter-sections where cereal crop yields are missing for certain years. The estimated yields are hypothetical.

The idea of a moving window approach is to predict the cereal crop yield in a year in which the quarter-section where cereal crop is not actually planted by using the cereal crop yields from neighboring quarter-sections. This is based on the assumptions that the neighboring quarter-sections have the same suitability for growing cereal crops, and that they are capable of producing similar yield.

By examining the spatial autocorrelation of cereal crop yields among quarter-sections, the above assumption is shown, with the exception for those under different farming practices, to be valid. Therefore, for each year, quarter-sections are divided into three classes based on three different farming practices. The yield estimation using moving window approach is conducted separately for each of three quarter-sections classes, because significant difference is found among the yields produced by different practices. A window size of 3 by 3 quarter-sections is used for "fallow" and "stubble" classes. Because the number of irrigated quarter-sections is very small in the reported dataset, a larger window size of 5 by 5 quarter-sections is used for the "irrigated" class to achieve a sufficient number of quarter-sections in which the missing yield data will be estimated. As such, there will be sufficient irrigated quarter-sections with cereal crop yields for all 14 years. The yields to be estimated are the average for all quarter-sections within the moving window. After applying the moving window approach to yield estimation, there are in total 4,005 quarter-sections with the cereal crop yield data for all 14 years. Among those quarter-sections, 2,200 are in "fallow" class, 1207 in "stubble" class and 598 are in "irrigated" class. Figure 3-2 presents the centroids of the 4,005 valid quarter-sections.
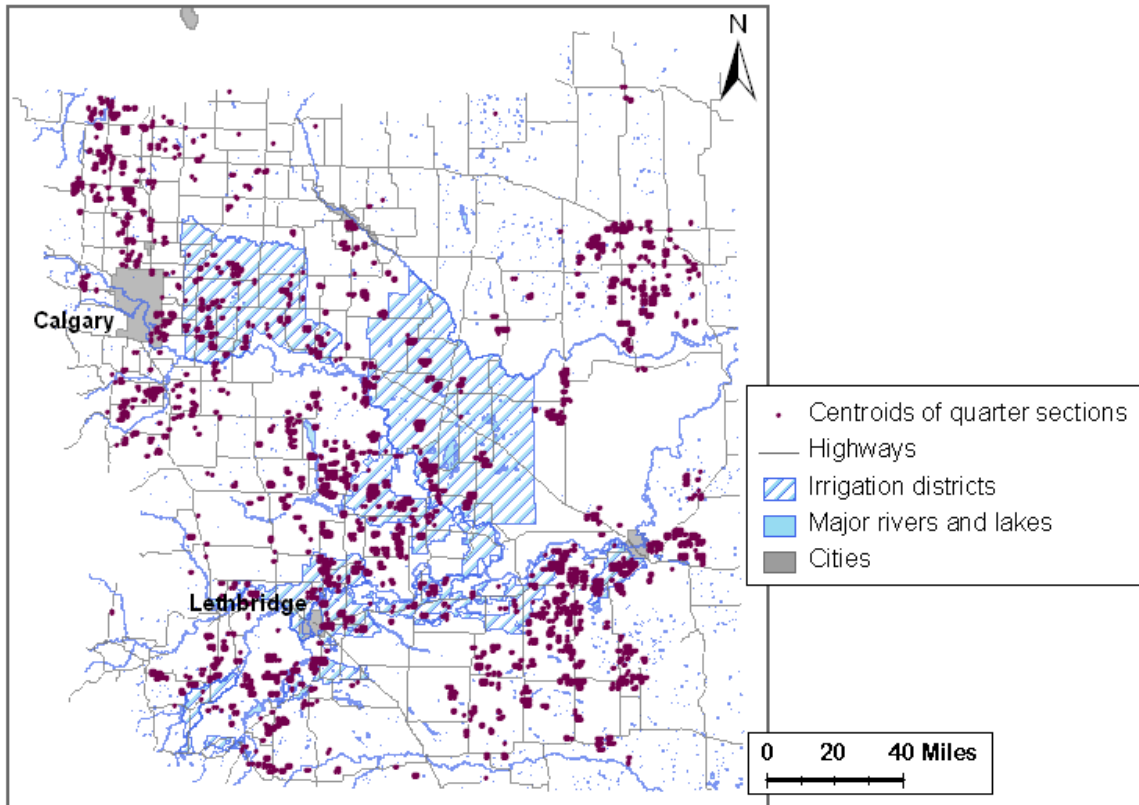
Figure 3-2 Centroids of quarter-sections where yield data is available

3.4.4 SPI calculation

In this study, a 40 year period from 1965 to 2004 is selected to calculate SPI based on precipitation records. Total monthly precipitation record is downloaded from the website of Environment Canada for each of the meteorological stations (479 stations in total) in the study area. Because none of the stations have meteorological records all through the 40 years, a total of 480 interpolated precipitation maps are generated using an inverse distance weighting (IDW) interpolator in ArcGIS software, so that for each month for these 40 years, spatially continuous data of precipitation is available. IDW method is chosen for all the data interpolation processes, because it provides a reasonable level of accuracy in data prediction while it is much less time consuming comparing to other interpolation methods such as Kriging. Three examples of the precipitation record

at meteorological stations and their interpolated continuous surface are presented in Figures 3-3, 3-4 and 3-5. The total monthly precipitation in August in 1999 is the highest among the three, while it is the lowest in 2001.
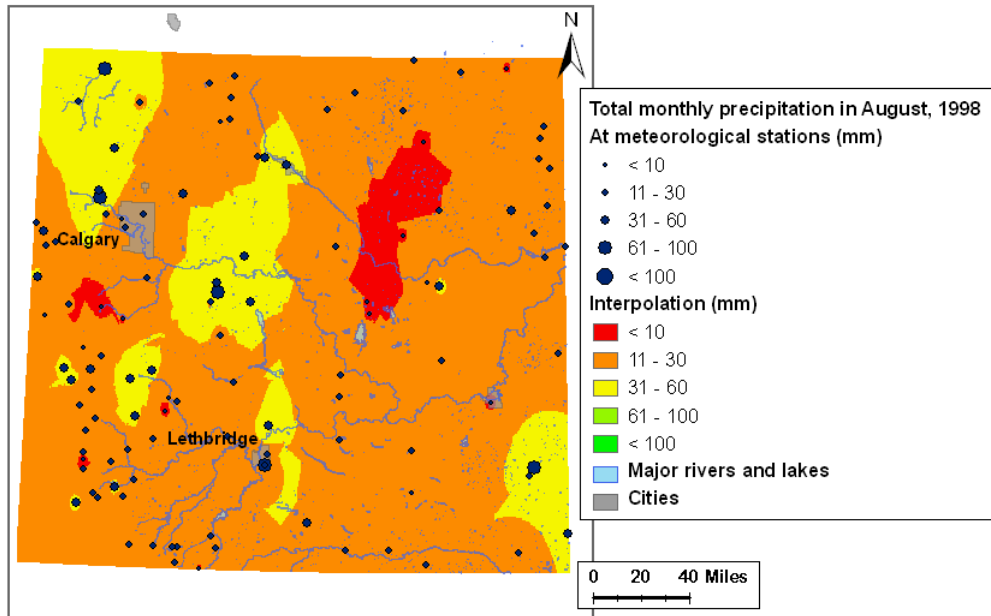
Figure 3-3 Spatial distribution of total monthly precipitation in August, 1998
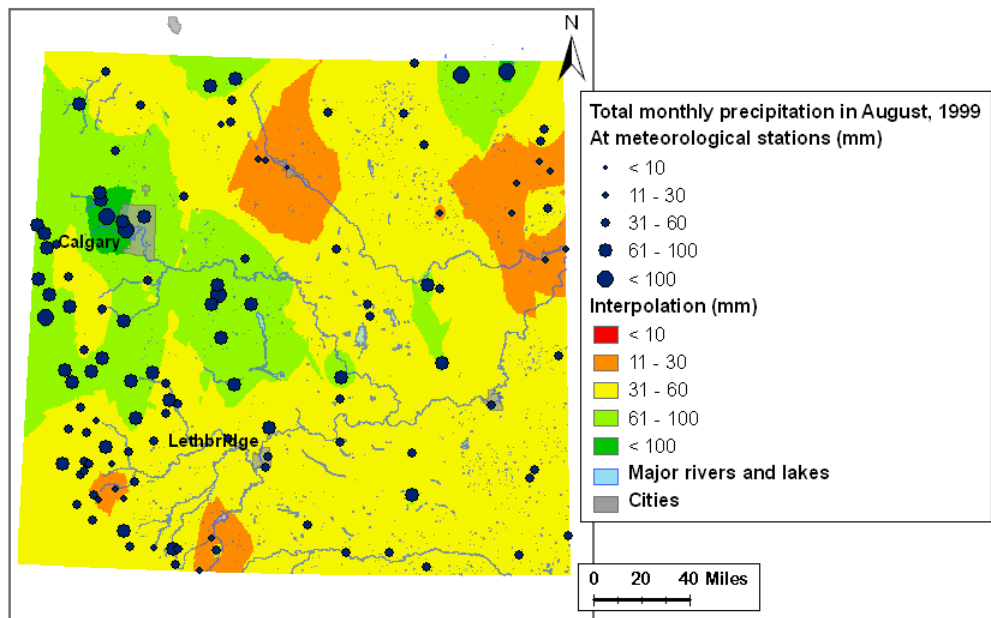
Figure 3-4 Spatial distribution of total monthly precipitation in August, 1999
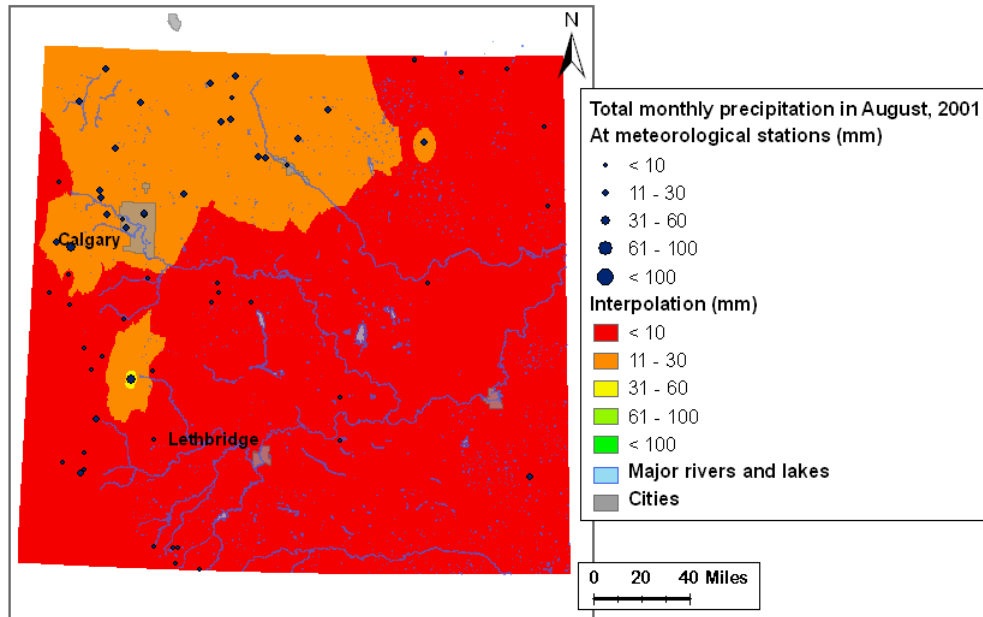
Figure 3-5 Spatial distribution of total monthly precipitation in August, 2001

The 480 precipitation maps are overlaid with the quarter-section map to derive the monthly precipitation data for each quarter-section for the last 40 years. The precipitation data is used to calculate the SPI value for each of the 4,005 quarter-sections, where the estimated cereal crops yield is available after moving window approach (see section 3.4.3).

The computation of SPI is conducted using a software program developed at the University of Nebraska and downloaded from the website of the National Drought Mitigation Center (NDMC, 2005). The SPI value for May, June, July and August at a 4 month scale is used as the measure of the stressor on the agricultural system in the study area. The SPI spatial distribution for 1998, 1999 and 2001 at the quarter-section central points are presented as examples in Figures 3-6, 3-7 and 3-8. The descriptive statistics for the SPI classes in each year are presented in Tables 3-1, 3-2 and 3-3.
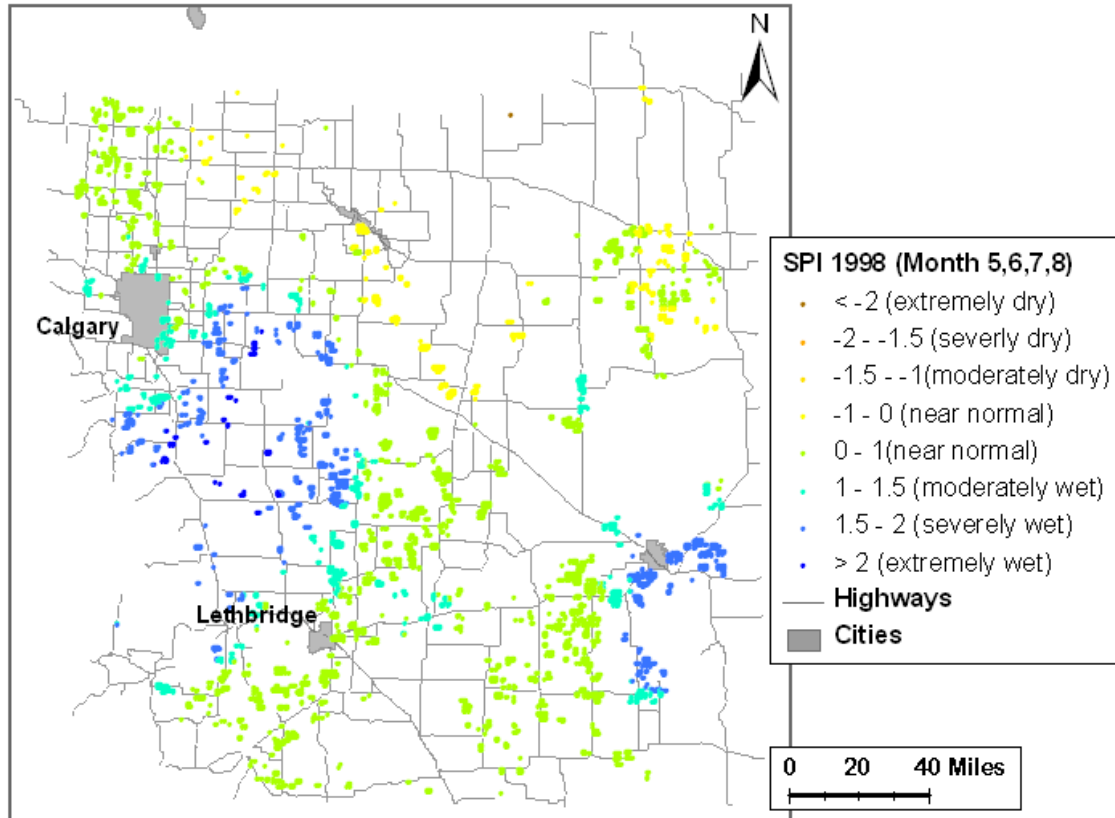
Figure 3-6 Spatial distribution of the growing season SPI in 1998

Table 3-1 Descriptive statistics of the growing season SPI in 1998

SPI classes	SPI value	Percentage of total valid quarter-sections	Mean	Standard deviation
Extremely to moderately dry	<-1	0.00%		
Near normal	-1- 0	8.34%	-0.28	0.23
Normal	0 - 1	55.98%	0.6	0.27
Moderately wet	1 - 1.5	15.26%	1.2	0.15
Severely wet	1.5 - 2	18.53%	1.72	0.11
Extremely wet	>2	1.90%	2.05	0.04
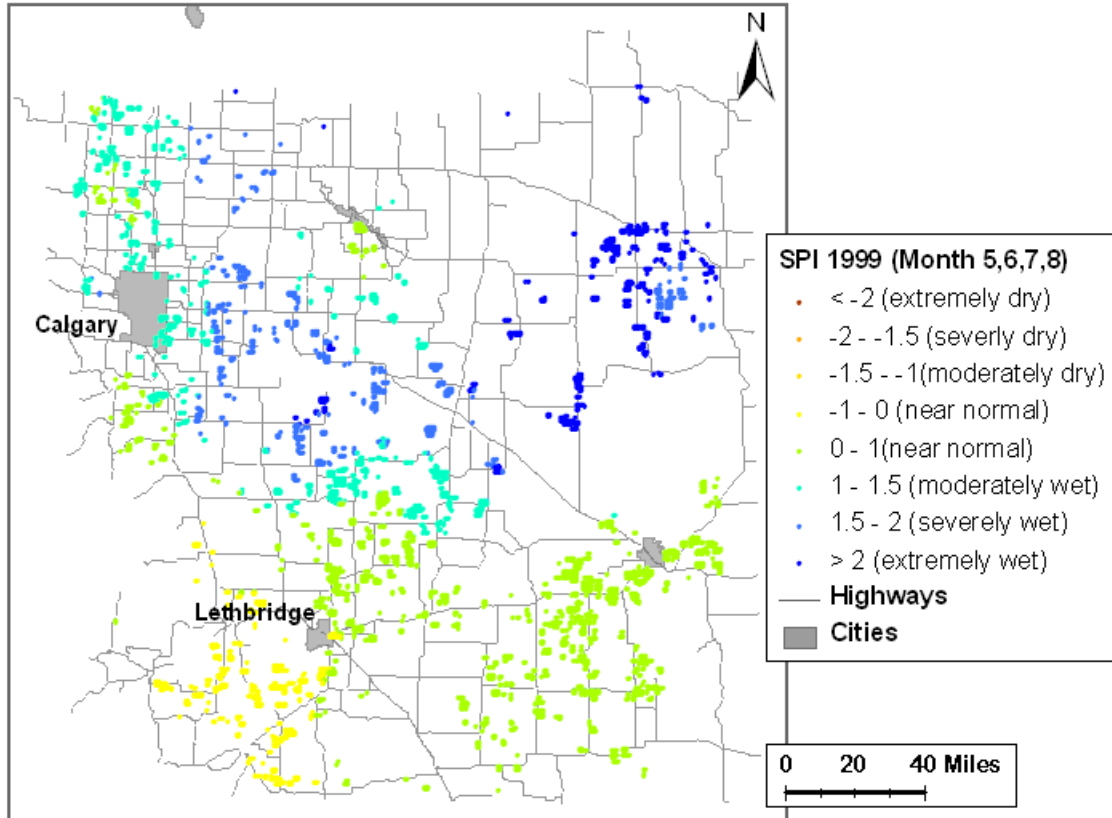
Figure 3-7 Spatial distribution of the growing season SPI in 1999

Table 3-2 Descriptive statistics of the growing season SPI in 1999

SPI classes	SPI value	Percentage of total valid quarter sections	Mean	Standard deviation
Extremely to moderately dry	<-1	0.00%		
Near normal	-1- 0	10.39%	-0.22	0.12
Normal	0 - 1	42.72%	0.55	0.22
Moderately wet	1 - 1.5	21.90%	1.27	0.15
Severely wet	1.5 - 2	13.66%	1.74	0.15
Extremely wet	>2	11.34%	2.27	0.21

For both 1998 and 1999, there was not a quarter-section associated with an SPI value lower than –1. The majority of the quarter-sections were classified as having a near normal precipitation condition during the growing season. There were more quarter-sections having moderately wet to extremely wet condition in 1999 than in 1998. In 1999, 11.34% of the quarter-sections had an extremely wet condition.
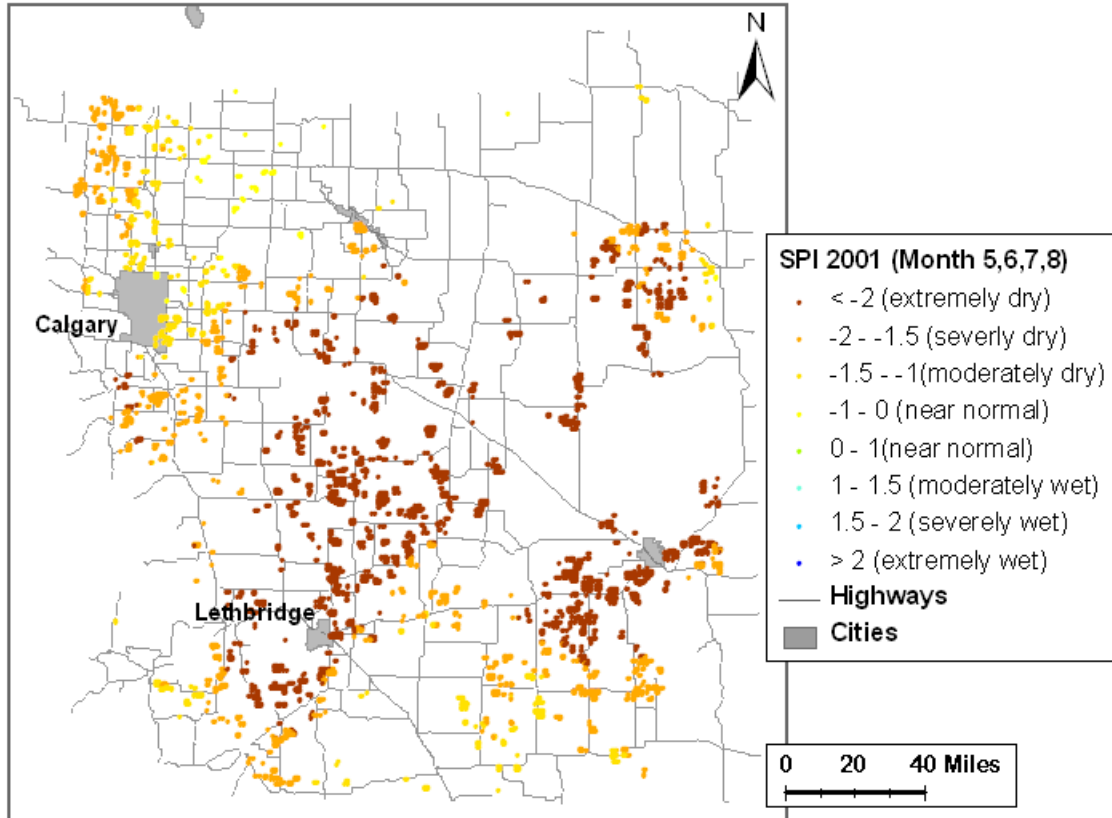
Figure 3-8 Spatial distribution of the growing season SPI in 2001

Table 3-3 Descriptive statistics of the growing season SPI in 2001

SPI classes	SPI value	Percentage of total valid quarter sections	Mean	Standard deviation
Extremely dry	<-2	55.71%	-2.33	0.22
Severely dry	-2 - -1.5	30.71%	-1.77	0.15
Moderately dry	-1.5 -1	12.16%	-1.32	0.13
Near normal	-1 - 0	1.42%	-0.63	0.32
Near normal to extremely wet	>0	0.00%		

The distribution of SPI values in 2001 is very different from those in 1998 and 1999. More than half of the quarter-sections exhibited extremely dry condition during the growing season in 2001; and about 31% of the quarter-sections were associated with severely dry conditions. There was no quarter-section associated with an SPI value larger than 0.

3.5   A Remote Sensing Approach for Assessing Agricultural Vulnerability

3.5.1   Data source

To assess agricultural vulnerability to drought at a detailed level, remotely sensed imagery is employed in the empirical analysis. As in the empirical approach based on the farm reported data. The years of 1998, 1999 and 2001 are selected as the years that provide a representative variation in precipitation conditions. Since multi-date satellite imagery can often generate superior land use and cover classification accuracy, and consequently generate better yield estimation, two Landsat TM/ETM+ images for each selected year are acquired. The determination of image date is mainly restricted by data availability: 1) the temporal resolution (the time between two overpass dates for a particular location) of Landsat satellite sensor is 16 days; and 2) large cloud coverage prevents some images from being usable. Images for the dates listed in Table 3-4 are selected for analysis in this study. The study area is defined as the overlapping area covered by all six acquired Landsat TM/ETM+ scenes over path 41 and row 25 (see Figure 3-1b). Each of the obtained imageries contains seven spectral bands of information. Six bands (band 1: 0.45-0.52 µm; band 2: 0.52-0.60 µm; band 3: 0.63-0.69 µm; band 4: 0.76-0.90 µm; band 5: 1.55-1.75µm; and band 7: 2.08-2.35µm) have a spatial resolution of 30 meters for each spectral pixel, and one thermal band (band 6: 10.4-12.5 µm) has a spatial resolution of 60 meters, which is excluded in the image analysis.

Table 3-4 Remote sensing images acquired

1998		1999		2001	
May 4th	July 23rd	May 23rd	August 3rd	July 7th	August 16th
Landsat 5 TM	Landsat 5 TM	Landsat 5 TM	Landsat 7 ETM+	Landsat 7 ETM+	Landsat 5 TM

3.5.2   Specifying the factors for vulnerability quantifying functions

In this approach, cereal crop yields estimated from the remotely sensed imagery are used as the measure of Y_i and Y_0 in Equation 3-5. The estimated yield for each representative year is used as the well-being state (Y_i in Equation 3-5). The average estimated yield for the three selected years is used as the relative damage threshold (Y_0 in Equation 3-5). Although the estimated yield can also be used for the sensitivity calculation, it requires data of a sufficient number of years to generate a steady trend line (regression line) for the slope calculation. We selected only three years for crop yield estimation, which is insufficient to generate the steady trend line suitable for sensitivity estimation. Therefore, the sensitivity value is adopted from the approach based on the farm reported data, which is already detailed above. The SPI calculation is the same as that presented in Section 3.4.4. V_{NEXP} is the average V_{NEXPi} over 1998, 1999 and 2001 (see Equations 3-1 and 3-2).

The data preparations for quantifying vulnerability are presented in detail in the following subsections.

3.5.3   Image preprocessing

3.5.3.1 Image orthorectification and atmospheric correction

The raw images are first orthorectified using orbital information and national road network vector data with a positional error of less than 0.5 pixel of[1]. All images are atmospherically corrected using the ATCOR2 algorithm implemented in PCI software by three general steps: 1) digital number of the image is first converted to at-sensor radiance using the gain and offset calibration information provided with the data, 2) by comparing

---

[1] Image orthorectification was done by David Rolfson at the image laboratory of Agricultural Research Station in Lethbridge.

the statistics of the haze versus clear regions of the scene for each sector and each channel, haze are removed, and 3) a ground reflectance image is calculated for each spectral band. The result of ATCOR2 is a ground reflectance image in each spectral band with a relative error of approximately 10 %. The output of ATCOR2 is an 8-bit image rather than a 32-bit floating point image, because the file size of 8-bit image is much more manageable. The pixel brightness values of the output images range from 0 to 255, with the following correlation: a value of 255 represents 65.535% reflectance, while the incremental value is 0.257% reflectance. As an example, the result of the atmospheric correction of image from August 3rd 1999 is presented in false color composite in comparison with the non-corrected image (Figure 3-9): A_1 and A_2 are subsets of the non-corrected image; B_1 and B_2 are subsets of the atmospherically corrected image. Comparing B_1 with A_1, the effects of thin haze are removed by the atmospheric
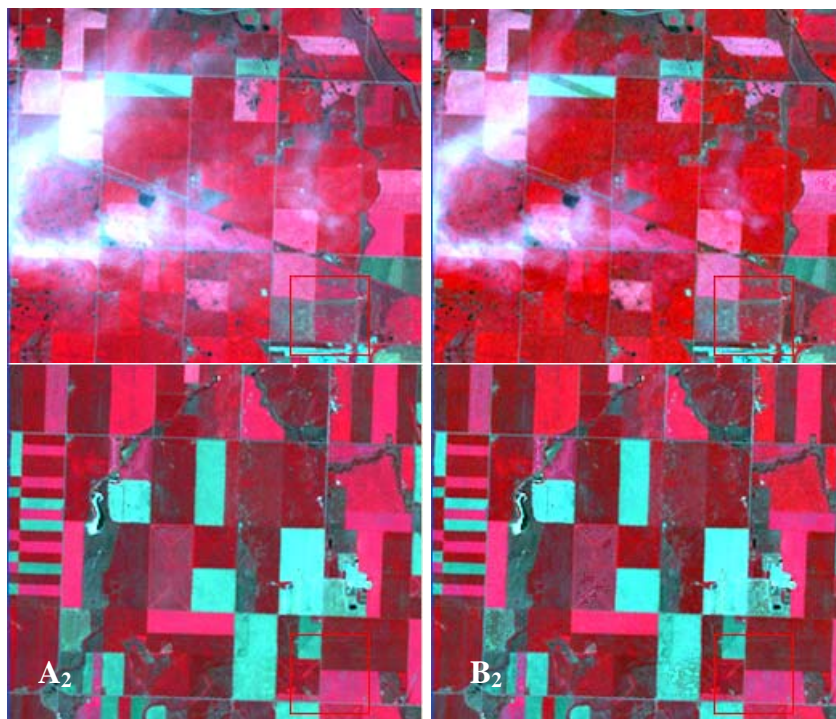
Figure 3-9 Image atmospheric correction: A_1 is the uncorrected haze area; A_2 is the uncorrected clear area; B_1 is the corrected haze area; and B_2 is the corrected clear area.

correction. Visually, no significant difference is presented at clear area (B_2 and A_2) between atmospherically corrected and non-corrected images.

3.5.3.2 Layer stacking and non-agricultural land masking

To ensure the best possible land use classification results in the study, both the single data imagery and two overpass date stacked imagery of each year are used for land use classification. The classification result from the single date image is compared with that from the two-date stacked image, and the comparison will be presented in Chapter 4.

It is indicated that the image atmospheric correction may not be necessary for land use classification (Champagne et al., 2005). To avoid the possible error in haze removal procedure of ATCOR2 algorithm, cloud and haze covered areas and shadows are visually detected and manually masked out based on the orthorectified image without atmospheric correction. Settlements and water bodies are masked with available vector data. A buffer of 150 pixels is created around the area with an elevation of 1300m or above to mask out the forestry land cover in the high elevation area. The masked image of August 3rd, 1999 is shown in Figure 3-10 as an example. Black area is either area outside the image coverage or masked non-agriculture area.

Figure 3-10 False color composite image with non-agricultural areas masked, August 3rd 1999

3.5.4   Data preparation for land use classification and yield estimation

3.5.4.1 Defining land use classification training and validation data

The farm reported crop dataset from AFSC is used with a supplemental dataset from Alberta Agriculture, Food and Rural Development (AAFRD) to define the training and validation data for land use classification. Different crop type classifications are used to overcome the semantic differences among these two datasets and to make the optimum use of these two training datasets. Table 3-5 presents possible land use classes and their corresponding descriptions from the corrected image; B_1 and B_2 are subsets of the atmospherically corrected image. Comparing B_1 with A_1, the effects of thin haze are removed by the atmospheric correction. Visually, no significant difference is presented at clear area (B_2 and A_2) between atmospherically corrected and non-corrected images.

Table 3-5 Dataset combination of AAFRD dataset and AFSC dataset

Crop name in AAFRD data	Crop Name in AFSC data	Classes for image classification
SUGAR BEETS	Sugar beets	Sugar beets
BARLEY	Barley	Barley
MALT BARLEY		
BARLEY SILAGE		
BARLEY SILAGE UNDERSEED		
CORN SILAGE	Corn (Fresh)	Corn
FRESH CORN (SWEET)	Corn (G)	
GRAIN CORN		
OATS	Oats	Oats
OATS SILAGE		
RYE	Rye-S	Rye
TRITICALE	Trit-S	Triticale
DURUM WHEAT	Wht-Durum	Durum wheat
HARD SPRING WHEAT	Wheat-HRS	Hard spring wheat
SOFT WHEAT	Wheat-SWS	Soft wheat
CPS WHEAT	Wht-Other	Other wheat
ALFALFA 2 CUT	Alfalfa	Alfalfa
ALFALFA 3 CUT		
ALFALFA HAY		
ALFALFA SEED		
ALFALFA SILAGE		
TIMOTHY HAY		
CANOLA	Canola	Canola
MUSTARD	Mustard-Br	Mustard
	Mustard-Ye	
DRY BEANS	Beans-Dry	Beans
	Bean-GrNor	
	Bean-Pinto	
	Beans-Pink	
	Beans-Red	
LENTILS	Lentils	Lentils
DRY PEAS	Peas-Field	Peas
FRESH PEAS		
POTATO	Potatoes	Potatoes
SEED POTATOES		
BROME HAY		Grass
GRASS HAY		
GRASS SEED		
	Trit-W	Winter triticale *
WINTER WHEAT	Wheat-HRW	Winter wheat *

FLAX	Flax	Flax*
SAFFLOWER	Safflower	Safflower*
SUNFLOWER	Sunflower	Sunflower*
	Cabbage	Cabbage*
ONIONS	Onions	Onions*
GREEN FEED		Green Feed*
SUMMER FALLOW		Summer Fallow*
CARAWAY		Caraway*
CARROTS		Carrots*
DILL		Dill*
HYOLA		Hyola*
NATIVE PASTURE		Native pasture*
TAME PASTURE		Tame pasture*
LINOLA		Linola*
MARKET GARDENS		Market Gardens*
MINT		Mint*
NURSEY		Nursery*
TURF SOD		Turf_Sod*
SMALL FRUIT		Small Fruit*
	Rye-F	Fall rye *
	MixedGr	Mixed grain*
MISC.		Miss-classified*

Note: 1) the crop types followed by a * in classes column is not considered in land use classification; 2) since the land covered with native range has obvious difference from other land uses, the training and validation data of native range class is visually detected and randomly defined in the study area.

Both the AFSC and AAFRD datasets recorded the crop type and acreage at the quarter-section level. For each year of the imagery, these two datasets are combined and linked with the quarter-section boundaries using the unique location IDs. The combined dataset is then overlaid on the remote sensing image for the corresponding year. The homogeneous crop areas on the remote sensing image within quarter-section boundaries are then identified and the acreage is verified using the data provided in AFSC and AAFRD datasets. These homogeneous crop areas are divided into classes of different crop types. In the quarter-sections, about two thirds of the homogeneous crop area in each class are randomly selected and defined as the training Region of Interests (ROIs), and

the remaining one third is defined as the validation ROIs. Examples of defined training and validation ROIs are presented in Figure 3-11. On the right side, the ROIs are presented in blue, white, green, red, and purple and so on, and each color represents one crop class, while true color image subsets are presented on the left hand as a reference.
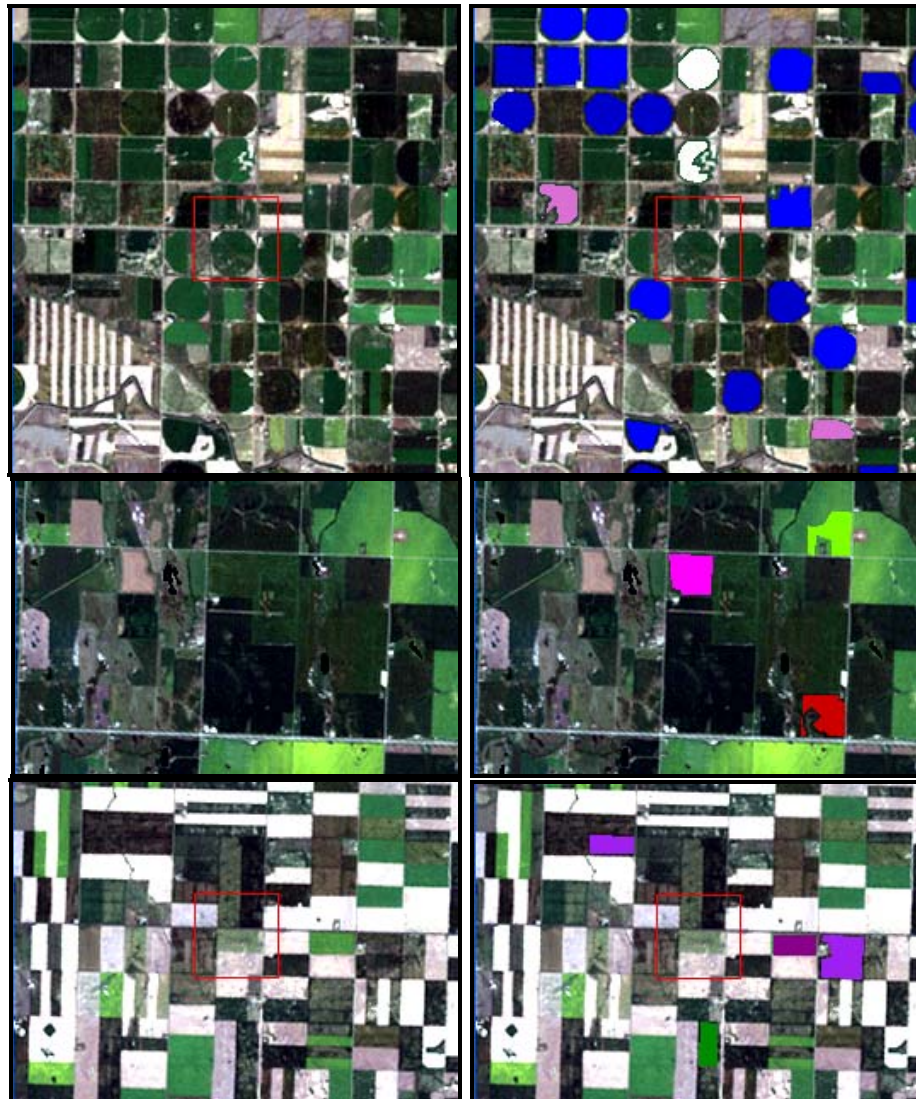
Figure 3-11 Examples of defined training and validation ROIs (on the right side)

The spectral characteristics of each crop type might differ across soil zones and vary spatially because of different water supply capacities. To insure high classification accuracy, the soil type and irrigation possibility zones (STIPZs) are identified by using

various soil zone and irrigation district boundaries. Six STIPZs are listed in Table 3-6. STIPZs are used to refine further the training ROIs for each crop class. The utility of STIPZs grouped classification training is discussed in Chapter 4.

Table 3-6 The definition of six STIPZs

STIPZs	Soil zones	Inside or outside of irrigation districts
BLI	Black	Inside
DBI	Dark brown	Inside
BRI	Brown	Inside
BLD	Black	Outside
DBD	Dark brown	Outside
BRD	Brown	Outside

In this study, the classification accuracy will be reported in overall accuracy, producer accuracy (short as Prod. Acc.) and user accuracy (short as User Acc.). The definition of these accuracies is as follows:

1) Overall accuracy is calculated by summing the number of pixels classified correctly and dividing by the total number of pixels.

2) Producer accuracy is a measure indicating the probability that a pixel belong to Class A in the given ground truth reference is classified as Class A by the classifier.

3) User accuracy is a measure indicating the probability that a pixel classified as Class A by the classifier is belongs to Class A in the given ground truth reference.

Since the yield estimation will be conducted based on the classified images, it is more important to ensure that what is classified as Class A is Class A in reality (according to ground truth validation data). Therefore, for the selection of the suitable classification approach, user accuracy is more of a concern than producer accuracy.

3.5.4.1 Yield estimation method

In this study, the yield estimation models are defined as the multiple regression models of the crop yield on a set of the related independent variables. The dependent variable is the farm reported cereal crop yield. The primary independent variable of the yield estimation model is the NDVI value that is calculated based on the remotely sensed images with Equation 2-3, where ℓ_1 and ℓ_2 are the pixel brightness values of the Landsat TM/ETM bands 3 (red) and 4 (NIR), respectively.

After achieving the acceptable accuracies of land use classification (see Section 4.2 for details), only image areas that are classified as cereal crops are retained, and all other non-cereal crop areas are excluded from the following analysis. Vector datasets of quarter-section boundaries and road systems in the image area are employed to mask out quarter-section boundaries and roads. The summer fallow areas are masked out by setting an NDVI threshold under which areas are found to be fallow. The utility of this pre-masking procedure for avoiding the confusion (noise) is illustrated in Chapter 4

The NDVI values calculated based on atmospherically corrected and non-corrected images from 1999 are tested for yield estimation and compared in terms of their suitability for yield estimation (see Section 4.3.1). The approach generating better NDVI estimation is then applied to other imageries of 1998 and 2001.

In addition to the dependent variable of NDVI in the regression model, two numerical variables and four binary variables are considered to improve the explanatory power of the yield estimation regression models. Location coordinates, soil type and irrigation are included in testing individual models for the respective years. The selections of these independent variables are based on the investigation of the regression

residuals and residual maps. The model that generates the best yield estimation results is employed for each year. The result of the regression model selection and crop yield estimates are presented and discussed in detail in Chapter 4.

CHAPTER 4 REMOTE SENSING IMAGERY ANALYSES RESULTS

4.1   Introduction

To assess agricultural vulnerability to climate variability, the crop yields of various types need to be estimated. This chapter presents and compares the crop classification results of different remote sensing classification approaches using 1999 imagery as the base. The tested approach that achieves the best classification result is then selected to classify crops using the imagery from 1998, 1999 and 2001. Based on the classified imagery, linear regression models are developed for each year and used to estimate yields of cereal crops from the classified remotely sensed imagery.

4.2   Image Classification

As introduced in Chapter 3, two Landsat TM digital images are obtained for 1998, 1999, and 2001. For each year, the training and validation ROIs are identified based on the seeded crop recorded in the AFSC and AAFRD combined dataset (see Section 3.5.4.1 for detail). Using the supervised maximum likelihood classifier, a series of processes are first applied to the 1999 imagery to determine a suitable approach for crop classification in the study area. The suitable classification approach is then employed to classify 1998 and 2001 images.

4.2.1   Identification of a suitable classification approach base on 1999 imagery

The ROI separability calculation is first conducted based on the training ROIs for 1999, where each crop type (see table 3-5) is defined as one training class. This calculation provides the information about the spectral similarity or difference of each pair of training ROIs. The calculated Jeffries-Matusita index is reported in Table 4-1 (see Richards, 1999 for Jeffries-Matusita index calculation). The Jeffries-Matusita index value

ranges from 0 to 2, where values over 1.9 (highlighted using light yellow color) indicate that the ROI pairs have a good separability. For ROI pairs with a lower separability value, it is suggested to consider combining them with other ROI pairs.

Table 4-1 Jeffries-Matusita index values

	Alfalfa	Barley	Beans	Canola	Corn	Flax	Grass	Lentils	Mustard	Oats	Pasture	Peas	Pota-toes	Rye	Sugar-beets	Triticale	Wheat-HRS	Wht-Durum	Wht-Other	Wht-Soft
Alfalfa		1.53	1.88	1.98	1.78	1.88	0.80	1.98	1.95	1.58	1.00	1.92	1.85	1.93	1.91	1.73	1.82	1.83	1.84	1.79
Barley	1.53		1.53	1.88	1.36	1.49	1.73	1.97	1.72	0.94	1.62	1.62	1.73	1.63	1.67	1.27	0.95	1.14	0.92	1.06
Beans	1.88	1.53		1.95	1.23	1.69	1.95	1.94	1.88	1.55	1.85	1.77	1.40	1.59	1.72	1.79	1.51	1.29	1.67	1.55
Canola	1.98	1.88	1.95		1.95	1.90	1.98	1.98	1.32	1.94	1.97	1.49	1.97	1.99	1.87	1.96	1.93	1.93	1.93	1.96
Corn	1.78	1.36	1.23	1.95		1.54	1.92	1.94	1.92	1.42	1.81	1.84	1.31	1.71	1.57	1.45	1.58	1.59	1.51	1.55
Flax	1.88	1.49	1.69	1.90	1.54		1.95	1.99	1.88	1.45	1.87	1.77	1.88	1.77	1.61	1.54	1.36	1.46	1.46	1.54
Grass	0.80	1.73	1.95	1.98	1.92	1.95		1.98	1.98	1.76	0.83	1.97	1.93	1.98	1.93	1.79	1.92	1.93	1.91	1.87
Lentils	1.98	1.97	1.94	1.98	1.94	1.99	1.98		1.88	1.98	1.99	1.95	1.95	2.00	1.99	1.98	1.99	1.99	1.99	1.99
Mustard	1.95	1.72	1.88	1.32	1.92	1.88	1.98	1.88		1.86	1.94	1.48	1.95	1.97	1.91	1.95	1.80	1.77	1.86	1.92
Oats	1.58	0.94	1.55	1.94	1.42	1.45	1.76	1.98	1.86		1.58	1.79	1.82	1.74	1.79	1.50	1.18	1.17	1.30	1.27
Pasture	1.00	1.62	1.85	1.97	1.81	1.87	0.83	1.99	1.94	1.58		1.94	1.88	1.95	1.91	1.79	1.85	1.85	1.86	1.82
Peas	1.92	1.62	1.77	1.49	1.84	1.77	1.97	1.95	1.48	1.79	1.94		1.92	1.92	1.87	1.90	1.67	1.66	1.79	1.88
Potatoes	1.85	1.73	1.40	1.97	1.31	1.88	1.93	1.95	1.95	1.82	1.88	1.92		1.87	1.60	1.89	1.89	1.87	1.89	1.83
Rye	1.93	1.63	1.59	1.99	1.71	1.77	1.98	2.00	1.97	1.74	1.95	1.92	1.87		1.91	1.81	1.64	1.64	1.63	1.48
Sugar-beets	1.91	1.67	1.72	1.87	1.57	1.61	1.93	1.99	1.91	1.79	1.91	1.87	1.60	1.91		1.75	1.87	1.88	1.85	1.80
Triticale	1.73	1.27	1.79	1.96	1.45	1.54	1.79	1.98	1.95	1.50	1.79	1.90	1.80	1.81	1.75		1.53	1.62	1.30	1.23
Wheat-HRS	1.82	0.95	1.51	1.93	1.58	1.36	1.92	1.99	1.80	1.18	1.85	1.67	1.89	1.64	1.87	1.53		0.46	0.53	1.04
Wht-Durum	1.83	1.14	1.29	1.93	1.59	1.46	1.93	1.99	1.77	1.17	1.85	1.66	1.87	1.64	1.88	1.62	0.46		1.02	1.07
Wht-Other	1.84	0.92	1.67	1.93	1.51	1.46	1.91	1.99	1.86	1.30	1.86	1.79	1.89	1.63	1.85	1.30	0.53	1.02		0.93
Wht-Soft	1.79	1.06	1.55	1.96	1.55	1.54	1.87	1.99	1.92	1.27	1.82	1.88	1.83	1.48	1.80	1.23	1.04	1.07	0.93	

By investigating the separability values presented in Table 4-1, a high spectral similarity (low separability value) exist among many class pairs. Therefore, the spectrally similar classes are combined to avoid excessive classification errors. The above twenty land use cover types are combined to form five crop cover types as the initial classification scheme (see Table 4-2). A few tests are conducted using this scheme, and the classification results are compared in terms of their classification accuracy. Further modifications to the image classification scheme are presented later in this section.

Table 4-2 Class grouping details and classification accuracy of scheme A

Classes (see Table 3-5)	Classification scheme A		
	Overall Accuracy (%)	86.0	
		Prod. Acc. (%)	User Acc. (%)
Grass	Alfalfa	82.7	92.7
Alfalfa			
Pasture			
Rye	Cereal crops	84.7	89.4
Oats			
Barley			
Hard spring wheat			
Durum wheat			
Soft wheat			
Other wheat			
Triticale			
Beans	Broadleaf crops	78.0	86.3
Lentils			
Peas			
Potatoes			
Sugarbeets			
Corn			
Canola	Canola+Mustard	93.5	75.0
Mustard			
Native Range	Native range	97.6	99.8

As presented in Chapter 3, since spectral characteristics of each crop may vary across different soil type and irrigation possibility zones (STIPZs). The training data are further divided into six groups by STIPZs. Two single date images and one two-date stacked imagery are classified based on the training data with and without the STIPZ grouping. As such, a total of six supervised maximum likelihood classifications are performed to identify the optimum image classification method. For all classification results based on the STIPZ grouped training data, the pixels that belong to the same crop class but are associated with different STIPZs are combined using a post-classification method, "combine". The results of classification accuracy are presented in Tables 4-3 and 4-4.

Table 4-3 Image classification accuracies using single date and two-date stacked imagery without the STIPZ grouping

	May 23th image		August 3rd image		Two-date stacked image	
Overall accuracy (%)	58.8		77.4		83.9	
	Prod. Acc. (%)	User Acc. (%)	Prod. Acc. (%)	User Acc. (%)	Prod. Acc. (%)	User Acc. (%)
Alfalfa	82.0	90.2	79.5	76.1	83.7	87.3
Cereal crops	14.8	61.8	80.9	77.1	82.3	84.1
Broadleaf crops	58.2	57.1	48.2	72.5	70.4	79.2
Canola+Mustard	82.0	21.1	90.4	67.8	93.8	65.5
Native Range	97.9	97.9	95.7	98.2	97.6	99.7

Table 4-4 Inage classification accuracies using single date and two-date stacked imageries with the STIPZ grouping

	May 23th Image		August 3rd image		Two-date stacked image	
Overall accuracy (%)	54.3		79.1		84.7	
	Prod. Acc. (%)	User Acc. (%)	Prod. Acc. (%)	User Acc. (%)	Prod. Acc. (%)	User Acc. (%)
Alfalfa	80.9	90.6	65.9	81.1	83.2	89.6
Cereal crops	21.5	60.7	81.2	81.9	81.5	86.4
Broadleaf crops	38.6	38.0	71.7	65.4	77.4	75.9
Canola+Mustard	55.3	15.6	91.5	74.5	92.3	68.1
Native Range	97.1	98.3	94.0	98.8	96.9	99.7

As indicated in Tables 4-3 and 4-4, the overall classification accuracy ranges from 54.3 to 84.7%. As expected, the classifications based on a two-date stacked imagery produce a higher overall accuracy. For the classifications with and without the STIPZ grouping of training data, there is a slight difference in image classification accuracies. The overall classification accuracy for the single data imagery taken in the late growing season and two-date stacked imagery is higher with the STIPZ grouping of training data than that without the STIPZ grouping (Tables 4-3 and 4-4). The accuracy for the single imagery taken in the early growing season without the STIPZ grouping of training data is higher than that with the STIPZ grouping.

Because the image classification based on the two-date stacked imagery with the STIPZ grouping of training data achieves the highest overall accuracy as well as the user accuracies, this approach is used for the digital image classification throughout this study.

To improve the user accuracy further, several post-classification methods are tested using the classified image of the two-date stacked imagery based on the STIPZ grouping of training data. The test results are demonstrated using a subset of the classified image as an example (see Figure 4-1).

As shown in classified image in Figure 4-1 (a), there are numerous isolated pixels in each of the classified land cover classes. These isolated pixels are often considered as classification noise. While the complete removal of classification noise is impossible, a number of post-classification operations can be carried out to improve the appearance of the output thematic image. Removing high-frequency spatial variation or noise from the classified image can often be achieved by analyzing the neighboring pixel and removing the scatter single pixels ('sieve' process), and then merging the small patches of pixels together to make more continuous and coherent units ('clump' process). In the image sieving process, the sieve threshold is a parameter that specifies the minimum size of the adjacent pixel groups to be maintained in the output. For example, assuming 50 is set as the sieve threshold, if a group of adjacent pixels less than 50 are classified as Class A and they are isolated from any other pixels in class A, these pixels will be assigned as unclassified in sieve output. In this study, different sieve thresholds are tested, and the classification accuracy results are reported in Table 4-5.
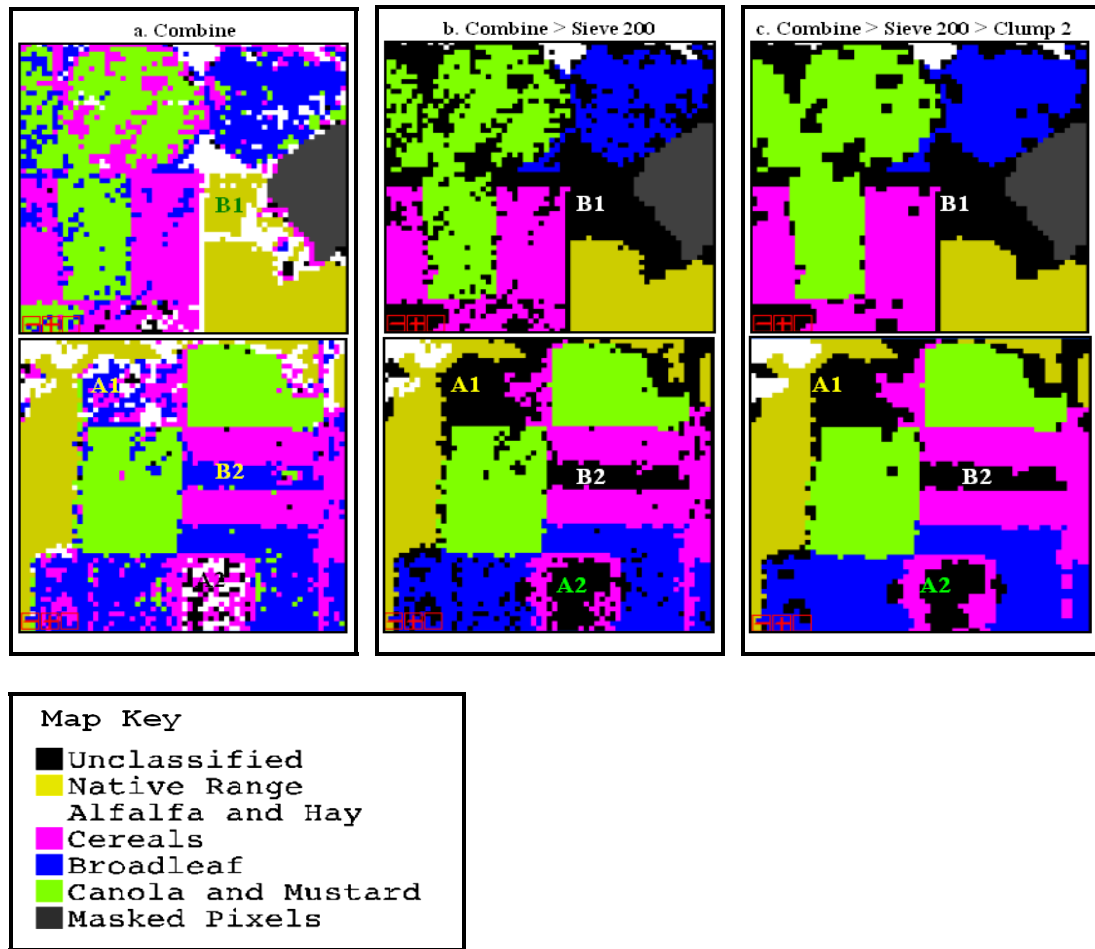
Figure 4-1 Image subset of three steps of classification and post-classification
a - STIPZ combined classes; b - sieved with a threshold of 200, based on a; c - clumped
by two pixels, based on b.

Figure 4-1(b) and Figure 4-1(c) illustrate how the sieving and clumping processes change the classified image. Some areas of confusion are eliminated from the classification result (e.g., A1 and A2), as well as some small classified pixel patches that may not be correctly classified (e.g. B1 and B2).

Table 4-5 Post-classification accuracy resulted with various parameter specifications

Sieve threshold (Pixels)			25		50		100		200		200	
Clump operator size (Pixels)											2	
Overall accuracy (%)	84.7		84.2		84.1		83.8		83.1		86.0	
	Prod. Acc. (%)	User Acc. (%)	Prod. Acc. (%)	User Acc. (%)	Prod. Acc. (%)	User Acc. (%)	Prod. Acc. (%)	User Acc. (%)	Prod. Acc. (%)	User Acc. (%)	Prod. Acc. (%)	User Acc. (%)
Alfalfa	83.2	89.6	82.9	91.9	82.7	92.3	82.4	92.8	82.1	93.1	82.7	92.7
Cereal crops	81.5	86.4	80.9	88.6	80.9	88.9	80.8	89.1	80.5	89.4	84.7	89.4
Broadleaf crops	77.4	75.9	76.1	82.2	75.7	82.9	75.0	84.3	72.8	86.8	78.0	86.3
Canola+ Mustard	92.3	68.1	92.2	73.1	92.2	74.1	91.7	75.2	90.8	77.0	93.5	75.0
Native Range	96.9	99.7	96.9	99.8	96.9	99.8	96.9	99.8	96.9	99.8	97.6	99.8

As indicated in Table 4-5, when the sieve threshold size increases, the number of unclassified pixels escalates. This is resulted from an increasing number of both mis-classified pixels and correctly classified pixels that are sieved out from a designated class. As a result, the overall accuracy declines while the sieve threshold goes up. Also, the producer accuracy decreases while user accuracy increases, when the sieve threshold rises. The decline of overall accuracy indicates, among the pixels sieved out of classes, there are more correctly classified pixels than mis-classified pixels. The clump process can be employed to solve this problem. A clump operator size of 2 pixels is used. This procedure assigns any single or two isolated pixels into the class that most of the surrounding pixels belong to. This procedure improves the overall accuracy by almost 3% while the user accuracy for most of the classes remains proximally the same. Compared to the classification result without noise removal procedures, the overall

accuracy of the image after the above post-classification procedures is increased by 1%. More importantly, the user accuracy of cereal crop classes is increased by more than 3%.

To further improve the classification accuracy, especially the user accuracy of cereal crops, alternative land use and land cover classification are adopted. The classification scheme used above is refined. The broadleaf crops in the above classification scheme are divided into three crop types, i.e. broadleaf crop (refined); row crop; corn in the alternative classification scheme (see Table 4-6).

Table 4-6 Class grouping details and classification accuracy comparison of two schemes

Classes (see Table 3-5)	Classification scheme A			Classification scheme B		
	Overall Accuracy (%)	86.0		Overall Accuracy (%)	83.7	
		Prod. Acc. (%)	User Acc. (%)		Prod. Acc. (%)	User Acc. (%)
Grass	Alfalfa	82.7	92.7	Alfalfa	82.4	93.9
Alfalfa						
Pasture						
Rye	Cereal crops	84.7	89.4	Cereal crops	82.1	92.7
Oats						
Barley						
Hard spring wheat						
Durum wheat						
Soft wheat						
Other wheat						
Triticale						
Beans	Broadleaf crops	78.0	86.3	Broadleaf crops (refined)	64.2	75.9
Lentils						
Peas						
Potatoes				Row crop	71.9	93.6
Sugarbeets						
Corn				Corn	80.5	92.7
Canola	Canola+Mustard	93.5	75.0	Canola+Mustard	91.4	85.4
Mustard						
Native Range	Native range	97.6	99.8	Native range	97.6	99.8

Comparing the classification results based on two different classification schemes (Table 4-6), most land classes based on Classification Scheme B are associated with higher user accuracy although the overall accuracy using this scheme is lower. Only the broadleaf crop class under the Classification Scheme B has lower user accuracy than that under the classification scheme A. More importantly, the user accuracy of cereal crops is

3.3% higher. The result based on the Classification Scheme B is a desirable improvement because this study focuses on the yield estimation of cereal crops. As a result, the classification scheme B is chosen to classify the imagery of 1998 and 2001.

In sum, the above classification and post-classification procedures are tested to derive an optimum classification framework for this study. These procedures are summarized systematically into a prototypical image classification framework. Figure 4-2 presents the prototypical framework that is implemented in classifying all of the imageries in this study.
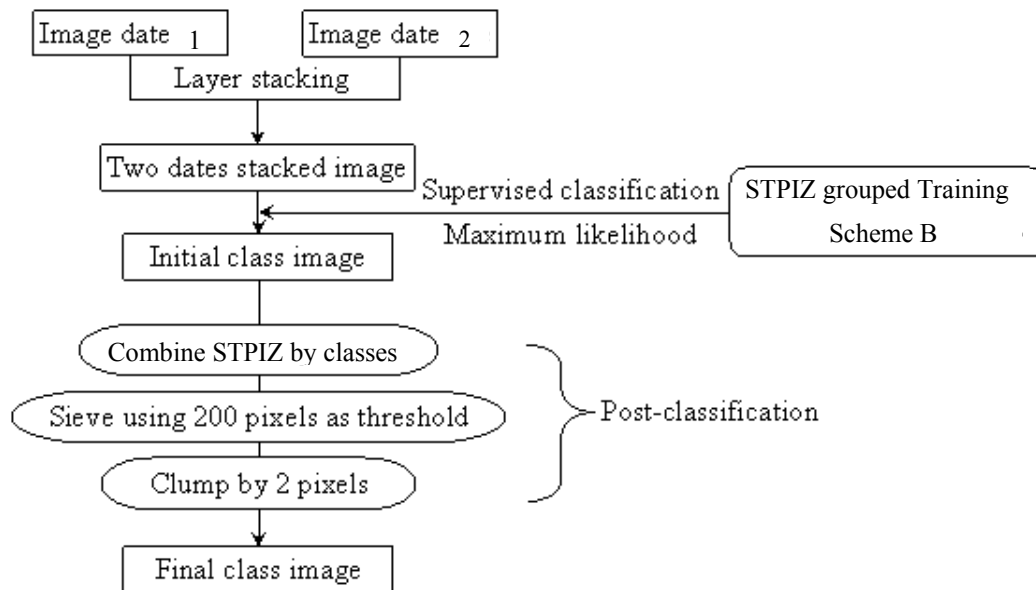
Figure 4-2 Image classification protocol

4.2.2   Classification results of 1998, 1999 and 2001

The image classification accuracies for 1998, 1999, and 2001 are presented in Table 4-7. The classification of the 1998 imagery produces an undesirably low overall accuracy. By examining the accuracies for each land use class, the low overall accuracy is primarily caused by a very poor classification of corn class. Since corn is not a dominant crop in the study area, it is eliminated from training dataset. The overall

classification accuracy (without considering corn) is 86.4% (see Table 4-7). The overall

classification accuracy is 83.7% and 81.0% for the 1999 and 2001 imageries, respectively.

Corn crop class is not excluded for 1999 and 2001, because it can be classified with

acceptable accuracy. User accuracy of all three years is close to 90% or higher.

Table 4-7 Classification accuracies of three years

Years	1998		1998 (Corn excluded)		1999		2001	
Overall Accuracy (%)	76.4		86.4		83.7		81.0	
	Prod. Acc. (%)	User Acc. (%)	Prod. Acc. (%)	User Acc. (%)	Prod. Acc. (%)	User Acc. (%)	Prod. Acc. (%)	User Acc. (%)
Alfalfa	80.7	86.7	80.7	87.0	82.4	93.9	62.7	88.8
Cereal crop	68.3	95.8	81.7	94.7	82.1	92.7	87.5	89.8
Broadleaf crop (refined)	51.9	83.2	53.8	80.4	64.2	75.9	64.9	97.2
Row crop	68.2	87.0	73.9	88.2	71.9	93.6	78.5	90.9
Corn	57.1	23.2			80.5	92.7	88.1	73.1
Canola+ Mustard	86.4	93.4	86.4	93.4	91.4	85.4	81.5	90.8
Native Range	98.5	99.8	98.5	99.8	97.6	99.8	97.1	99.4

Table 4-8 presents the coverage of the classified land use and cover classes. The

cereal crops represent the dominant crops in all three years, and their yields will be

estimated for assessing agricultural vulnerability to drought.

Table 4-8 Coverage of classified land used and cover classes, 1998, 1999, and 2001

Classe	1998		1999		2001	
Total acreage	6172824		6316672		6638637	
	Percentage	Acreage	Percentage	Acreage	Percentage	Acreage
Alfalfa	16.9%	1040829	19.7%	1241549	8.9%	592224
Cereal crop	33.3%	2054899	32.8%	2071163	38.2%	2533672
Canola+Mustard	6.4%	394766	6.3%	395184	3.6%	238149
Corn			0.5%	32683	0.8%	53427
Broadleaf crop (refined)	2.4%	147959	1.8%	112065	2.1%	137217
Row Crops	1.0%	59763	0.6%	36878	0.7%	43553
Native Range	17.5%	1079545	17.5%	1107088	18.4%	1219598
Unclassified	22.6%	1395064	20.9%	1320062	27.4%	1820796

4.3   Yield Estimation

In this section, a standard image pre-processing procedure for yield estimation is

first developed based on the 1999 imagery. This standard procedure is then applied to

processing the 1998 and 2001 imagery. Multiple regression analysis is used to establish the yield estimation models. Different regression variable sets are tested to determine the best estimation result.

4.3.1   Image pre-processing standard for yield estimation

As indicated in Chapter 3, the original imagery is masked and only the areas classified as cereal crops are retained. The methods for atmospheric correction and NDVI calculation are presented in Chapter 3, and are applied to the imagery used in this study. The image NDVI is first calculated at the pixel level, and it is then used to generate the average NDVI of a quarter-section by using the "Zonal statistics" function available in ArcGIS software. A set of boundary files are employed to mask out irrelevant image areas to avoid the possible confusion (noise) in yield estimation:

1) Roads and quarter-section boundaries are masked using a 30 meters (one pixel size) buffer of the quarter-section boundaries;

2) Summer fallow areas are masked by a NDVI threshold under which the image area was detected to be fallow. This threshold is visually detected based on investigating the NDVI calculated from the atmospherically corrected image. The image taken from the later date of the growing season (August 3rd for 1999) is used. The reasons for using the atmospherically corrected later growing season image for threshold detections are: a) the corrected imagery after removing the atmospheric effects represents the spectral property of the vegetations more accurately, and b) imagery from later in the growing season provides more variability in the NDVI values, and therefore is preferred for visually detecting the difference between vegetation and summer fallow. The detected the threshold for fallow masking is NDVI value 0.4 for 1999. The detailed pre-processing

procedure is illustrated in a flowchart in Figure 4-3. The processing results indicated in the shaded boxes are tested in the following steps in terms of their efficiency for yield estimation.
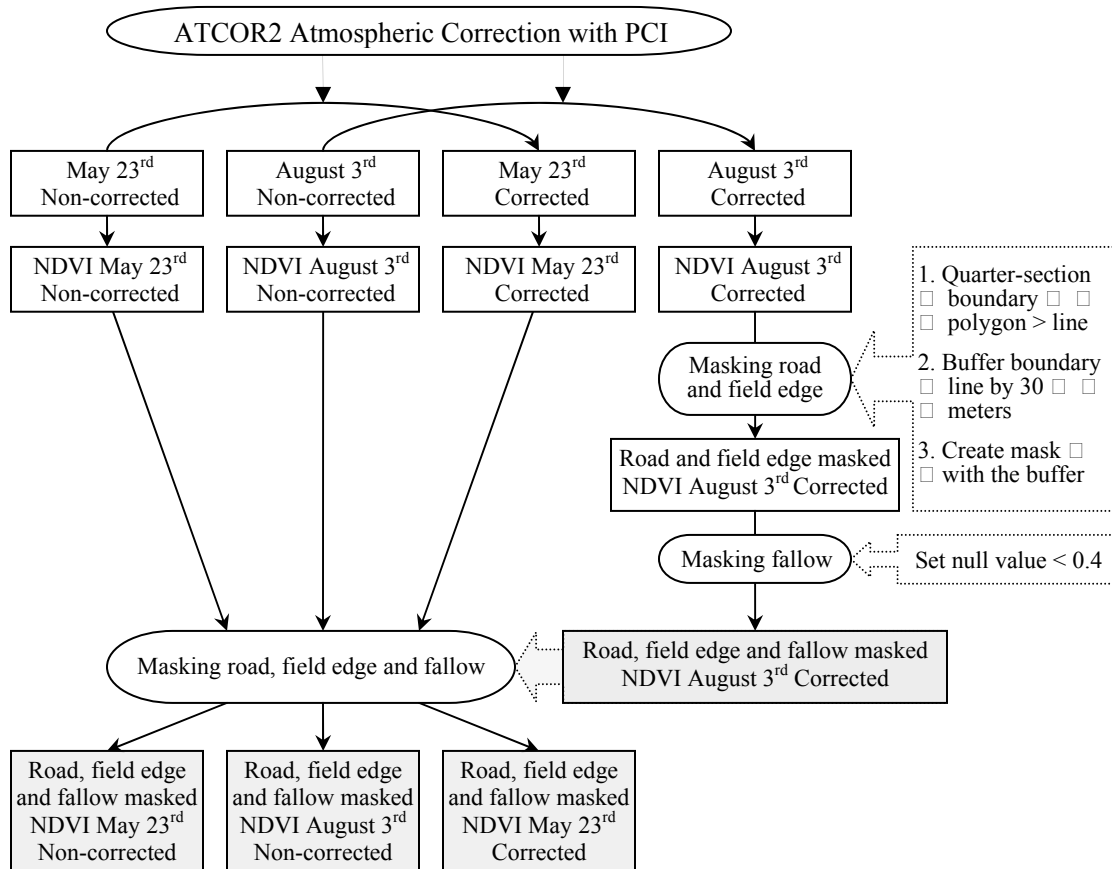
Figure 4-3 Pre-processes for yield estimation, 1999

The utility of these pre-processes in improving yield estimation performance is discussed by comparing the yield estimation results using NDVI with and without pre-processing. In addition, the NDVI calculated based on both atmospherically corrected and non-corrected imagery is tested and compared to see if the atmospheric correction method would generate better yield estimates of cereal crops. Also, the NDVI from the image of the later date in the growing season alone and NDVIs of both images are used for yield estimation. The results are compared in terms of their utility for yield estimation.

Both simple and multiple linear regression models are used to test the usefulness of the above pre-processing and atmospheric correction procedures in crop yield estimation. Using the farm reported yields as the two available training datasets e dependent variable and the quarter-section average of NDVI values from the differently pre-processed imagery as the independent variable, a total of four yield estimation models was conducted. The estimation results are simply compared in their R-square coefficients of regression models (see Table 4-9). As presented in Table 4-9, masking out confusion areas (with pre-processing) improves the estimation effectiveness for both atmospherically corrected NDVI (ATCOR2) and non-corrected NDVI (Orig). However, it is found that the regression based on the non-corrected NDVI has R-square values higher than that of the corrected NDVI (see Table 4-.9), which is not expected.

Table 4-9 Tested regression R-square values for crop yield estimation based on NDVI with varying pre-processing procedures

Variables		R^2			
NDVI		Without pre-processing		With preprocessing	
May 23rd	Aug. 03rd	Orig	ATCOR2	Orig	ATCOR2
	√	0.225	0.214	0.291	0.273
√	√	0.260	0.260	0.313	0.293

By plotting the histogram and Q-Q plot of the atmospherically corrected NDVI, it is discovered that these NDVI values are not perfectly normally distributed (see Figure 4-4). Therefore a log-transform of NDVI data (see Equations 4-1and 4-2) is then applied to improve the NDVI values' normality. Comparing the histograms and Q-Q plots of the log-transformed NDVI data to the non-transformed NDVI data presented in Figure 4-4, the transformed data approximate more to a normal distribution curve.

$$T\_NDVI\_0523 = ln(NDVI\_0523 \times 10) \qquad\qquad (4\text{-}1)$$

$$T\_NDVI\_0803 = ln[(1 - NDVI\_0803) \times 10]$$ (4-2)
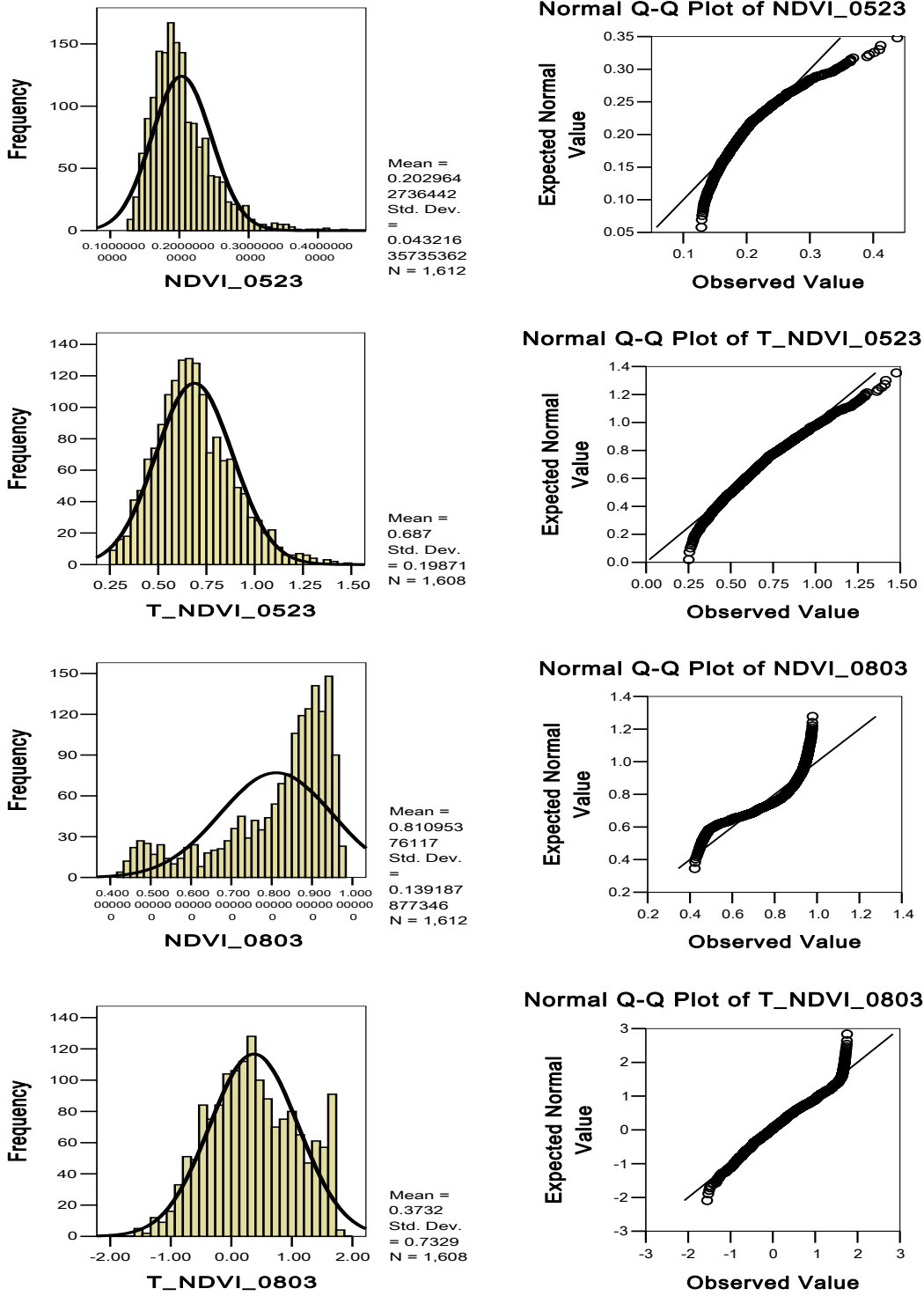
Figure 4-4 Histogram and Q-Q plot of atmospherically corrected 1999 NDVI (NDVI_0523, NDVI_0803) and their transformation (T_NDVI_0523, T_NDVI_0803)

Table 4-10 Tested regression R-square values for crop yield estimation based on transformed NDVI with varying pre-processing procedures

Variables		R^2			
Transformed NDVI		Without pre-processing		With preprocessing	
May 23rd	Aug. 03rd	Orig	ATCOR2	Orig	ATCOR2
	√	0.260	0.294	0.310	0.319
√	√	0.283	0.319	0.322	0.330

Based on the transformed NDVI data, simple regression analysis is conducted again to test any change in R-square value in the regression models. As expected, the R-square values increased consistently in all of the regression models (see Tables 4-9 and 4-10). Moreover, the atmospherically corrected NDVI shows an advantage over non-corrected NDVI in crop yield estimation. The regression tests also show that the masking procedures of removing possible confusion areas contribute to a better estimation of crop yields. The atmospherically corrected NDVI data for 1998 and 2001 are examined (see Figure 4-5 and Figure 4-6). Similar to the 1999 NDVI data, the 1998 and 2001 NDVI data are not normally distributed. The log-transformation procedures are applied to the data. The individual transformation equations are listed below (see Equations 4-3, 4-4, 4-5, 4-6).

$$T\_NDVI\_0504 = ln(NDVI\_0504 \times 10) \tag{4-3}$$

$$T\_NDVI\_0723 = ln[(1 - NDVI\_0723) \times 10] \tag{4-4}$$

$$T\_NDVI\_0707 = ln[(1 - NDVI\_0707) \times 10] \tag{4-5}$$

$$T\_NDVI\_0816 = ln(NDVI\_0816 \times 10) \tag{4-6}$$
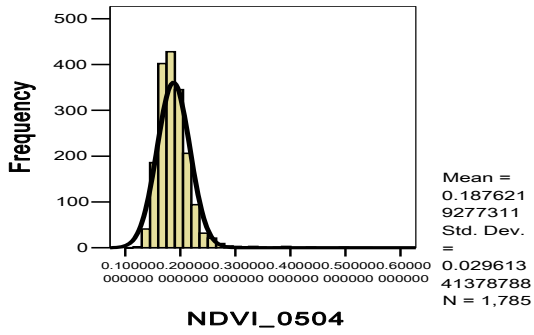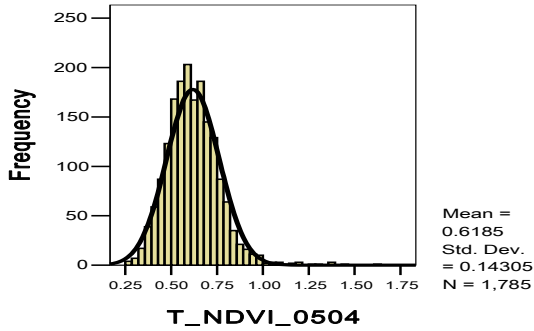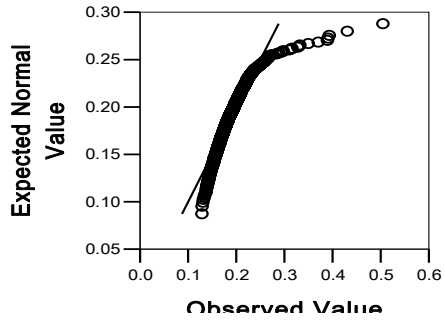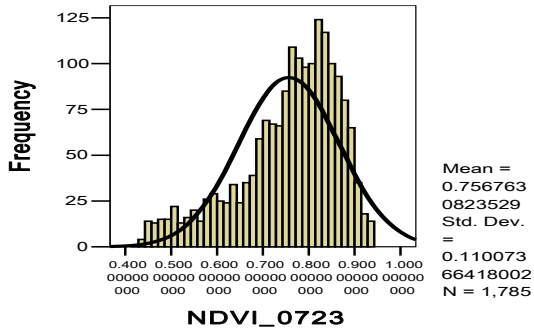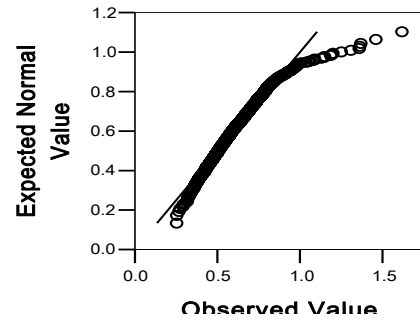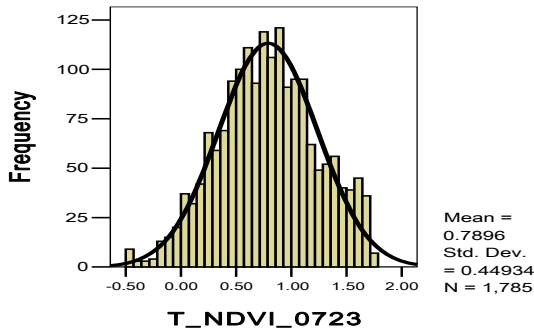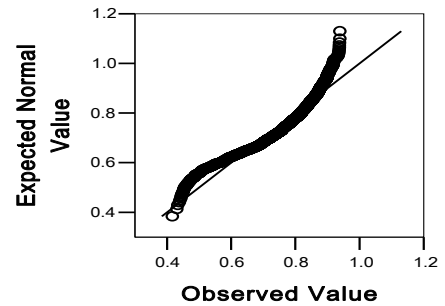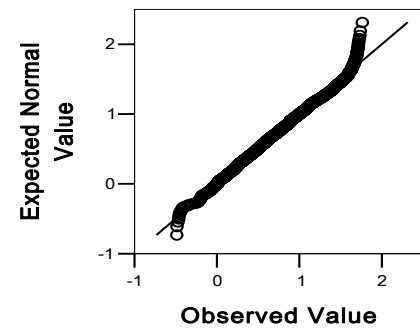
Figure 4-5 Histogram and Q-Q plot of atmospherically corrected 1998 NDVI (NDVI_0504, NDVI_0723) and their transformation (T_NDVI_0504, T_NDVI_0723)
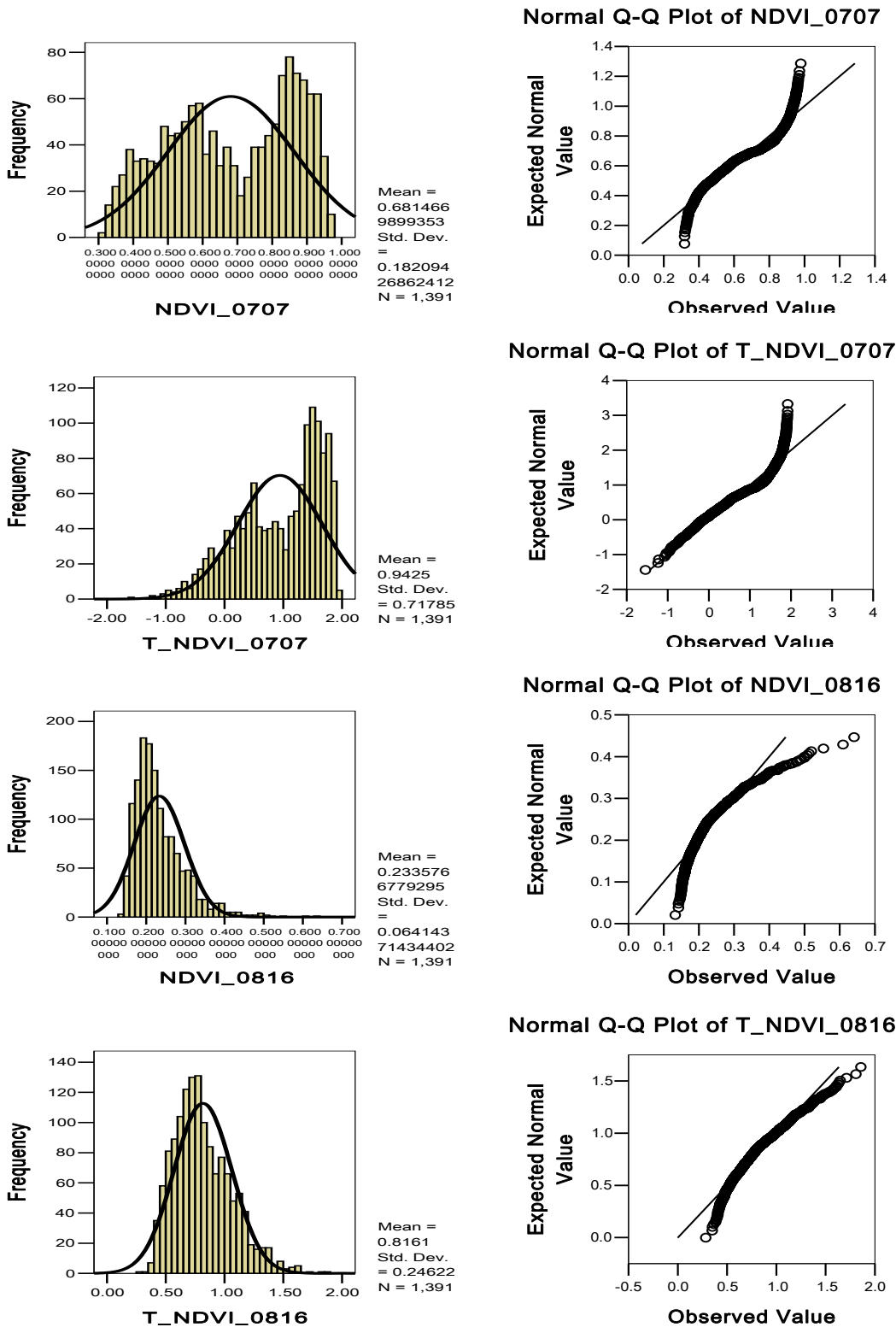
Figure 4-6 Histogram and Q-Q plot of atmospherically corrected 2001 NDVI (NDVI_0707, NDVI_0816) and their transformation (T_NDVI_0707, T_NDVI_0816)

Based on the above analysis and discussions, the standard pre-processing procedure for crop yield estimation modeling is established for this study. The procedure includes the following steps: 1) applying atmospheric correction using the ATCOR2 procedure to the digital images, 2) transforming the NDVI data derived from the above corrected images, and 3) masking out road, field edge and fallow areas. For 1998, the NDVI threshold for fallow masking was set at 0.4 based on the NDVI data of July 23rd. For 2001, it is set to 0.3 based on NDVI of July 7th.

4.3.2 Multiple regression analysis for yield estimation

As introduced in Chapter 3, the yield estimation in this study is based on a multiple regression analysis. The dependent variable is the farm reported yield of each quarter-section, and the primary independent variable is the transformed NDVI data. To improve the explanatory power of the regression model, several additional independent variables are included in the regression model based on the analysis of regression residuals. Two numerical variables and four binary variables are considered in the regression model specification for individual datasets, and tests are conducted to identify the suitable regression models for each year.

4.3.2.1 Linear regression analysis of cereal yield estimation for 1998

An initial regression model is established for estimating the yields of cereal crops. The model is then assessed and refined to generate an effective model. As presented in table 4-11, the initial model includes the log-transformed NDVI data. The transformed NDVI from both dates are employed. The geographic coordinates of the centroid of each quarter-section are also included to account for spatial correlation of the crop yields. Recognizing that the variation in soil types may contribute to the variation in crop growth,

two binary variables are also included in the initial model. One binary variable is included in the model to account for the variation in irrigation. The results of the initial regression analysis are presented in Table 4-11.

Table 4-11 Results of the initial regression model testing for 1998

Regression coefficients	Standardized Beta coefficients	T-statistics	Significance
(Constant)		2.716	0.007
T_NDVI_0504	-0.012	-0.525	0.599
T_NDVI_0723	-0.424	-20.155	0.000
Longitude	0.079	1.757	0.079
Latitude	-0.055	-2.112	0.035
Irrigation district	0.337	14.075	0.000
Black soil	0.061	1.853	0.064
Brown soil	0.061	1.920	0.055
Model F-statistics	131.531		
Model significance	0.000		
R^2	0.341		
Adjusted R^2	0.339		

The model is statistically significant at a 99% confidence level. It explains 34.1% of variation in the yield of cereal crops. While all independent variables are associated with the expected sign, several independent variables are not statistically significant. In particular, the log-transformed NDVI variable from the May 4th imagery is not significant in the model. This may be explained that the image is taken before the summer growing season, and hence do not show sufficient information on the variation of crop growth. The independent variables longitude and soil types do not show high significance values in the model either. By examining the regional soil distribution, it is found that the three soil zones in the study area are distributed essentially parallel from west to east. The longitude variable may be sufficient to account for spatial variation in soil types.

Based on the above analysis, the initial regression model was adjusted by excluding the log-transformed NDVI of the May 4th and soil zone binary variables. The results of the adjusted regression analysis are shown in Table 4-12. The model is

statistically significant at the 99% confidence level. The model explains 33.7% of the variation in cereal crop yield. In the regression, the independent variable latitude is not significant. Since year 1998 was a relatively wet year, the yields of cereal crops may have not varied significantly from south to north in the study area.

Table 4-12 Results of the adjusted regression model testing for 1998:

Regression Coefficients	Standardized Beta Coefficients	t-statistics	Significance
(Constant)		5.908	0.000
T_NDVI_0723	-0.425	-20.863	0.000
Irrigation district	0.344	14.564	0.000
Longitude	0.092	3.742	0.000
Latitude	-0.034	-1.364	0.173
Model F-statistics	226.088		
Model significance.	0.000		
R^2	0.337		
Adjusted R^2	0.335		

The adjusted model is then further refined by excluding the independent variable latitude. The final regression for estimating the 1998 cereal crop yields includes three impendent variables, i.e., the log-transformed NDVI from the July 23rd imagery, the binary variable of irrigation district, and longitude. The results of the final model are given in Table 4-13. The model is statistically significant at the 99% confidence level. All of the coefficients are statistically significant, and are with expected signs. The derived model explains 33.6% of the variation in cereal crops (R^2=0.336). While the R^2 value is not very high, considering the large sample size (N=1785), it is acceptable. This model is used as the final model for estimating the 1998 cereal crop yield (see Equation 4-7). The crop yield estimates and associated yield map are presented later for comparison of 1998, 1999, and 2001 estimations.

$$Y = 12312.182 - 424.582 \times T\_NDVI\_072\ 3 + 95.55 \times Longitude$$
$$+ 311.359 \times Irri\_dis$$

(4-7)

Table 4-13 Results of the final regression model for 1998

Regression Coefficients	Standardized Beta Coefficients	t-statistics	Significance
(Constant)		6.105	0.000
T_NDVI_0723	-0.427	-20.964	0.000
Irrigation district	0.111	5.379	0.000
Longitude	0.327	16.190	0.000
Model F-statistics	300.684		
Model significance	0.000		
R^2	0.336		
Adjusted R^2	0.335		

4.3.2.2 Linear regression analysis of cereal yield estimation for 1999

The analytical procedure discussed in estimating the 1998 crop yield is repeated here for establishing the 1999 crop yield. Six independent variables are included in the initial regression analysis. The model is statistically significant at the 99% confidence level. It explains 46.9% of the 1999 crop yield variation. The results of the initial model are shown in Table 4-14.

Table 4-14 Results of the initial regression model testing for 1999

Regression Coefficients	Standardized Beta Coefficients	t-statistics	Significance
(Constant)		3.716	0.000
T_NDVI_0523	0.109	5.577	0.000
T_NDVI_0803	-0.532	-22.471	0.000
Longitude	0.042	1.003	0.316
Latitude	-0.217	-7.804	0.000
Irrigation district	0.377	16.089	0.000
Black	0.052	1.637	0.102
Brown	0.040	1.327	0.185
Model F-statistics	202.210		
Model significance	0.000		
R^2	0.469		
Adjusted R^2	0.467		

As indicated in Table 4-14, variable longitude, and two binary soil zones variables are not statistically significant in the model.

By excluding the longitude variable and binary soil zones variables from the initial regression model, the final regression model for estimating the 1999 crop yield is

derived. The results of the model are presented in Table 4-15. The log-transformed NDVI for both dates, the latitude coordinate, and the binary variable for irrigation district are used as independent variables. The model is statistically significant, and it accounts for 46.6% of the crop variation with an R^2 value slightly higher than that of the 1998 model. All four independent variables are statistically significant with the expected signs. The regression model used to estimate the 1999 crop yield is given as Equation 4-8.

$$
\begin{aligned}
Y = {}& 12541.280 + 269.846 \times T\_NDVI\_0523 \\
& - 350.340 \times T\_NDVI\_0803 - 224.429 \times Latitude \\
& + 429.465 \times Irri\_dis
\end{aligned}
\tag{4-8}
$$

Table 4-15 Results of the final regression model for 1999

Regression Coefficients	Standardized Beta Coefficients	t-statistics	Significance
(Constant)		10.583	0.000
T_NDVI_0523	0.112	5.776	0.000
T_NDVI_0803	-0.538	-23.624	0.000
Latitude	-0.231	-9.498	0.000
Irrigation district	0.401	19.732	0.000
Model F-statistics	349.336		
Model significance	0.000		
R^2	0.466		
Adjusted R^2	0.464		

4.3.2.3 Linear regression analysis of cereal yield estimation for 2001

The initial regression analysis for the 2001 crop yield estimation also includes six independent variables. The results of the initial regression are shown in Table 4-16. The model is statistically significant at the 99% confidence level. It explains 69% of the crop yield variation in the study area. While all of coefficients are associated with the expected sign, three independent variables are not statistically significant in the regression model, including the log-transformed NDVI from the August 16th imagery, longitude and binary

variable of brown soil zone. The insignificant constant coefficient indicates that this

model is not stable, and consequently it is not suitable for crop yield estimation.

Table 4-16 Results of the initial regression model testing for 2001

Regression Coefficients	Standardized Beta Coefficients	t-statistics	Significance.
(Constant)		0.707	0.480
T_NDVI_0707	-0.844	-38.942	0.000
T_NDVI_0816	0.037	1.886	0.059
Longitude	-0.029	-0.900	0.368
Latitude	-0.095	-4.598	0.000
Irrigation district	0.153	8.170	0.000
black	-0.118	-4.605	0.000
brown	0.013	0.567	0.571
Model F-statistics	440.640		
Model significance	0.000		
R^2	0.690		
Adjusted R^2	0.689		

Table 4-17 Results of the regression model testing for 2001

Regression Coefficients	Standardized Beta Coefficients	t-statistics	Significance.
(Constant)		5.654	0.000
T_NDVI_0707	-0.856	-40.736	0.000
Latitude	-0.085	-4.262	0.000
Irrigation district	0.142	7.993	0.000
black	-0.092	-4.266	0.000
Model F statistics	768.303		
Model significance	0.000		
R^2	0.689		
Adjusted R^2	0.688		

The initial model is adjusted to include four variables, and the results of

regression analysis are presented in Table 4-17. The model is statistically significant at

the 99% confidence level. It explains 68.9% of the variation of dependent variable. All

three independent variables are significant with expected signs. This model is used to

estimate yield of the 2001 cereal crops (see Equation 4.9).

$$
\begin{aligned}
Y = \ & 4990.551 \ - 568.151 \ \times T\_NDVI\_070 \quad 7 \\
& - 75.136 \ \times Latitude \ + 159.439 \times Irri\_dis \\
& - 91.877 \ \times black
\end{aligned}
\tag{4.9}
$$

4.3.2.4 Cereal crop yield estimation model for three years

In order to ensure the quality of crop yield estimates, residuals of the regression models developed above are scrutinized further using histograms and Q-Q plots (see Figures 4-7, 4-8 and 4-9). As indicated in Figures 4-7, 4-8 and 4-9, the regression residuals of the 1998, 1999, and 2001 yield estimation models are normally distributed, although there are a few outliers in the residual data. The residual distribution results not only validate that the data meet the normality assumptions in the regression exercise, but also indicate the models have accounted for spatial dependency of crop yields in the study area.
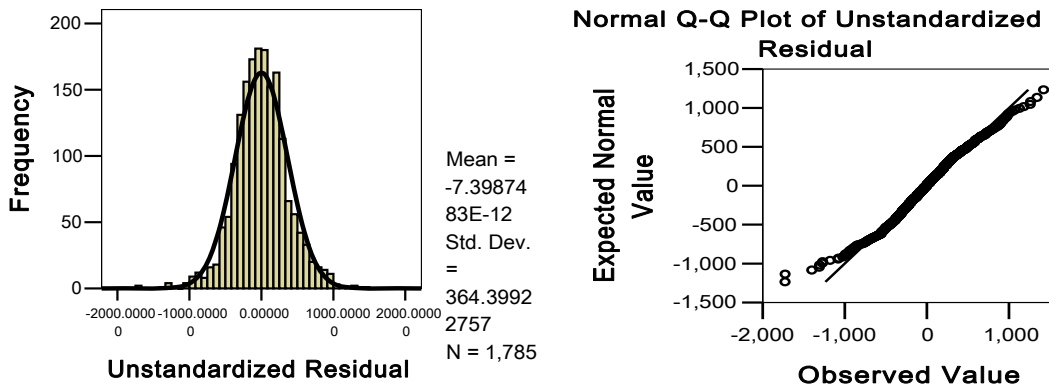
Figure 4-7 Histogram and Q-Q plot of 1998 regression model residuals
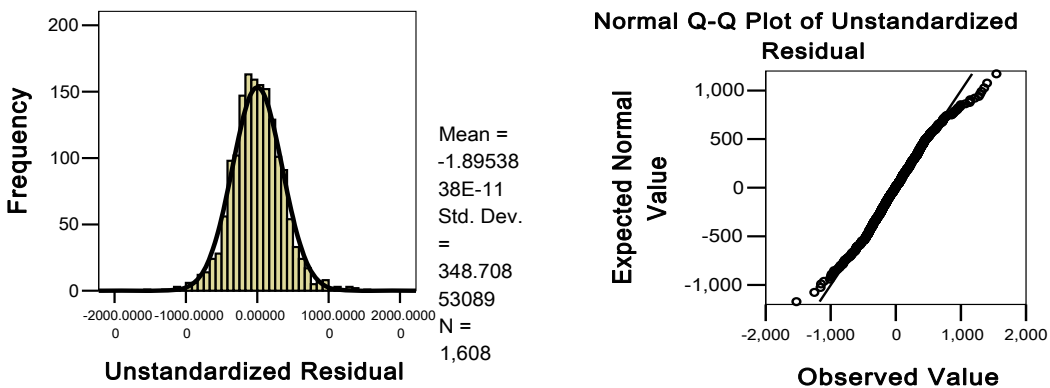
Figure 4-8 Histogram and Q-Q plot of 1999 regression model residuals
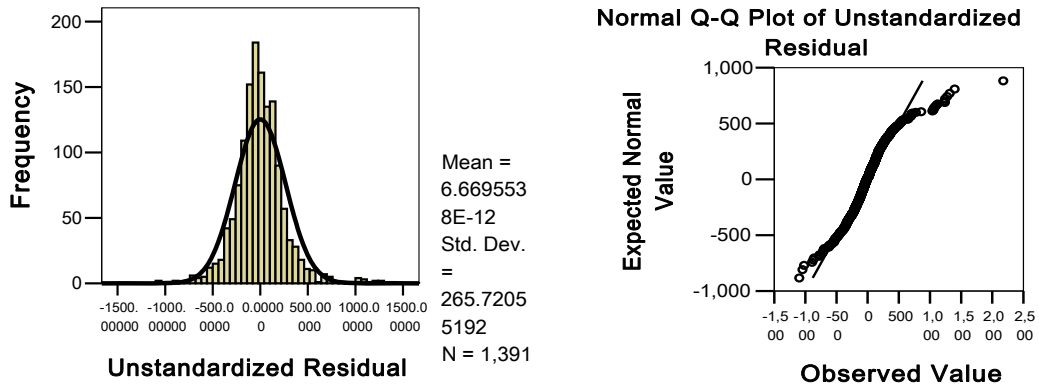
Figure 4-9 Histogram and Q-Q plot of 1998 regression model residuals

The estimates of cereal crop yields for 1998, 1999, and 2001 based on the regression models are presented as maps in Figures 4-10, 4-11 and 4-12. The descriptive statistics for the estimated yield are summarized in Tables 4-18, 4-19 and 4-20
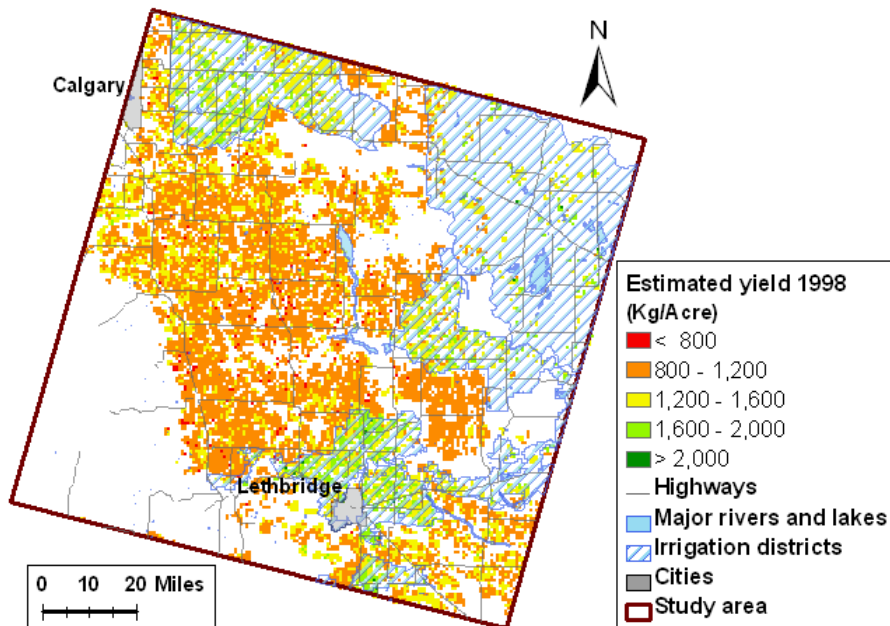
Figure 4-10 Spatial distribution of 1998 estimated cereal crop yield

Table 4-18 Descriptive statistics of 1998 estimated cereal crop yield

Yield range (kg /acre)	Percentage of area	Mean (kg /acre)
< 800	2.26%	762
800 - 1200	46.45%	1026
1200 - 1600	40.02%	1363
1600 - 2000	10.48%	1743
> 2000	0.80%	2084
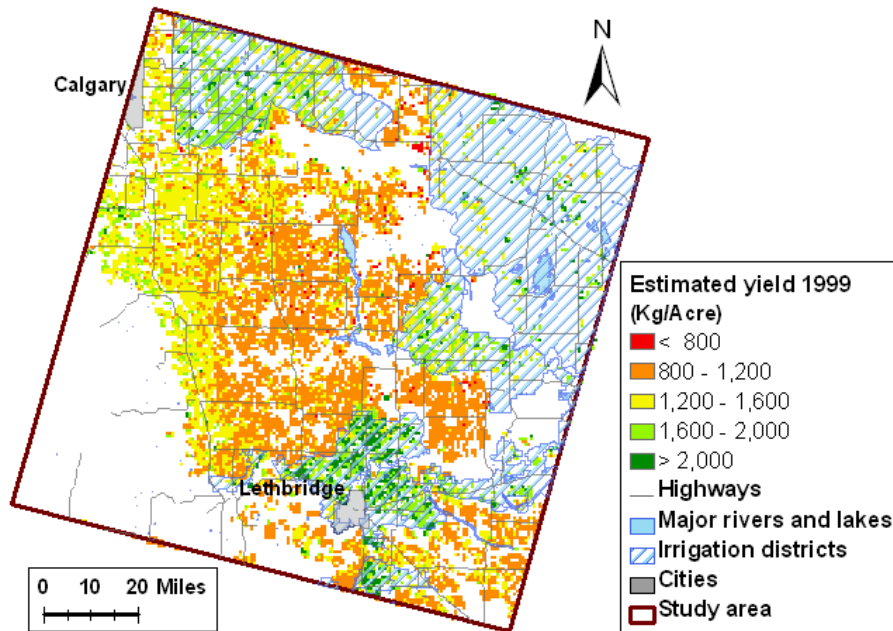
Figure 4-11 Spatial distribution of 1999 estimated cereal crop yield

Table 4-19 Descriptive statistics of 1999 estimated cereal crop yield

Yield range (kg/acre)	Percentage of area	Mean (kg /acre)
< 800	1.10%	747
800 - 1200	38.27%	1047
1200 - 1600	37.45%	1374
1600 - 2000	16.15%	1771
> 2000	7.04%	2245
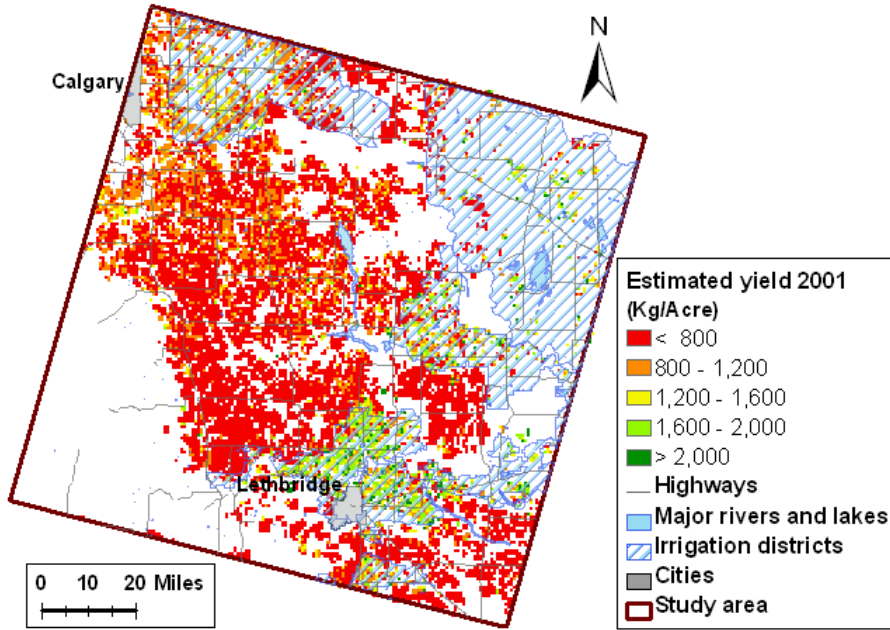
Figure 4-12 Spatial distribution of 2001 estimated cereal crop yield

Table 4-20 Descriptive statistics of 2001 estimated cereal crop yield

Yield range (kg/acre)	Percentage of area	Mean (kg /acre)
< 800	57.57%	491
800 - 1200	23.57%	977
1200 - 1600	10.31%	1371
1600 - 2000	4.85%	1777
> 2000	3.70%	2375

As presented in the Figures 4-10, 4-11, 1-12, and Tables 4-18, 4-19, 4-20, the overall estimated yields of 1998 and 1999 are similar. The majority of the mapped area has a cereal crop yield of 800 to 1600 kg/acre. There were more areas associated with a higher yield (above 1600 kg/acre) in 1999 than those in 1998. The estimated yield in 2001 was obviously lower than that in 1998 and 1999. Over 50% of the mapped area in 2001 had a yield less than 800 kg/acre. As indicated in Figures 4-10, 4-11, and 4-12, most of the areas in the Southern irrigation districts maintained a high yield of above 1600 kg/acre in all three years.

The average yield for the three years are calculated and mapped in Figure 4-13. Table 4-21 presents the descriptive statistics of estimated average yields over three years.

About 59.3% of the cereal crop field had an average yield between 800 to 1200 kg/acre. There were 10.89% of the cereal crop fields that produce an average yield of more than 1600 kg/acre. Only 7.87% of the cereal crop fields had an average yield of less than 800 kg/acre. As expected, the irrigated regions were normally associated with higher average yields in the study area in the selected years.
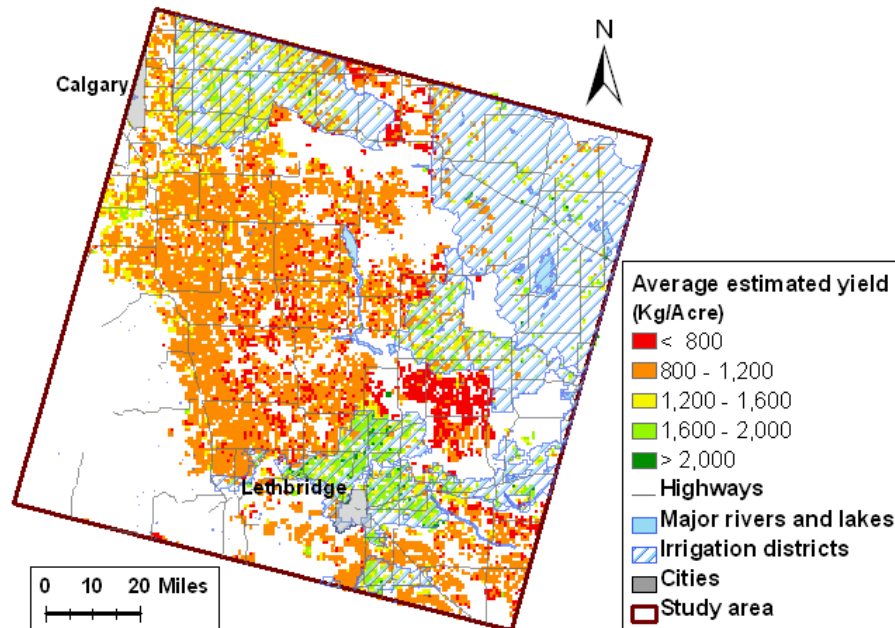
Figure 4-13 Spatial distribution of average cereal crop yield (1998, 1999, and 2001)

Table 4-21 Descriptive statistics of average cereal crop yield (1998, 1999, and 2001)

Yield range (kg/acre)	Percentage of area	Mean (kg/acre)
< 800	7.87%	739
800 - 1200	59.30%	990
1200 - 1600	21.94%	1364
1600 - 2000	8.69%	1763
> 2000	2.20%	2143

4.4   Chapter Summary

Based on analyzing the imagery from 1999, an image classification framework is developed for this study. Using the combined imagery from two dates in a grow season for crop classification provides better results than a single date imagery. The training

datasets with the STIPZ grouping perform the image classification better than that without the STIPZ grouping. Post-classification methods including sieving and clumping are helpful in terms of removing isolated pixels and increasing classification accuracy. Crops that are spectrally similar are grouped as one class in this study, and different types of cereal crops are not separable using our classification approach. The developed classification framework is applied to the 1998 and 2001 imageries. The overall classification accuracies are 86.4% (1998), 83.7% (1999), and 81.0% (2001). Because the cereal crop yields are used as a measure of agricultural wellbeing in the following agricultural vulnerability assessment, a relatively high classification user accuracy of cereal crop class is needed. The user accuracies for the cereal crop class are 94.7% (1998), 92.7% (1999), and 89.8% (2001).

The NDVI value of the image areas classified as cereal crops is employed as a primary independent variable for yield estimation in the regression analysis. Roads, field edges and fallow areas are masked off. The log-transformed NDVI from the atmospherically corrected image shows an advantage in yield estimation.

Multiple regression analyses are used for yield estimation. Variables such as field location, irrigation capacity and soil type are considered in the regression models in addition to the NDVI value. Non-significant variables are excluded step by step. Final yield estimation models for three years are all statistically significant at a 99% confidence level. All independent variables in the models are also significant. The R^2 values of the final yield estimation models are 0.336 (1998), 0.466 (1999), and 0.689 (2001). The regression residuals for all three models are normally distributed. These models are directly employed to generate yield maps of cereal crops at the image pixel level. These

yield estimates will be employed directly as a measure of agricultural wellbeing for assessing agricultural vulnerability in the region.

CHAPTER 5 VULNERABILITY ASSESSMENT

5.1   Introduction

In this chapter, the empirical results on agricultural vulnerability to different levels of drought conditions are presented. The assessment is based upon the methods described in Chapter 3. The farm reported yields of cereal crops at a quarter-section level and the estimated yield of cereal crops from the remotely sensed imagery at a 30 meter by 30 meter pixel level are employed as the main data sources to measure agricultural well-being in the study area. The expected agricultural vulnerability to a possible future drought condition and its spatial distribution are also described based on the expected increasing drought frequency.

This chapter is divided into three main sections. In the first section, components of the vulnerability function and agricultural vulnerability to different levels of droughts are assessed based on the farm reported yields of cereal crops at a quarter-section level. In the second section, agricultural vulnerability is assessed based on the yield estimates from the remotely sensed imagery and the sensitivity estimates using the quarter-section yield data. The spatial patterns of agricultural vulnerability are presented in maps. In the third section, the expected agricultural vulnerability to an increasing drought propensity in the study area is assessed.

5.2   Agricultural Vulnerability to Drought at the Quarter-section Level

5.2.1   Estimated sensitivity

Agricultural sensitivity is estimated for the point data at the centroid locations of the valid quarter-sections using the method described in Chapter 3. The point data is interpolated to generate a continuous surface representation of agricultural sensitivity.

The spatial distribution of sensitivity is presented in Figure 5-1. The descriptive statistics for each sensitivity class are presented in Table 5-1.
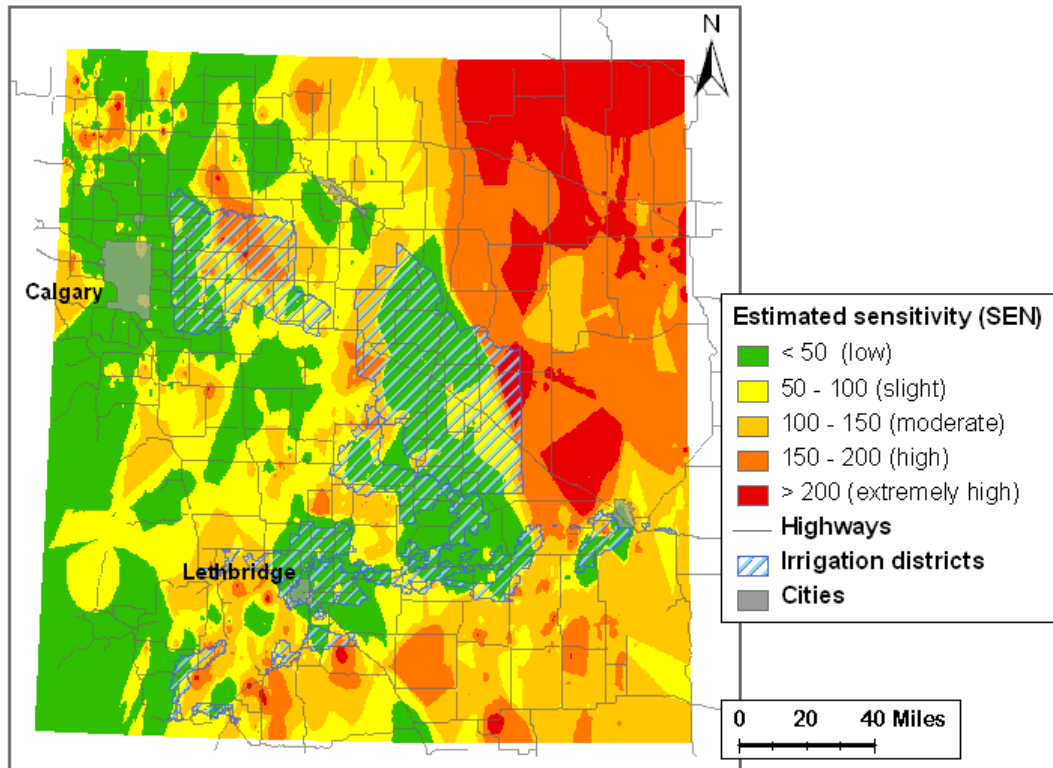
Figure 5-1 Spatial distribution of *SEN:* estimated agricultural sensitivity to meteorological drought in growing season

Table 5-1 Descriptive statistics for *SEN* classes: estimated agricultural sensitivity to meteorological drought in growing season

SEN classes	*SEN* value	Percentage coverage	Mean	Standard deviation
Low	< 50	30.06%	-0.15	42.68
Slight	50 - 100	22.29%	75.70	14.87
Moderate	100 - 150	22.45%	122.75	13.82
High	150 - 200	16.64%	172.76	14.81
Extremely high	> 200	8.57%	219.01	11.98

Over 30% of the study area has a sensitivity value less than 50. Most of the areas with a low sensitivity are located within or close to irrigation districts (see Figure 5-1). Nevertheless, there are some areas within irrigation districts that are estimated more sensitive than it is expected. This is because not all agricultural land within irrigation

districts is actually irrigated every year. For example, the total area of the irrigation district east of Calgary (Western Irrigation District) is about half million acres, within which about 95,000 acres are contracted on the water role and only less than 55,000 acres actually requested for irrigation service in 2004 (WID, 2004). The southwest corner of the study area also has a low value. This is mostly non-agricultural areas with mountains and hills. Slight and moderate sensitive areas are at central longitude areas and the southeast of the study area. These two classes cover about 44% of the study area. Most of the central-east and northeast areas are classified as having a high to extremely high sensitivity. About 9% of the study area is associated with an extremely high sensitivity value.

A small portion of the study area is associated with a negative sensitivity value. In these areas, agricultural production is more sensitive to the extremely wet condition rather than to the extreme dry condition might be. Due to the orientation and scope of this study, agricultural vulnerability to the extremely wet condition will not be discussed.

5.2.2   Vulnerability without exposure

Using Equation 3-1, agricultural vulnerability without exposure (V_{NEXPi}) is calculated for three selected years (1998, 1999 and 2001). Because the yield data from AFSC is confidential, spatial distribution of W_i and W_0 is not presented. The interpolated surface representations of V_{NEXPi} for the three years are mapped in Figures 5-2, 5-3, and 5-4.

A three-year average V_{NEXP} value is calculated based on the interpolated V_{NEXPi} values in the selected years (see Equation 3-2), and its spatial distribution is presented in Figure 5-5. V_{NEXP} is classified based on the classification ranges used for classifying the

sensitivity data. The descriptive statistics of V_{NEXPi} and V_{NEXP} classes are presented

accordingly in Tables 5-2, 5-3, 5-4 and 5-5.
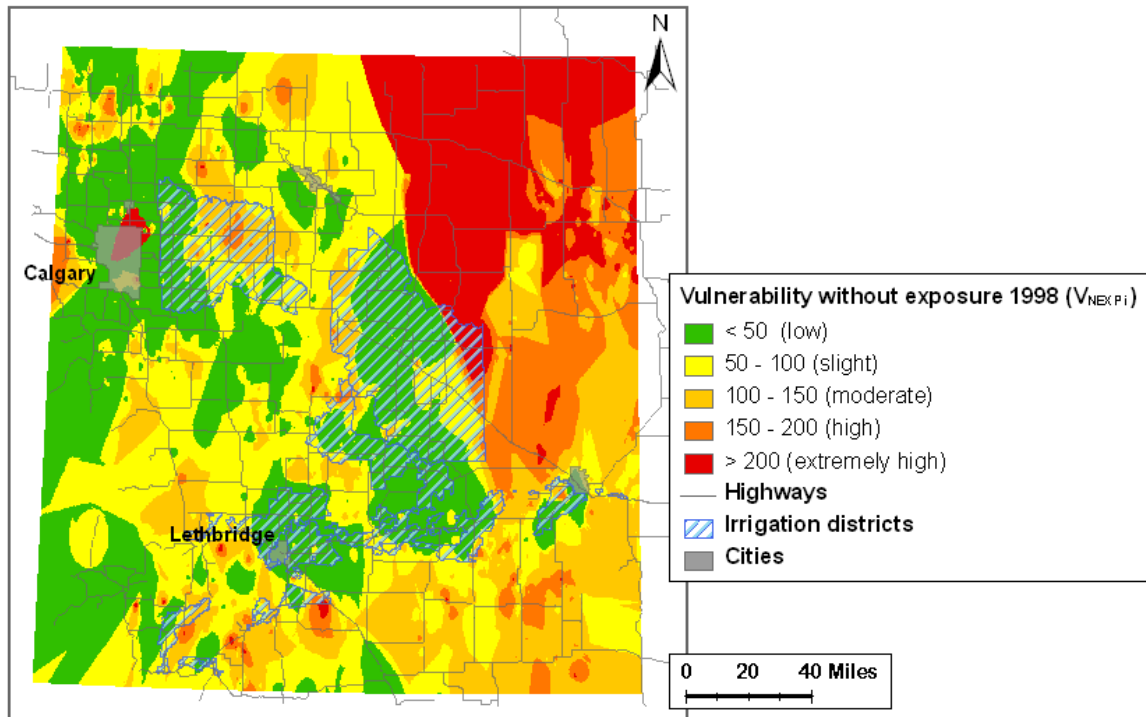
Figure 5-2 Spatial distribution of V_{NEXPi}: agricultural vulnerability to meteorological drought in 1998 growing season, without considering exposure

Table 5-2 Descriptive statistics for V_{NEXPi} classes: agricultural vulnerability to meteorological drought in 1998 growing season, without considering exposure

V_{NEXPi} Classes	V_{NEXPi} value	Percentage coverage	Mean	Standard deviation
Low	< 50	29.30%	-4.07	48.08
Slight	50 - 100	28.01%	76.31	13.99
Moderate	100 - 150	20.44%	122.14	14.32
High	150 - 200	9.26%	171.87	14.40
Extremely high	> 200	12.98%	1191.15	2382.85

As indicated in Figure 5-2 and Table 5-2, the areas with a low to moderate

vulnerability value covered a major part of the study area. In particular, the irrigation

areas tended to be associated with low to moderate vulnerability values. About 13% of

the study area was classified as having an extremely high vulnerability. The area was

mostly located in the northeast part of the study area. In 1998, without considering the exposure factor, the eastern part of the study area tended to be more vulnerable than the western part.
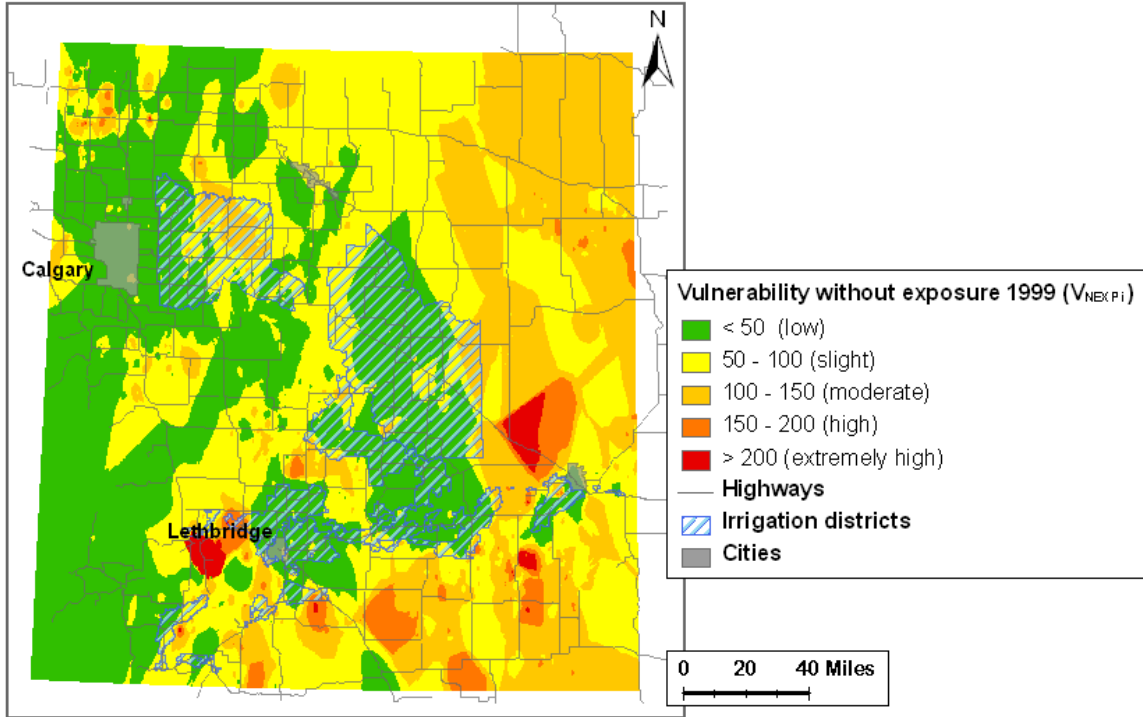
Figure 5-3 Spatial distribution of V_{NEXPi}: agricultural vulnerability to meteorological drought in 1999 growing season, without considering exposure

Table 5-3 Descriptive statistics for V_{NEXPi} classes: agricultural vulnerability to meteorological drought in 1999 growing season, without considering exposure

V_{NEXPi} Classes	V_{NEXPi} value	Percentage coverage	Mean	Standard deviation
Low	< 50	36.66%	-8.48	109.53
Slight	50 - 100	35.33%	76.85	13.56
Moderate	100 - 150	24.14%	118.10	12.11
High	150 - 200	2.99%	169.72	13.92
Extremely high	> 200	0.89%	1033.65	1549.37

It can be seen clearly from Figure 5-3 and in Table 5-3 that the spatial pattern of vulnerability to drought in 1999 was quite similar to that in 1998. Overall, agricultural production in the study area was less vulnerable. About 96% of the study area was

associated with a low, slight or moderate vulnerability. Only 3% of the area was associated with a high vulnerability, and less than 1% of the area had an extremely high vulnerability. The pockets of highly vulnerable areas were scattered in the south and southeast of the study area.
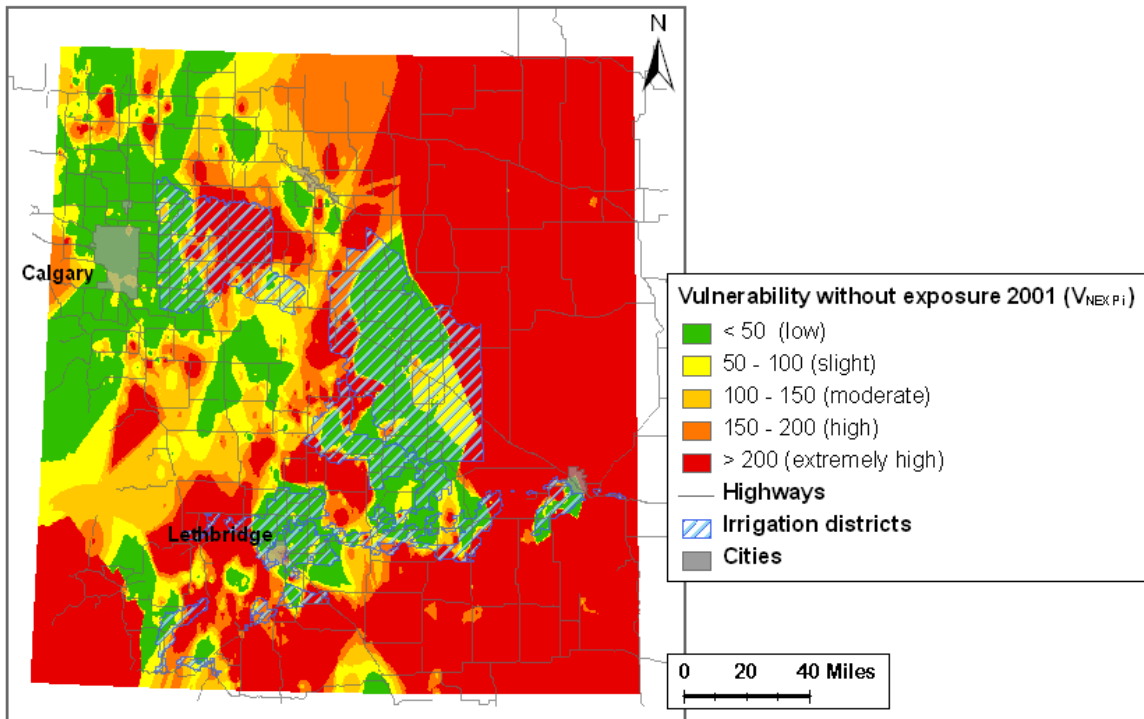
Figure 5-4 Spatial distribution of V_{NEXPi}: agricultural vulnerability to meteorological drought in 2001 growing season, without considering exposure

Table 5-4 Descriptive statistics for V_{NEXPi} classes: agricultural vulnerability to meteorological drought in 2001 growing season, without considering exposure

V_{NEXPi} classes	V_{NEXPi} value	Percentage coverage	Mean	Standard deviation
Low	< 50	20.27%	-7.41	39.82
Slight	50 - 100	9.62%	75.55	14.28
Moderate	100 - 150	10.24%	123.55	14.27
High	150 - 200	9.08%	172.97	13.91
Extremely high	> 200	50.79%	806.77	716.57

Agricultural vulnerability without considering exposure in 2001 is presented in Figure 5-4 and Table 5-4. There was a drastic contrast in the spatial pattern of agricultural

vulnerability between 2001 and 1998 or 1999. For 2001, over 50% of the study area was classified as having an extremely high vulnerability. With an exception for the regions surrounding the City of Calgary and most of the irrigation districts, a large part of the study area was considered to be highly vulnerable. Even some irrigated area in the north was considered as extremely vulnerable (Figure 5-5). About 30% of the study area showed a low to slight vulnerability values (Table 5-5).
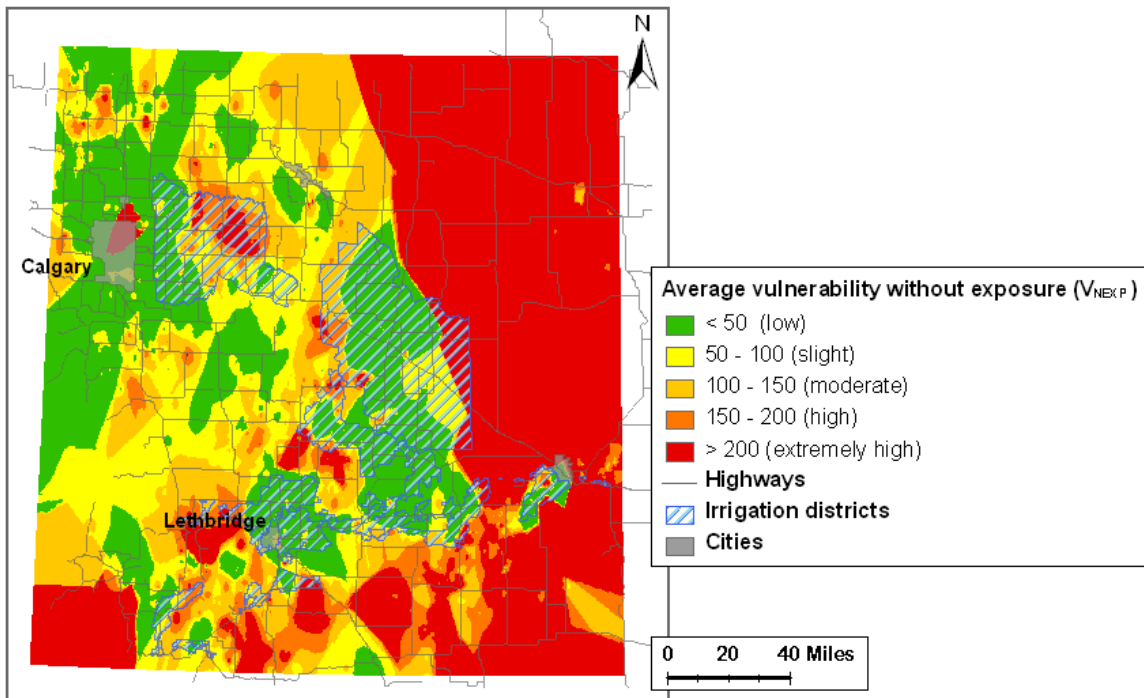
Figure 5-5 Spatial distribution of V_{NEXP}: average agricultural vulnerability to meteorological drought in growing seasons (1998, 1999 and 2001), without considering exposure

Table 5-5 Descriptive statistics for V_{NEXP} classes: average agricultural vulnerability to meteorological drought in growing seasons (1998, 1999, and 2001), without considering exposure

V_{NEXP} classes	V_{NEXP} value	Percentage coverage	Mean	Standard deviation
Low	< 50	23.91%	-12.42	67.46
Slight	50 - 100	16.01%	75.65	14.05
Moderate	100 - 150	16.26%	122.08	14.26
High	150 - 200	6.23%	171.15	14.05
Extremely high	> 200	37.60%	538.54	524.71

Figure 5-5 presents the three-year average vulnerability in the study area based on the vulnerability values in 1998, 1999, and 2001. Overall, across these three years, about 24% of the study area showed a low vulnerability without considering exposure (see Table 5-5). The area was located approximately where a low sensitivity was estimated. Most of the irrigation districts were associated with low vulnerability values. Slight and moderate vulnerability values were found in the areas between the west and the irrigation districts. These two vulnerability classes covered 32.3% of the study area. Most of the eastern part of the study area was classified as extremely highly vulnerable to drought. This area accounted for 37.6% of study area.

5.2.3 Vulnerability with exposure to meteorological drought

As described in Chapter 3, the exposure to the stressor in this study is measured by the proportion of SPI value under or over a harmful level in a concerned period. Assuming that a severely dry condition is harmful to cereal crop production, the exposure is calculated as the proportion of the growing season SPI value less than -1.5 in the period from 1965 to 2004 (EXP_L). This measure describes the long term frequency of the exposure to a severely dry condition. In order to understand the effect of a short term exposure, the proportion of the SPI value less than -1.5 in the period from 1991 to 2004 (EXP_S) is also calculated. Both exposure measures are derived at the quarter-section level. To generate a surface representation of the exposure measures for the entire study are, an IDW interpolator is applied. The interpolated spatial distributions of EXP_L and EXP_S measures are presented in Figures 5-6 and 5-7, and their descriptive statistics are presented in Table 5-6 and 5-7, respectively.
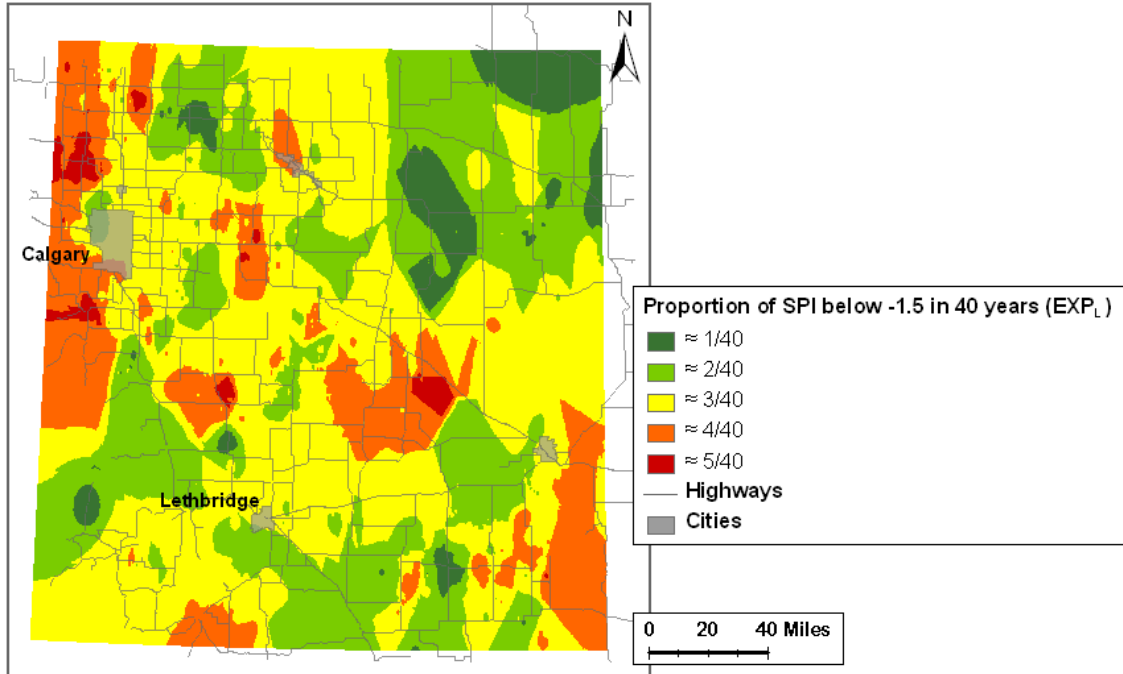
Figure 5-6 Spatial distribution of EXP_L: long-term exposure to severe meteorological drought in growing season, from 1965 to 2004

Table 5-6 Descriptive statistics for EXP_L classes: long-term exposure to severe meteorological drought in growing season, from 1965 to 2004

Occurrence of SPI under -1.5	Percentage coverage	Mean	Standard deviation
≈ 1/40	5.56%	0.0312	0.0039
≈ 2/40	29.87%	0.0515	0.0059
≈ 3/40	46.99%	0.0742	0.0054
≈ 4/40	16.30%	0.0976	0.0054
≈ 5/40	1.28%	0.1173	0.0036

As summarized in Table 5-6, for all the locations in the study area from 1965 to 2004, there was at least one year of severe meteorological drought during the growing season. The severe meteorological drought happened twice for 30% of the study area and three times for 47% of the study area. About 17.5% of the area experienced at least four severe meteorological droughts during the growing season between 1965 and 2004.

Figure 5-7 Spatial distribution of EXP_S: short-term exposure to severe meteorological drought in growing season, from 1991 to 2004

Table 5-7 Descriptive statistics for EXP_S classes: short-term exposure to severe meteorological drought in growing season, from 1991 to 2004

Occurrence of SPI under -1.5	Percentage coverage	Mean	Standard deviation
≈ 0/14	9.36%	0.0104	0.0109
≈ 1/14	34.71%	0.0731	0.0145
≈ 2/14	37.40%	0.1401	0.0146
≈ 3/14	18.52%	0.2082	0.0102

Figure 5-7 and Table 5-7 present the distribution and frequency data of severe meteorological drought over a short and more recent period. Less than 10% of the study area did not experience any severe meteorological drought in the growing season between 1991 and 2004. About 72% of the study area had one or two severely dry growing seasons. There was 18.5% of the area that even experienced severely dry growing season three times over 14 years. The area with the highest frequency of the severely meteorological drought was located mostly in the central-south part of the study area, around Lethbridge.

Based on the exposure data presented above, the vulnerability of cereal crop production to the severe meteorological drought with exposure (V_{EXP}) is estimated. V_{EXPL} and V_{EXPS} values are estimated using EXP_L and EXP_S measures, respectively, that are defined as the exposure factor in Equation 3-3. The three-year average vulnerability map presented in Figure 5-4 is used in estimating V_{EXPL} and V_{EXPS} values. The spatial distributions of V_{EXPL} and V_{EXPS} values are mapped (see Figures 5-8 and 5-9). The descriptive statistics of V_{EXPL} and V_{EXPS} values classes are presented in Tables 5-8 and 5-9.
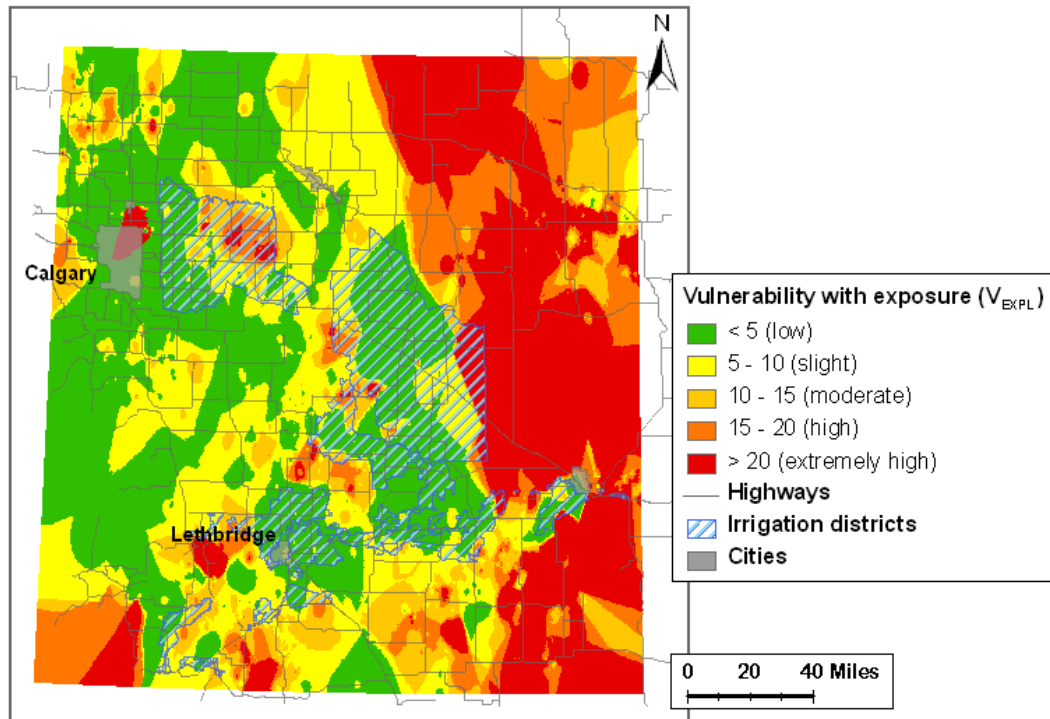
Figure 5-8 Spatial distribution of V_{EXPL}: agricultural vulnerability to severe meteorological drought in growing season, from 1965 to 2004

Table 5-8 Descriptive statistics for V_{EXPL} classes: agricultural vulnerability to severe meteorological drought in growing season, from 1965 to 2004

V_{EXPL} classes	V_{EXPL} value	Percentage coverage	Mean	Standard deviation
Low	< 5	32.26%	0.26	4.83
Slight	5 - 10	22.34%	7.33	1.35
Moderate	10 - 15	11.23%	12.34	1.48
High	15 - 20	11.52%	17.31	1.36
Extremely high	> 20	22.65%	42.81	39.02

The overall pattern of agricultural vulnerability to the severe drought over a long term was uneven in the study area. From the west to the east, agricultural vulnerability increased gradually. Most of the eastern part of the study area was associated with a very high V_{EXPL} value, representing agricultural sectors which were extremely vulnerable (Figure 5-8). In total, about 22.65% of the study area was associated with an extremely high vulnerability index value (Table 5-8).

In the central part of the study area, particularly towards the south-central area, there were pocket areas where crop production tended to be highly to extremely highly vulnerable to severe drought (Figure 5-9). About 34% of the study area had a slight to moderate vulnerability index value. The low vulnerability areas were essentially associated with a low sensitivity value (see Figure 5-9). Overall, about a third of the study area had a low vulnerability value.

Figure 5-9 Spatial distribution of V_{EXPS}: agricultural vulnerability to severe meteorological drought in growing season, from 1991 to 2004

Table 5-9 Descriptive statistics for V_{EXPS} classes: agricultural vulnerability to severe meteorological drought in growing season, from 1991 to 2004

V_{EXPS} classes	V_{EXPS} value	Percentage coverage	Mean	Standard deviation
Low	< 5	27.84%	-1.97	9.01
Slight	5 - 10	12.75%	7.70	1.45
Moderate	10 - 15	13.66%	12.38	1.42
High	15 - 20	10.58%	17.24	1.42
Extremely high	> 20	35.17%	44.95	34.01

Agricultural vulnerability to drought over a short run from 1991 to 2004 is presented in Figure 5-9 and Table 5-9. Most of the low sensitivity areas (Figure 5-1 and Table 5-1) were associated with a low agricultural vulnerability to the severe meteorological drought from 1991 to 2004. They were mostly located in the northwest of the study area. The areas covered by a slight and moderate vulnerability value accounted for 26.4% of the study area. These areas were distributed along a corridor to the east of Calgary running from the northeast to the southwest. More than 35% of the study area was considered as extremely highly vulnerable to the severe drought. The extremely highly vulnerable region was not just confined to the east, but was also clustered in the southern part of the study around Lethbridge.

Considering that a moderate drought might be harmful enough to cause damage in cereal crop production, agricultural vulnerability to the moderate meteorological drought in the study area over a long run is also assessed. The exposure to a moderate meteorological drought condition is calculated as the proportion of the year with the SPI value less than −1 during 1965 to 2004 (EXP_L'). The spatial distribution of EXP_L' is presented in Figure 5-10, and the descriptive statistics of EXP_L' are presented in Table 5-10.
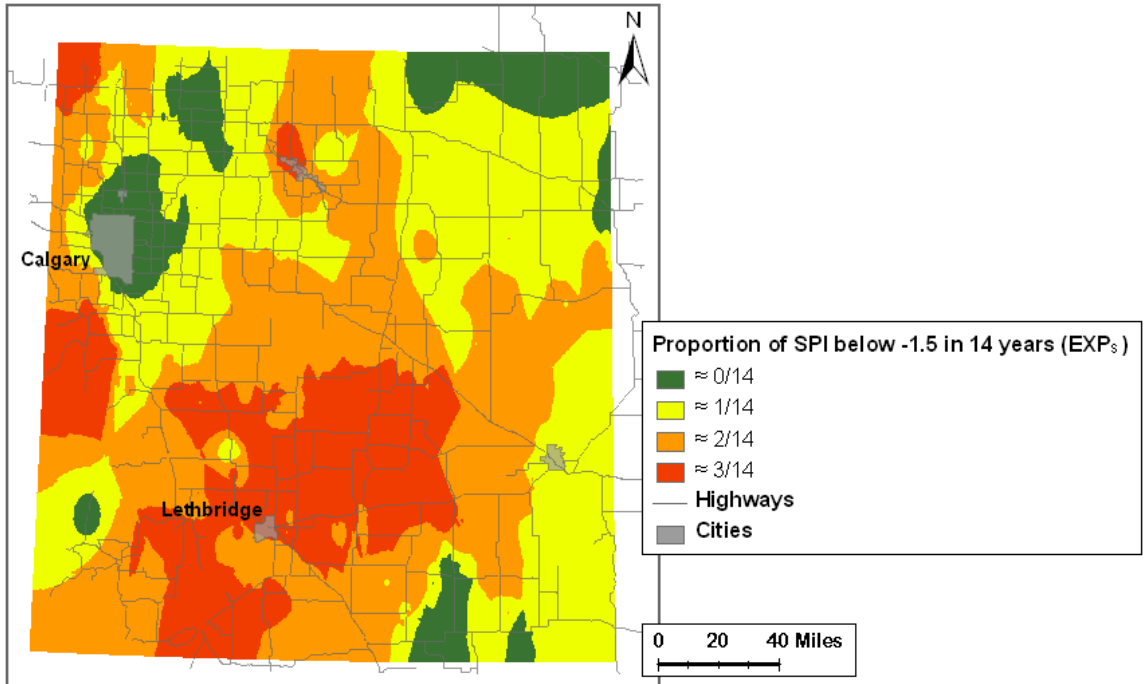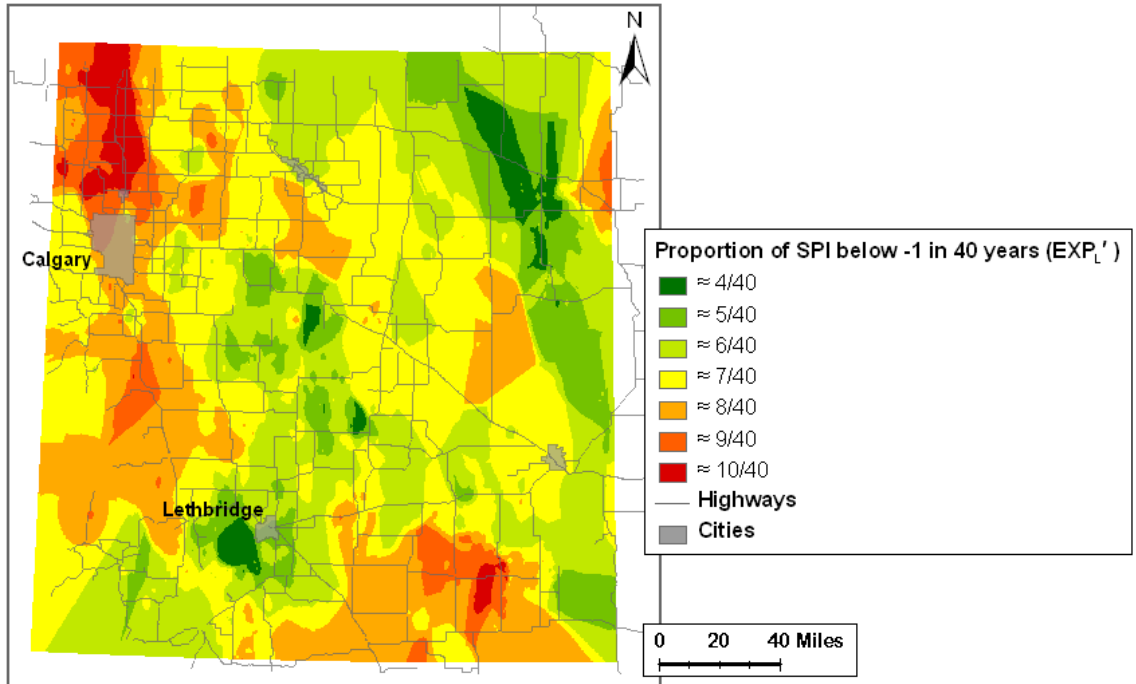
Figure 5-10 Spatial distribution of EXP_L': long-term exposure to moderate meteorological drought in growing season, from 1965 to 2004

Table 5-10 Descriptive statistics for EXP_L' classes: long-term exposure to moderate meteorological drought in growing season, from 1965 to 2004

Occurrence of SPI under -1	Percentage coverage	Mean	Standard deviation
≈ 4/40	2.28%	0.1048	0.0059
≈ 5/40	9.81%	0.1279	0.0060
≈ 6/40	28.21%	0.1510	0.0058
≈ 7/40	32.40%	0.1750	0.0061
≈ 8/40	20.42%	0.1983	0.0055
≈ 9/40	4.82%	0.2224	0.0059
≈ 10/40	2.07%	0.2506	0.0074

As presented in Table 5-10, at least four growing seasons were considered to be moderately dry in the study area during period 1965 to 2004. Over 80% of the study area experienced six to eight moderately dry growing seasons. The highest exposure to the moderate meteorological drought was 10 out of 40 years.

V_{EXPL}' is then estimated using EXP_L' as the exposure factor in Equation 3-3. Again, the three-year average vulnerability value of 1998, 1999, and 2001 is used to

estimate V_{EXP} (see Figure 5-5). The spatial distribution of V_{EXPL}' to the moderate drought is mapped (see Figure 5-11), and its descriptive statistics are presented in Table 5-11. As expected, a very large part of the study area (78.91%) was considered to be extremely vulnerable to a moderate drought condition. Only 13.58% of the study area was associated with a low vulnerability, most of which was associated with the irrigation districts. As indicated by the vulnerability map, even some areas that had low sensitivity values were associated with high to extremely high vulnerability to a moderate drought condition in the study area.
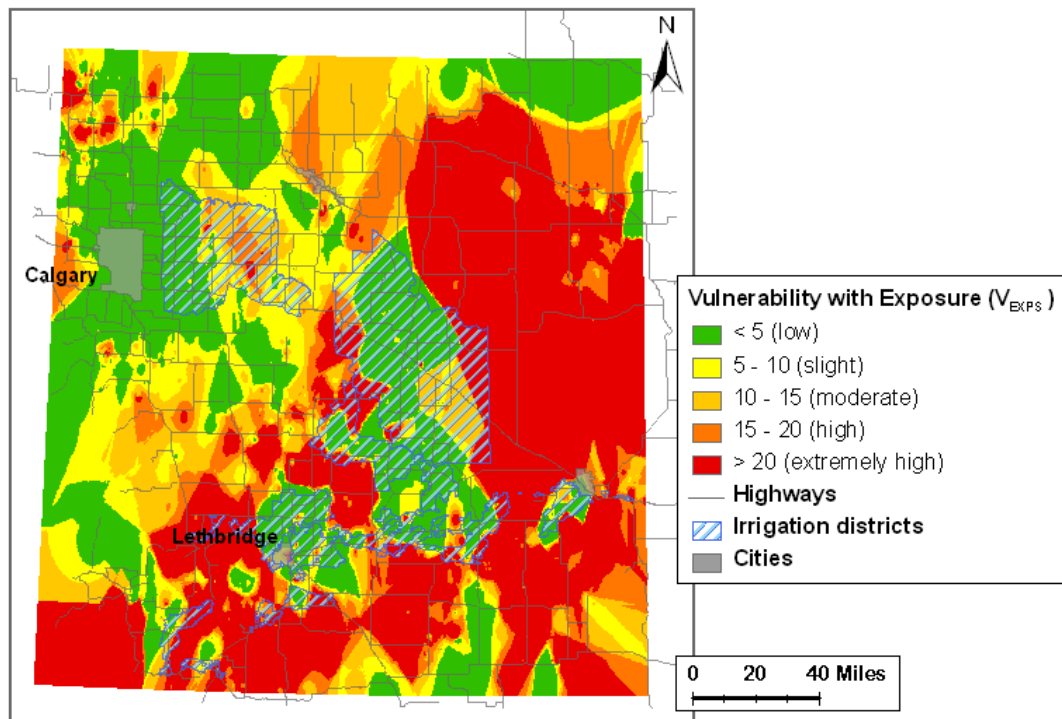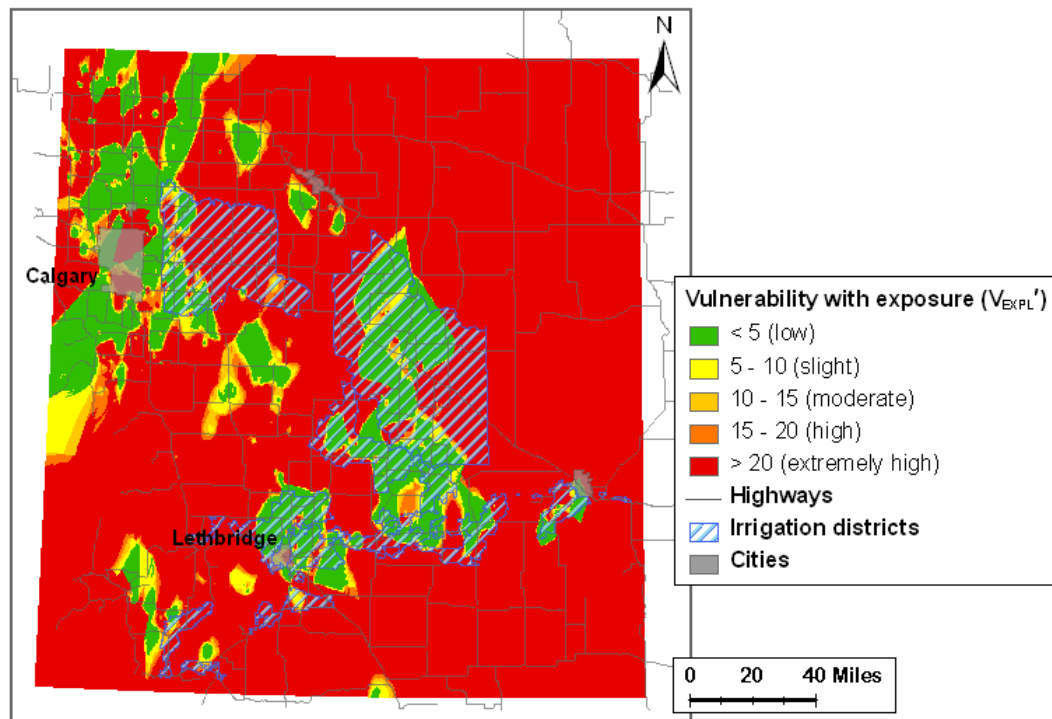

Figure 5-11 Spatial distribution of V_{EXPL}': agricultural vulnerability to moderate meteorological drought in growing season, from 1965 to 2004

Table 5-11 Descriptive statistics for V_{EXPL}' classes: agricultural vulnerability to moderate meteorological drought in growing season, from 1965 to 2004

V_{EXPL}' classes	V_{EXPL}' value	Percentage coverage	Mean	Standard deviation
Low	< 5	13.58%	-22.12	35.10
Slight	5 - 10	2.78%	7.60	1.43
Moderate	10 - 15	2.36%	12.44	1.47
High	15 - 20	2.37%	17.61	1.45
Extremely high	> 20	78.91%	148.59	197.21

5.3 Agricultural Vulnerability to Drought at the Pixel Level

In this section, the areas classified as cereal crop fields in 1998, 1999 and 2001 (see section 4.2) are defined as the study area. The basic spatial unit of the assessment is the agricultural field defined by 30 meter by 30 meter pixel. The vulnerability of cereal crop production to different drought severities is assessed based on the yield estimates derived in Chapter 4. The sensitivity and exposure factors of the vulnerability function estimated above are used here. The cereal crop yield estimated from the remotely sensed data is used to measure agricultural well-being, denoted as W_i in Equation 3-1. The yield data are already presented in Figures 4-10, 4-11, 4-12 and Tables 4-18, 4-19, and 4-20 in the previous chapter. The three-year average of the estimated yields is treated as W_0 in Equation 3-1, and its spatial distribution is already presented in Figure 4-13 and Table 4-21. V_{NEXPi} is estimated for 1998, 1999, and 2001 using Equation 3-1. Figures 5-12, 5-13, and 5-14 present the spatial distributions of V_{NEXPi} for each year, respectively. A three-year V_{NEXP} average is calculated based on Equation 3-2, and its spatial distribution is mapped in Figure 5-15. V_{NEXPi} and V_{NEXP} are classified using the same classification ranges as those used for classifying the sensitivity data. The descriptive statistics of V_{NEXPi} and V_{NEXP} classes are presented in Tables 5-12, 5-13, 5-14 and 5-15.

5.3.1   Agricultural vulnerability to drought without considering exposure

Figure 5-12 Spatial distribution of V_{NEXPi} at image pixel level: agricultural vulnerability to meteorological drought in 1998 growing season, without considering exposure

Table 5-12 Descriptive statistics for V_{NEXPi} classes at image pixel level: agricultural vulnerability to meteorological drought in 1998 growing season, without considering exposure

V_{NEXPi} classes	V_{NEXPi} value	Percentage coverage	Mean	Standard deviation
Low	< 50	41.07%	1.54	46.34
Slight	50 - 100	40.94%	73.44	13.61
Moderate	100 - 150	14.80%	119.34	13.66
High	150 - 200	2.74%	166.28	12.63
Extremely high	> 200	0.45%	236.70	39.61

As presented in Table 5-12, the total area of the low to slight vulnerability classes in 1998 covered 82% of the study area including the irrigation districts and the main agricultural regions from Calgary to Lethbridge (see Figure 5-12). About 14.8% of the study area was associated with a moderate vulnerability. Only 3.19% of the study area had high to extremely high vulnerability. According to the vulnerability map given in

Figure 5-12, these vulnerable regions were scattered in places where irrigations were not

available.

Figure 5-13 Spatial distribution of V_{NEXPi} at image pixel level: agricultural vulnerability to meteorological drought in 1999 growing season, without considering exposure

Table 5-13 Descriptive statistics for V_{NEXPi} classes at image pixel level: agricultural vulnerability to meteorological drought in 1999 growing season, without considering exposure

V_{NEXPi} classes	V_{NEXPi} value	Percentage coverage	Mean	Standard deviation
Low	< 50	44.89%	6.32	39.46
Slight	50 - 100	41.36%	73.77	13.35
Moderate	100 - 150	11.40%	118.52	13.41
High	150 - 200	2.17%	168.59	12.82
Extremely high	> 200	0.17%	220.13	22.86

The distribution of vulnerability ranges and the spatial pattern of agricultural

vulnerability in 1999 were quite similar to those of 1998. A majority part of the study

area had low to moderate vulnerability. Only 2.34% of the study area was estimated with

a high to extremely high vulnerability (see Figure 5-13 and Table 5-13).

Figure 5-14 Spatial distribution of V_{NEXPi} at image pixel level: agricultural vulnerability to meteorological drought in 2001 growing season, without considering exposure

Table 5-14 Descriptive statistics for V_{NEXPi} classes at image pixel level: agricultural vulnerability to meteorological drought in 2001 growing season, without considering exposure

V_{NEXPi} classes	V_{NEXPi} value	Percentage coverage	Mean	Standard deviation
Low	< 50	30.89%	-15.59	662.41
Slight	50 - 100	18.19%	75.85	14.28
Moderate	100 - 150	17.34%	123.86	14.42
High	150 - 200	12.31%	173.16	14.33
Extremely high	> 200	21.26%	341.73	864.44

The distribution of vulnerability ranges and its spatial pattern in 2001 were significantly different from those in 1998 and 1998. Almost half of the study area was associated with a low vulnerability, most of which was located in the north part of the study area or in the irrigation districts (see Figure 5-14 and Table 5-14). More than half of the study area was associated with a moderate to high or extremely high vulnerability value in 2001. About a third of the study area had high to extremely high vulnerability to

the drought. Most of these areas were in central to Southern part of the region where no

irrigation systems were available (Figure 5-14).

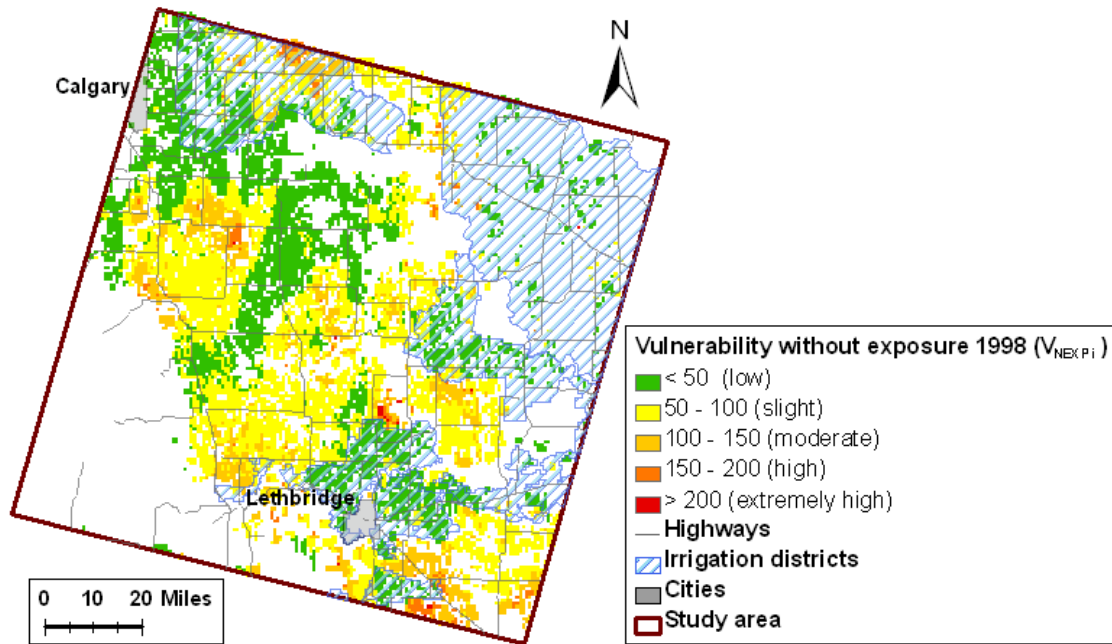
Figure 5-15 Spatial distribution of V_{NEXP} at image pixel level: average agricultural vulnerability to meteorological drought in growing season (1998, 1999 and 2001), without considering exposure

Table 5-15 Descriptive statistics for V_{NEXP} classes at image pixel level: average agricultural vulnerability to meteorological drought in growing season (1998, 1999 and 2001), without considering exposure

V_{NEXP} classes	V_{NEXP} value	Percentage coverage	Mean	Standard deviation
Low	< 50	34.72%	-5.34	223.04
Slight	50 - 100	28.42%	76.27	14.50
Moderate	100 - 150	23.28%	122.88	13.97
High	150 - 200	9.04%	170.34	13.88
Extremely high	> 200	4.54%	276.95	632.45

Assuming that 1998, 1999, and 2001 can be considered as representative crop

growth years, Figure 5-15 presents the spatial pattern of agricultural vulnerability using

the three-year average of V_{NEXP}. On average over the selected three years, almost 35% of

the study area was associated with a low vulnerability without considering exposure. The

area with a low vulnerability was where a low sensitivity was estimated. The areas with a

slight to moderate vulnerability value accounted for 51.7% of the study area. They were mainly located in the central part of the study area. A total of 13.58% of study area was estimated with a high to extremely high vulnerability (see Figure 5-15 and Table 5-15).

5.3.2   Agricultural vulnerability to drought with exposure

The EXP values presented in section 5.2.3 are employed here as the exposure factor for estimating agricultural vulnerability at the image pixel level. The vulnerability of cereal crop production to the severe meteorological drought is estimated using EXP_L and EXP_S as the exposure factor in Equation 3-3, respectively. The three-year average V_{NEXP} is used in calculating the V_{EXPL} and V_{EXPS} values at the pixel level. The spatial distributions of V_{EXPL} and V_{EXPS} values are presented in Figures 5-16 and 5-17. Their descriptive statistics of V_{EXPL} and V_{EXPS} classes are presented in Tables 5-16 and 5-17
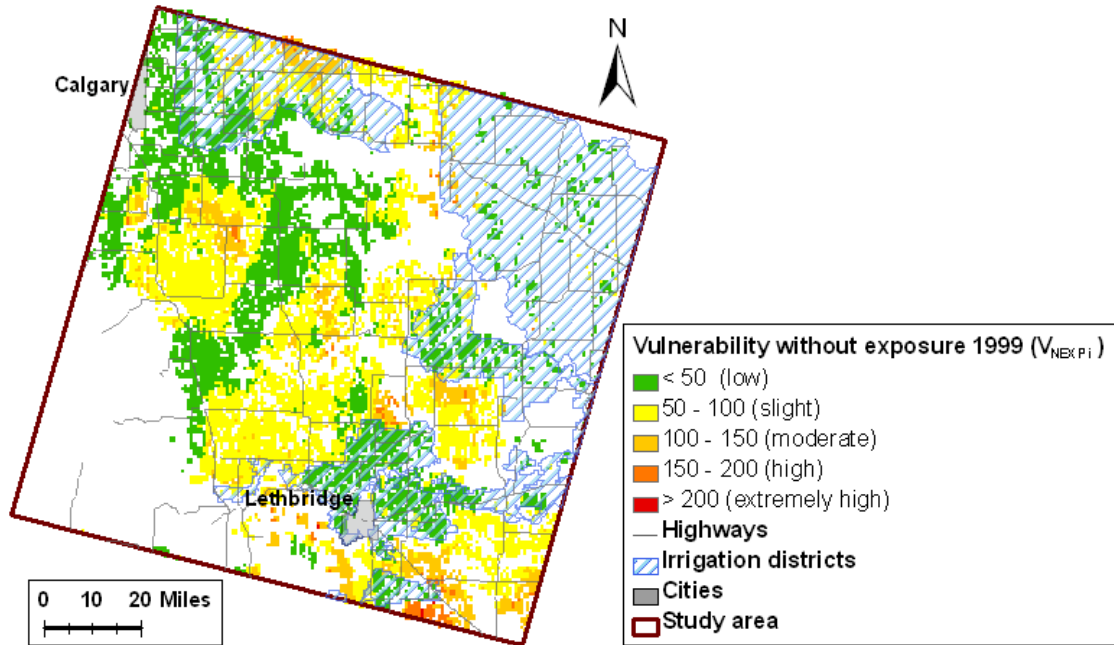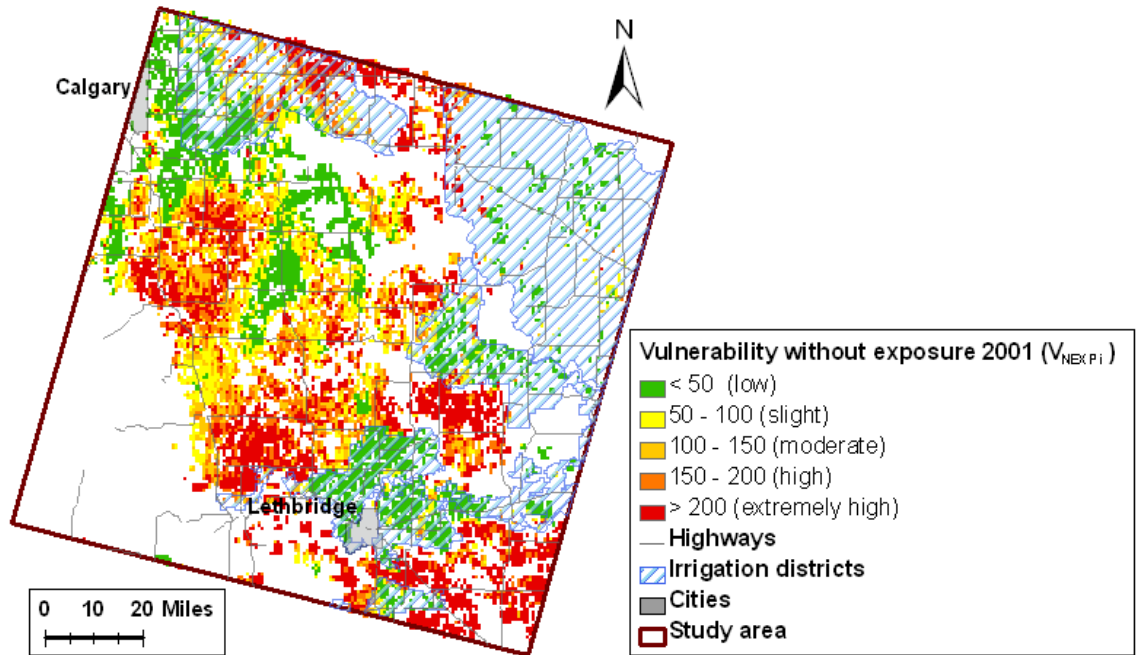

Figure 5-16 Spatial distribution of V_{EXPL} at image pixel level: agricultural vulnerability to severe meteorological drought in growing season, from 1965 to 2004

Table 5-16 Descriptive statistics for V_{EXPL} classes at image pixel level: agricultural vulnerability to severe meteorological drought in growing season, from 1965 to 2004

V_{EXPL} classes	V_{EXPL} value	Percentage coverage	Mean	Standard deviation
Low	< 5	50.92%	0.94	14.84
Slight	5 - 10	35.42%	7.09	1.35
Moderate	10 - 15	10.39%	12.04	1.37
High	15 - 20	2.47%	16.97	1.38
Extremely high	> 20	0.81%	33.92	105.81

Considering the long-term exposure, the vulnerability of cereal crop production to the severe meteorological drought ranged mainly from a low to slight. A total of 86.35% of the study area was with this range (Table 5-16), and the low to slight vulnerable area was associated with the irrigation districts and also in the central area between Calgary and Lethbridge (Figure 5-16), where a low sensitivity value was estimated (see Figure 5-1 and Table 5-1). Only 3.28% of the study area was estimated as highly or extremely highly vulnerable to the severe meteorological drought. The area was mainly located towards the north edge of the study area and in the area to the east of Lethbridge outside of the irrigation districts (Figure 5-16 and Table 5-16). About 10.4% of the study area had a moderate vulnerability index value.
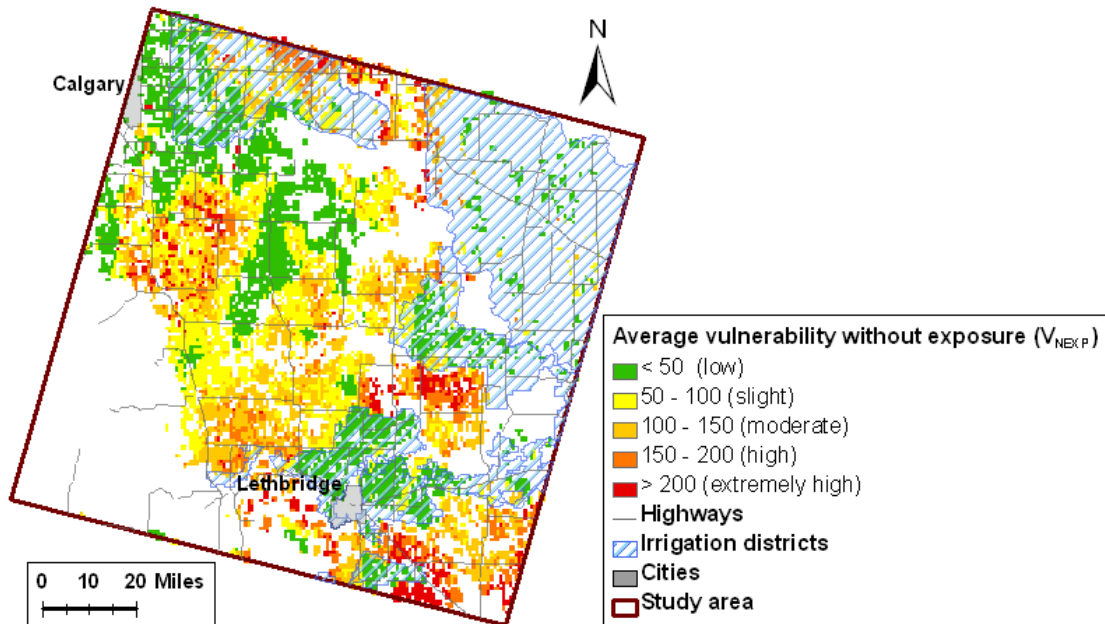
Figure 5-17 Spatial distribution of V_{EXPS} at image pixel level: agricultural vulnerability to severe meteorological drought in growing season, from 1991 to 2004

Table 5-17 Descriptive statistics for V_{EXPS} classes at image pixel level: agricultural vulnerability to severe meteorological drought in growing season, from 1991 to 2004

V_{EXPS} classes	V_{EXPS} value	Percentage coverage	Mean	Standard deviation
Low	< 5	33.56%	-1.91	10.37
Slight	5 - 10	21.12%	7.54	1.40
Moderate	10 - 15	16.02%	12.45	1.46
High	15 - 20	11.80%	17.37	1.45
Extremely high	> 20	17.50%	29.55	33.92

Figure 5-17 presents the spatial distribution of agricultural vulnerability in the growing season to the severe meteorological drought over a short period of time between 1994 and 2004. Because of the higher drought occurrence frequency over the recent decade, the study area displayed a higher vulnerability index value than that over a long period (see Figures 5-16 and 5-17). Less than 45% of the study area was associated with a low to slight vulnerability to the severe meteorological drought (Table 5-17). About

16% of the study area showed a moderate vulnerability, and it was distributed throughout the study area. Almost 30% of the study area was estimated as having a high to extremely high vulnerability to the drought. The highly and extremely highly vulnerable area could be seen throughout the study area, but it was particularly clustered in the area close to Lethbridge and in places where no irrigation systems were available.

To understand further the vulnerability of agricultural production to various drought conditions, vulnerability to the moderate meteorological drought condition is also assessed. The V_{EXPL}' value is estimated using EXP_L' as the exposure factor in Equation 3-3. The spatial distribution of V_{EXPL}' is presented in Figure 5-18, and its descriptive statistics are presented in Table 5-18. Similar to what was already identified with the farm reported yield data, a larger area was estimated as very vulnerable due to the higher occurrence of the moderate meteorological drought condition in the study are. A total of 46.92% of the study area was considered highly or extremely highly vulnerable to the moderate drought condition, particularly in the places outside of the irrigation districts. Only about a quarter of the study was not vulnerable, most of which was within the boundary of the irrigation districts (see Figure 5-18 and Table 5-18).
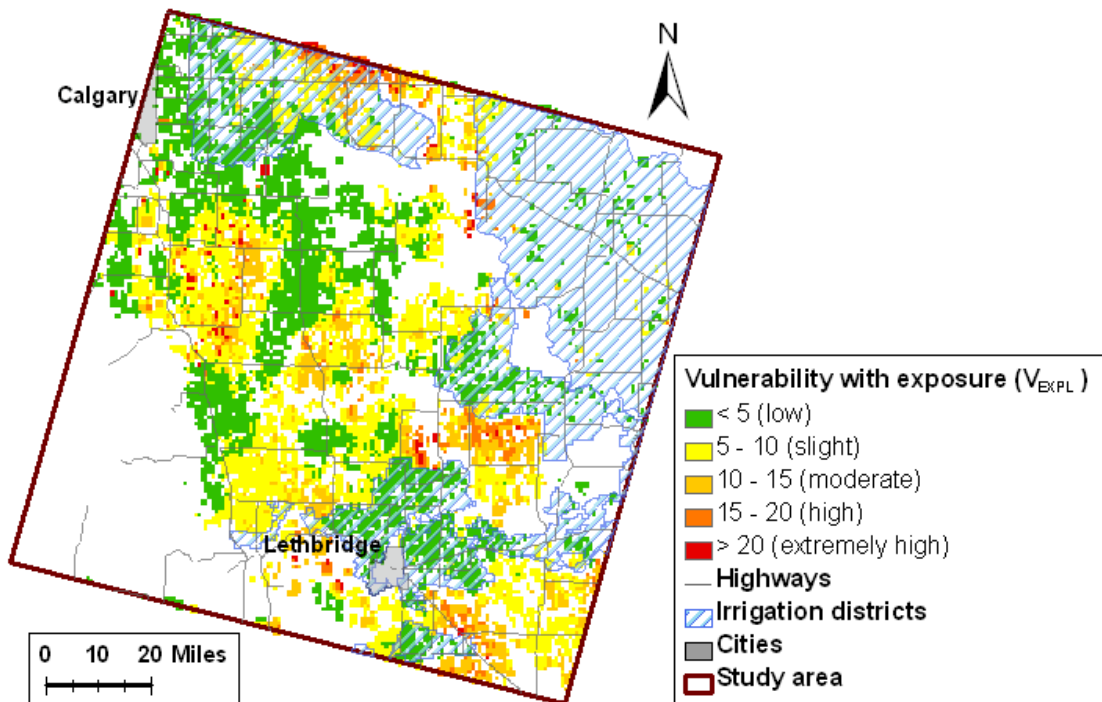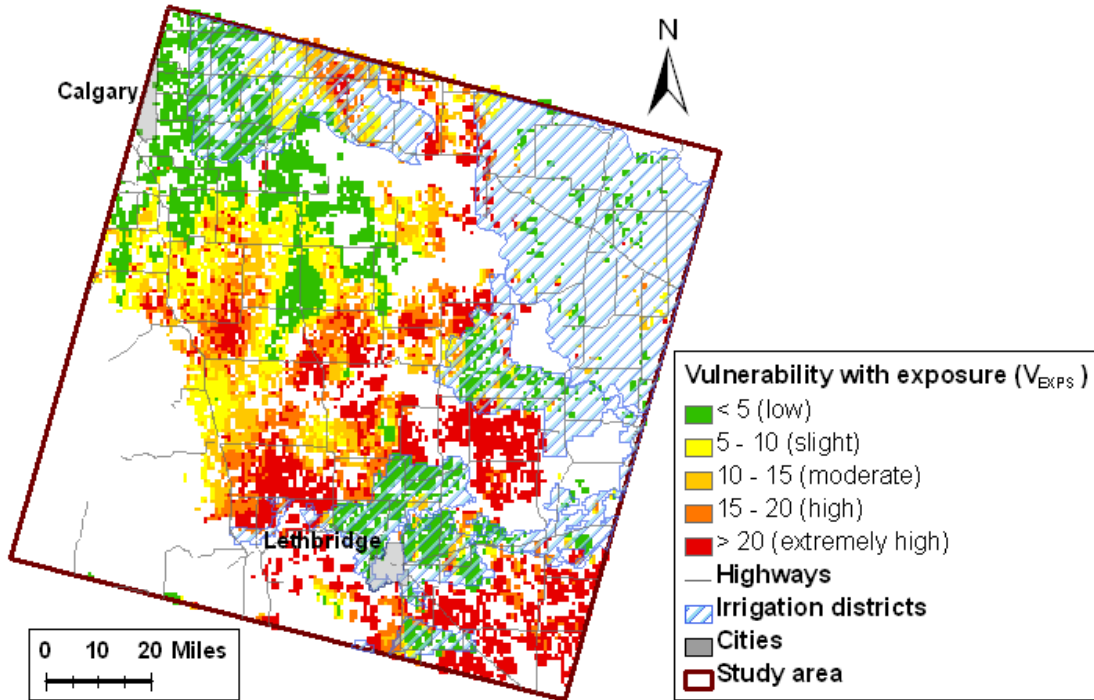
Figure 5-18 Spatial distribution of V_{EXPL}' at image pixel level: agricultural vulnerability to moderate meteorological drought in growing season, from 1965 to 2004

Table 5-18 Descriptive statistics for V_{EXPL}' classes at image pixel level: vulnerability to moderate meteorological drought in growing season, from 1965 to 2004

V_{EXPL}' classes	V_{EXPL}' value	Percentage coverage	Mean	Standard deviation
Low	< 5	26.76%	-2.95	49.21
Slight	5 - 10	11.53%	7.45	1.53
Moderate	10 -15	14.79%	12.54	1.42
High	15 - 20	16.67%	17.54	1.42
Extremely high	> 20	30.25%	28.50	48.33

5.4 Expected Agricultural Vulnerability to Drought in the Future

Based on the analytical approach introduced in Chapter 3, the exposure trend, denoted as T_{EXP} in Equation 3-7, is calculated as the ratio of the short-term exposure (EXP_S) to the long-term exposure (EXP_L). The T_{EXP} value presents the increasing or decreasing propensity of the drought over the recent period (1991 to 2004), and therefore can be employed to assess the prospective vulnerability of agricultural production given a changing, especially warming, trend of global climate. Figure 5-19 presents the spatial

distribution of exposure trend. The descriptive statistics of exposure trend is presented in Table 5-19.

About three quarters of the study area had a T_{EXP} value larger than 1, indicating that a majority of the study area experienced an increasing occurrence frequency of the severe drought condition in the recent decade. More than a third of the study area experienced severe meteorological drought during 1991 to 2004, twice as frequent as that between 1965 and 2004.
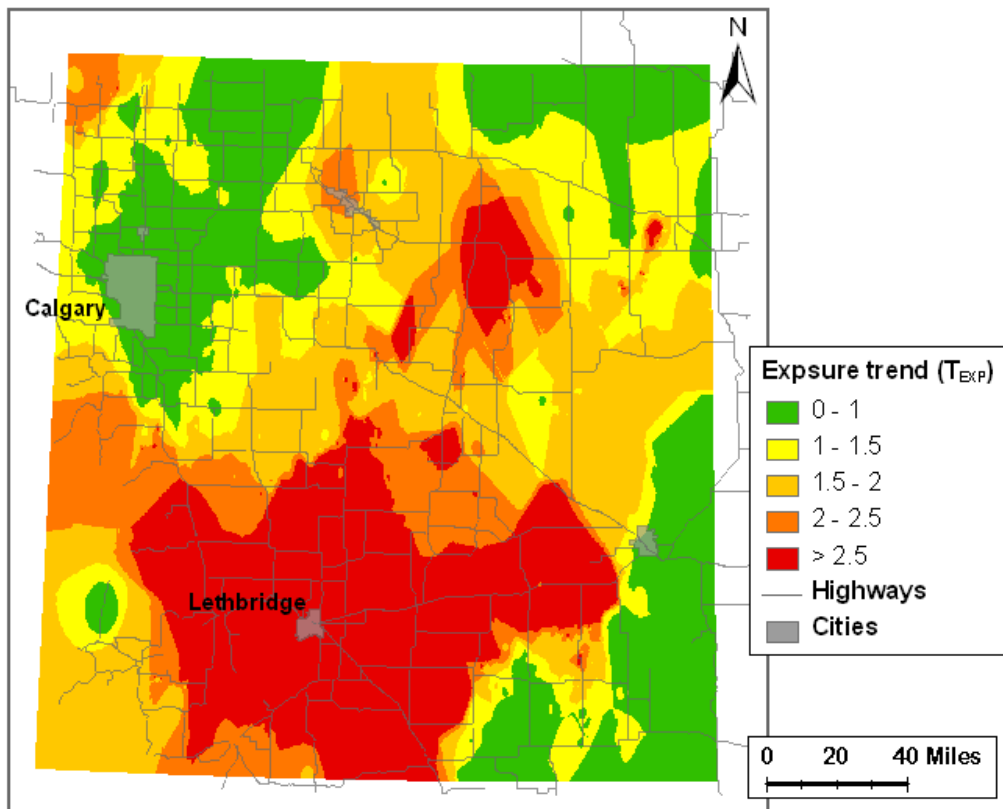
Figure 5-19 Spatial distribution of T_{EXP}: trend of exposure to meteorological drought in growing season

Table 5-19 Descriptive statistics for T_{EXP} classes: trend of exposure to meteorological drought in growing season

T_{EXP} value	Percentage coverage	Mean	Standard deviation
0 -1	23.40%	0.60	0.34
1 - 1.5	17.24%	1.27	0.15
1.5 - 2	25.00%	1.79	0.13
2 - 2.5	12.86%	2.18	0.12
> 2.5	21.50%	2.82	0.08

The expected exposure (*EEXP*) with an increasing exposure to drought is estimated using Equation 3-8. The spatial distribution of *EEXP* is given in Figure 5-20. While the expected exposure may not reflect the real situation of drought occurrence in the future, it sheds some light on the implications of a warming climate and consequently an increasing drought occurrence for agricultural production in the study area. As presented in Table 5-20, the extremely high exposure is expected to occur in 7.6% of the study area, particularly in the area around Lethbridge.
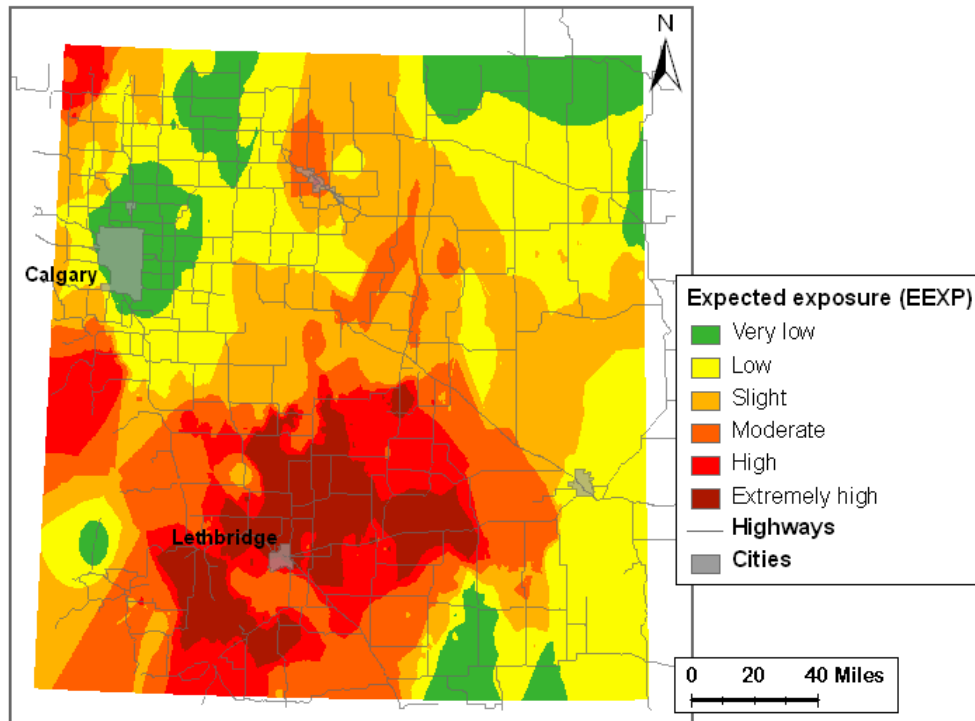
Figure 5-20 Spatial distribution of EEXP: expected exposure to meteorological drought in growing season

Table 5-20 Descriptive statistics for EEXP classes: expected exposure to meteorological drought in growing season

$EEXP$ classes	Percentage coverage	Mean	Standard deviation
Very low	10.76%	0.01	0.01
Low	28.69%	0.08	0.03
Slight	25.87%	0.23	0.04
Moderate	16.95%	0.37	0.05
High	10.14%	0.48	0.04
Extremely high	7.60%	0.61	0.01

Based on both the farm reported yield data and remotely sensed data, agricultural vulnerability with exposure to the severe meteorological drought was estimated using the expected exposure ($EEXP$) as the exposure factor in Equation 3-9. Figures 5-21 and 5-22 present the spatial distribution of the expected vulnerability with exposure (EV_{EXP}) at the quarter-section level and at a 30 meter by 30 meter pixel level. Although the expected exposure might have exaggerated the possible occurrence frequency of the severe drought, the data range of expected exposure is still 0 to 1. The same classification ranges used for classifying V_{EXP} are used to classify EV_{EXP}. The descriptive statistics of EV_{EXP} classes are presented in Tables 5-21 and 5-22.
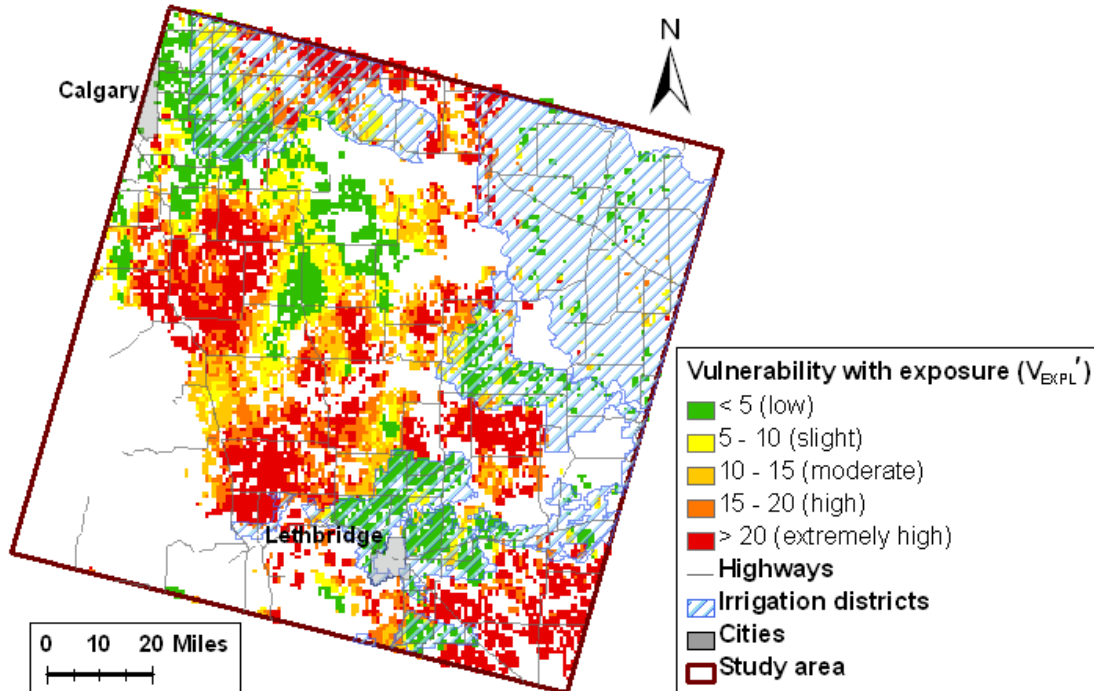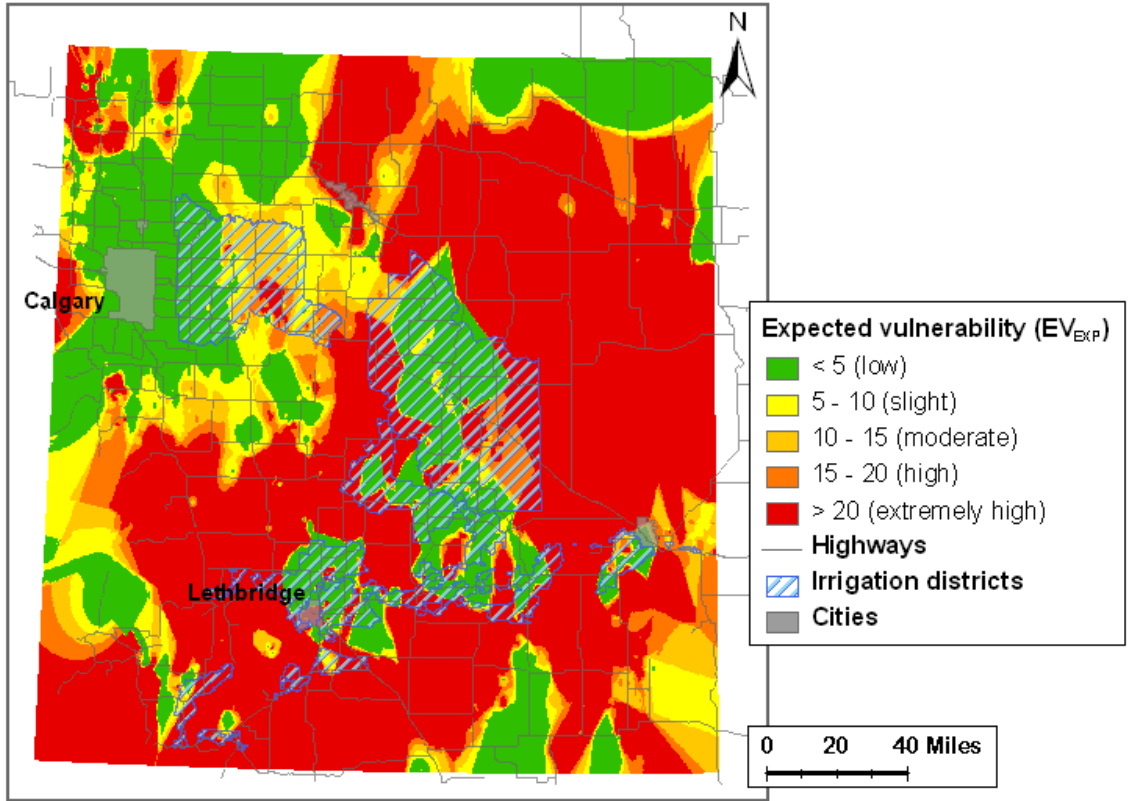
Figure 5-21 Spatial distribution of EV_{EXP}: expected agricultural vulnerability to severe meteorological drought in growing season

Table 5-21 Descriptive statistics for EV_{EXP} classes: expected agricultural vulnerability to severe meteorological drought in growing season

EV_{EXP} classes	EV_{EXP} value	Percentage coverage	Mean	Standard deviation
Low	< 5	25.06%	-6.63	19.07
Slight	5 - 10	8.73%	7.56	1.42
Moderate	10 - 15	8.09%	12.39	1.43
High	15 - 20	7.41%	17.50	1.38
Extremely high	> 20	50.71%	71.40	73.20
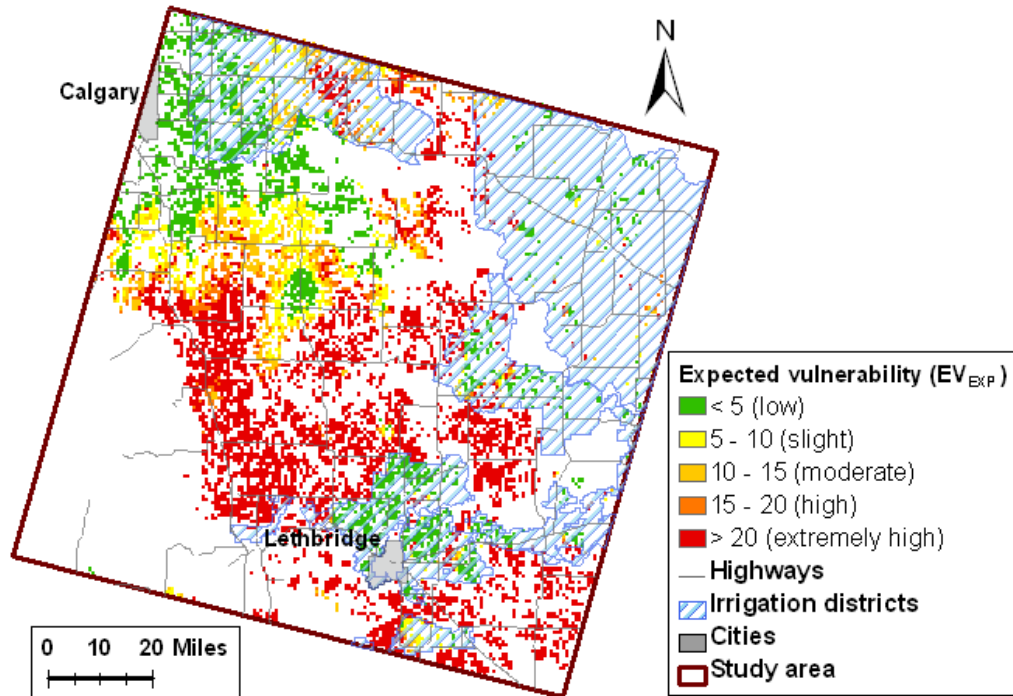
Figure 5-22 Spatial distribution of EV_{EXP} at the image pixel level: expected agricultural vulnerability to severe meteorological drought in growing season

Table 5-22 Descriptive statistics for EV_{EXP} classes at the image pixel level: expected agricultural vulnerability to severe meteorological drought in growing season

EV_{EXP} Classes	EV_{EXP} value	Percentage coverage	Mean	Standard deviation
Low	< 5	28.44%	-8.79	21.47
Slight	5 - 10	11.76%	7.55	1.44
Moderate	10 - 15	9.91%	12.23	1.37
High	15 - 20	5.55%	17.41	1.45
Extremely high	> 20	44.34%	52.13	48.24

As indicated in Figures 5-21 and 5-22, agricultural production in Southern Alberta is expected to be highly vulnerable given the increasing propensity of the severe drought event. Both the farm reported yield data and the estimated yield data based on the remotely sensed information provide a consistent picture of the possible agricultural vulnerability to the increasing severe drought conditions in the future. The study area using the quarter-section as the basic unit covers a larger area of Southern Alberta. Close to 60% of the study area is expected to have a high to extremely high vulnerability.

Almost the entire eastern part of the region and the area in the south without irrigation systems are expected to be highly vulnerable if the recent drought trend repeats in the near future.

The study area defined by the remotely sensed image covers a relatively smaller area. However, the spatial extent and pattern of the expected agricultural vulnerability within this area remains similar. About half of the study area is expected to be associated with a high to extremely vulnerability. The south part of the study area in the vicinity of Lethbridge is expected to be very vulnerable to increasing drought events in the near future if the drought trend in the recent past repeats. Both Figures 5-21 and 5-22 show that the irrigation systems will make a difference. Because of the enhanced adaptive capacity in the irrigation districts, not only is the current agricultural vulnerability in the districts relatively low, but also agricultural production is expected to be less vulnerable to the drought condition even if the propensity of the drought increases in the near future.

5.5   Chapter Summary

This chapter presents the empirical results of the agricultural vulnerability assessment. The method utilized in this study proves to be effective in capturing the spatial variability of vulnerability. The spatial distribution of the vulnerability function components that are estimated using the remotely sensed data are approximately the same as those estimated based on the farm reported data. Overall, the regions investigated in this study were susceptible to varying degrees of agricultural vulnerability to different drought conditions. The pocket regions in the eastern and southern parts were particularly vulnerable based on the historic data. With an increasing propensity of the drought occurrence in the recent past, more regions, especially in the east and south, are expected

to become highly vulnerable. The empirical results presented in this chapter also indicate that remote sensing data as well as the associated analytical approaches can be useful and powerful in assessing the spatial variability of agricultural vulnerability. Since the remotely sensed data are readily available at a relatively lower cost nowadays, such approaches can be frequently employed to assess the changing relationship between agricultural sectors and varying climate conditions in a timely manner.

CHAPTER 6 SUMMARY AND CONCLUSIONS

6.1   Summary

Agricultural vulnerability is generally referred to as the degree to which agricultural systems are likely to experience harm due to a stress. In this study, an existing analytical method to quantify vulnerability is adopted to assess the magnitude as well as the spatial pattern of agricultural vulnerability to varying drought conditions in Southern Alberta. Two approaches are developed to implement vulnerability assessment at two different scales. The first is designed to employ a farm reported dataset, and the second is based on remote sensing techniques. Considering the characteristics of the study area, especially the importance of cereal crop production in Alberta's agricultural system and the adverse effects of possible drought, the cereal crop yield is selected as the measure of agricultural system's well-being in this study, while the standard precipitation index (SPI) is used to measure the stress that the system is exposed to.

The approach based on the farm reported data is employed to analyze generated agricultural vulnerability to various drought conditions at a quarter-section level. The empirical results indicate that the agricultural system is vulnerable to both moderate and severe meteorological drought conditions in the study area, and the vulnerability patterns vary spatially and differ depending upon the drought level.

The study develops yield estimation models based on the remotely sensed imageries. Based on estimated crop yields, the agricultural vulnerability to various drought conditions is assessed at a 30 meter by 30 meter pixel level. The overall spatial patterns of vulnerabilities using the remotely sensed data are similar to those generated using from the farm reported dada. Most areas within irrigation districts are identified as

having lower vulnerability than the areas outside irrigation districts. The expected vulnerability highlighted that the area in the vicinity of Lethbridge is possibly the most vulnerable area in the study area in the future, as a result of expected exposing to a higher drought occurrence frequency.

Overall, the quantitative vulnerability assessment method adopted and modified based on the existing method is demonstrated to be effective in assessing the magnitude and spatial pattern of agricultural vulnerability to varying drought conditions in Southern Alberta.

6.2   Discussions of research findings

As an empirical study, this study supports the vulnerability assessment theories that have emerged recently in the literature. The research indicates that understanding of the vulnerability of a system as a function of sensitivity, exposure and its adaptive capacity provides an effective conceptual framework. Such understanding can be employed as heuristic guidance for implementing vulnerability assessment. This study also identifies that each theoretical component of the vulnerability framework varies geographically and over time. Therefore, further theoretical development on vulnerability assessments should incorporate explicitly the spatial and temporal dimensions. The results of this study also show that the vulnerability of a system at a specific place can be very complex, and hence implementing the theoretical vulnerability framework in examining regional systems remains very much a challenge.

Methodologically, this research demonstrates that various analytical approaches can and need to be integrated into vulnerability assessments. Findings from this research indicate that remote sensing techniques may provide a useful tool in assisting

vulnerability component estimation. It is found that the regression yield estimations coupled with a remote sensing technique are effective tools that can help the utilization of widely available remote sensing data for vulnerability assessment. The traditional vegetation indices such as NDVI derived from the remote sensing imagery and other auxiliary spatial attributes present valuable information for estimating crop yields at the regional level. The estimated cereal crop yield reaches the desirable accuracy, and the revealed vulnerability patterns enhance a detailed understanding of agricultural vulnerability to drought in the study area. Furthermore, the approach based on the remote sensing data provides a reasonable picture of the overall magnitude and spatial pattern of agricultural vulnerability to drought, and illustrates effectively the utility of remote sensing data in vulnerability assessment.

The study employs a relatively new drought measure of SPI. The results of the case study indicate the index can be employed effectively to portray the spatial and temporal variations in drought conditions. Also, the developed method for assessing the expected drought exposure and vulnerability can be used as an effective and powerful tool to reveal a possible spatial pattern of agricultural vulnerability to drought in the future.

Empirically, this study generates some valuable insights into the extent and spatial variation of agricultural vulnerability to drought condition in Southern Alberta. First, the findings from this research indicate that there is a sharp contrast in agricultural vulnerability to drought between irrigated districts and non-irrigated areas. While non-irrigated areas are vulnerable to varying drought conditions, irrigated agricultural areas are largely insensitive to droughts. Such findings confirm the importance of irrigation

practices in the regions. The installation of irrigation systems in the region has certainly elevated the adaptive capacity of agriculture systems to cope with drought related disturbances in the study area.

While the severe drought may cause devastating harm to agricultural sectors, only a relatively small portion of the region is very vulnerable to such possible hazards. For most of the study area, vulnerability to severe drought is low to moderate. However, a larger area is quite vulnerable to the moderate level drought. Although the moderate drought may not cause as devastating effects to agricultural production as those by severe drought, it still results in an obvious reduction in crop yields in the region.

The estimated trend of the drought occurrence frequency based on the historical data suggests that most of the study area might face an increasing possibility of exposure to drought conditions. The assessment of the expected vulnerability suggests agricultural crop production in the south of the study area, especially in the vicinity of Lethbridge will be possibly associated with the highest vulnerability due to the expected increasing drought occurrence frequency in this area.

There are also some limitations of the research approaches employed, and some errors and uncertainty are possibly introduced in the processes of data handling and manipulation. First, in processing the farm reported data, it is found that there are possible reporting and data recording errors in the farm reported data. Some deletion and averaging are done to make use of the data. The effects of such data processing procedures on the final outputs are largely unknown, although it is quite confident that the derived overall vulnerability pattern reflects the reality in the study area. Errors and uncertainties could also be introduced in handling and processing the remote sensing

imagery. For example, image orthorectification and atmospherically correction introduce minor errors into the data. The visual detection of cloud haze and shadow area, the establishment of NDVI threshold for fallow masking, and the manually verification of the classification training and validation ROIs could introduce some possible errors. Also, the interpolation procedures employed in predicting the data at un-sampled locations such as the moving window approach and the inverse distance weighting interpolation may be error-prone. While the above possible aspects of data processing errors are difficult to quantify and are consequently not directly reported, some uncertainties in the data analysis are quantified and reported explicitly, such as the land use classification accuracies and errors related to the yield estimation models.

6.3   Contributions of this research

There is a growing body of literature devoted to vulnerability studies. Global climate change and its possible environmental and economic effects at the regional and global scales push vulnerability assessment to the forefront in various disciplines. While the theoretical understanding and research methodologies on vulnerability assessment are being advanced steadily, the sufficient empirical evidence on the vulnerability of human and environmental systems is not available. Few have studied agricultural vulnerability in the semi-arid prairie region of Southern Alberta, part of the "bread basket" of the world.

This study employs the quantitative assessment method developed by Luers et al. (2003) for a semi-arid region, and demonstrates the suitability of this method for vulnerability assessment in this region. Several modifications to the adopted approach are made in this study, and the methodological adjustments may contribute to a further discussion on how to measure quantitatively the vulnerability and its components.

This study suggests that the actual value instead of absolute value for sensitivity calculation should be used. As such, it reflects more precisely the widely agreed definition of sensitivity, which is defined by IPCC (2001) as the degree to which a system will respond to a fluctuation in stress (force), including both the potential of being harmed or benefited. The study also illustrates a possible approach to assess the spatial variation of vulnerability by estimating all vulnerability components at the detailed quarter-section and image pixel levels. The method for assessing the expected vulnerability based on investigating the trend of the drought occurrence frequency expands the methodological possibility in agricultural vulnerability assessments.

In addition to methodological contributions to the vulnerability assessment literature, the empirical findings of this research may be of important interest to local and regional governments. The spatial distribution of the estimated agricultural vulnerability to various drought conditions can be used as reference information for formulating spatial coping policies to reduce future vulnerability of agricultural sectors in the study area. It can also provide a reference base for insurance institutions to refine their insurance policies. Also, the results of the study can also inform farmers and other stakeholders in this study area about their potential risk in terms of possible crop production decline in facing an increasing warming and variable climate at the regional and global scales.

6.4   Future research

Several areas of the future research can be identified as a result of this study. Firstly, agricultural systems are composed of multiple components and the interrelationships among them. The sustainability of agricultural systems involves not only economic viability, but also social vitality and environment integrity. The wellbeing

of agricultural systems is thus multidimensional, and the social, economic, and environmental aspects of well-being all need to be considered simultaneously (Xu and Mage, 2001). As a result, a more comprehensive vulnerability assessment seems desirable. A possible multidimensional measure of vulnerability can possibly be achieved by summing several weighted vulnerability values for different representative well-being and stress pairs. The possible mathematical function of a comprehensive method for quantifying vulnerability may take the following forms as Equations 6-1 and 6-2:

$$V_{ix} = SEN_{ix} \times (W_i / W_{i0}) \times EXP_x \tag{6-1}$$

$$V = \sum_{\substack{i=1 \\ x=1}}^{n} (w_{ix} \times V_{ix}) \tag{6-1}$$

Where,

V_{ix} is the vulnerability of any possible representative well-being to any possible concerned stress of a system in a place.

SEN_{ix} is the system's sensitivity defined as the change in the representative well-being i corresponding to a small change in concerned stress x.

W_i/W_{i0} is the relative proximity of the well-being i to its damage threshold.

EXP_x is the value of exposure defined as the occurrence frequency of the concerned level of stress x.

V indicates the vulnerability value of a comprehensive assessment, where several representative well-being factors and stresses are considered.

w_{ix} is the weighting coefficients of each coupled well-being and stress pairs, which quantify the importance of the specific pair.

Secondly, the remote sensing data can also be employed in the calculation of sensitivity when vulnerability assessment is based on crop production. The drought related crop stress level may be quantitatively measured based on the spectral information on the remotely sensed imagery through laboratory tests and quantitative modeling. This will generate sensitivity estimates spatially at a more detailed level, and will further enhance the value of remote sensing data in agricultural vulnerability assessment.

Finally, this study employs the SPI values that are calculated for each of the growing seasons over the last 40 years. SPI can be calculated monthly, seasonally, or annually. Because of the temporal flexibility in SPI calculation, the sensitivity as a component of vulnerability measure can also be estimated at different temporal scales of years. Identifying the most critical time window of a year in terms of the impact of drought occurrence will help portray a more precise picture of how vulnerable the agricultural system is. Such an undertaking still remains a challenging topic for future research on agricultural vulnerability to drought.

References Cited

AAFRD (2002). Southern Alberta Drought, Alberta Agriculture, Food and Rural Development http://www1.agric.gov.ab.ca/$department/deptdocs.nsf/all/irr4416.

AAFRD (2006). Agriculture and Food Value Chain Facts 2006, Alberta Agriculture, Food and Rural Development http://www1.agric.gov.ab.ca/$department/deptdocs.nsf/all/sdd3854.

Abou-Ismail, O., J. F. Huang and R. C. Wang (2004). "Rice yield estimation by integrating remote sensing with rice growth simulation model." Pedosphere **14**(4): 519-526.

Adger, W. N. (2006). "Vulnerability." Global Environmental Change-Human and Policy Dimensions **16**(3): 268-281.

Alberini, A., A. Chiabai and L. Muehlenbachs (2006). "Using expert judgment to assess adaptive capacity to climate change: Evidence from a conjoint choice survey." Global Environmental Change-Human and Policy Dimensions **16**(2): 123-144.

Alley, W. M. (1985). "The Palmer Drought Severity Index as a Measure of Hydrologic Drought." Water Resources Bulletin **21**(1): 105-114.

Anonymous (2003). "The vulnerability of cities: Natural disasters and social resilience." Environment and Urbanization **15**(1): 216-216.

Babar, M. A., M. van Ginkel, A. Klatt, B. Prasad and M. P. Reynolds (2006). "The potential of using spectral reflectance indices to estimate yield in wheat grown under reduced irrigation." Euphytica **150**(1-2): 155-172.

Badarinath, K. V. S., T. R. K. Chand and V. K. Prasad (2006). "Agriculture crop residue burning in the Indo-Gangetic Plains - A study using IRS-P6 AWiFS satellite data." Current Science **91**(8): 1085-1089.

Baethgen, W. E. (1997). "Vulnerability of the agricultural sector of Latin America to climate change." Climate Research **9**(1-2): 1-7.

Basnyat, P., B. McConkey, G. R. Lafond, A. Moulin and Y. Pelcat (2004). "Optimal time for remote sensing to relate to crop grain yield on the Canadian prairies." Canadian Journal of Plant Science **84**(1): 97-103.

Bastiaanssen, W. G. M., D. J. Molden and I. W. Makin (2000). "Remote sensing for irrigated agriculture: examples from research and possible applications." Agricultural Water Management **46**(2): 137-155.

Beeri, O. and A. Peled (2006). "Spectral indices for precise agriculture monitoring." International Journal of Remote Sensing **27**(9-10): 2039-2047.

Blaikie, P., T. Cannon, I. Davis and B. Wisner (1994). <u>At risk: natural hazards, people's vulnerability, and disasters</u>. London: Routledge.

Boruff, B. J., C. Emrich and S. L. Cutter (2005). "Erosion hazard vulnerability of US coastal counties." <u>Journal of Coastal Research</u> **21**(5): 932-942.

Boughton, D. A., E. R. Smith and R. V. O'Neill (1999). "Regional vulnerability: A conceptual framework." <u>Ecosystem Health</u> **5**(4): 312-322.

Bouman, B. A. M. (1995). "Crop Modeling and Remote-Sensing for Yield Prediction." <u>Netherlands Journal of Agricultural Science</u> **43**(2): 143-161.

Brooks, N., W. N. Adger and P. M. Kelly (2005). "The determinants of vulnerability and adaptive capacity at the national level and the implications for adaptation." <u>Global Environmental Change-Human and Policy Dimensions</u> **15**(2): 151-163.

Bullock, P. R. (2004). "A comparison of growing season agrometeorological stress and single-date Landsat NDVI for wheat yield estimation in west central Saskatchewan." <u>Canadian Journal of Remote Sensing</u> **30**(1): 101-108.

Burton, I. (1997). "Vulnerability and adaptive response in the context of climate and climate change." <u>Climatic Change</u> **36**(1-2): 185-196.

Chambers, R. (1989). "Vulnerability, Coping and Policy - Introduction." <u>Ids Bulletin-Institute of Development Studies</u> **20**(2): 1-7.

Champagne, C., J. Shang, H. McNairn and T. Fisette (2005). Exploiting Spectral Variation from Crop Phenology for Agricultural Land-Use Classification. <u>Remote Sensing and Modeling of Ecosystems for Sustainability II</u>. W. Gao and D. R, Shaw.

Chen, Y., Q. F. Chen and L. Chen (2001). "Vulnerability analysis in earthquake loss estimate." <u>Natural Hazards</u> **23**(2-3): 349-364.

Currens, K. P. and C. A. Busack (1995). "A Framework for Assessing Genetic Vulnerability." <u>Fisheries</u> **20**(12): 24-31.

Cutter, S. L. (1996). "Vulnerability to environmental hazards." <u>Progress in Human Geography</u> **20**(4): 529-539.

Cutter, S. L., B. J. Boruff and W. L. Shirley (2003). "Social vulnerability to environmental hazards." <u>Social Science Quarterly</u> **84**(2): 242-261.

Dadhwal, V. K. and V. N. Sridhar (1997). "A non-linear regression form for vegetation index-crop yield relation incorporating acquisition date normalization." <u>International Journal of Remote Sensing</u> **18**(6): 1403-1408.

De Sherbinin, A. (2000). "Climate change impacts on agriculture." Environment **42**(2): 3-3.

Descroix, L., M. Vauclin, D. Viramontes, M. Esteves, J. L. G. Barrios and E. Anaya (2003). "Water management in Northern Mexico: sharing resources affected by drought." Houille Blanche-Revue Internationale De L Eau(6): 46-52.

Dixon, B. (2005). "Applicability of neuro-fuzzy techniques in predicting ground-water vulnerability: a GIS-based sensitivity analysis." Journal of Hydrology **309**(1-4): 17-38.

Doerfliger, N., P. Y. Jeannin and F. Zwahlen (1999). "Water vulnerability assessment in karst environments: a new method of defining protection areas using a multi-attribute approach and GIS tools (EPIK method)." Environmental Geology **39**(2): 165-176.

Doraiswamy, P. C., S. Moulin, P. W. Cook and A. Stern (2003). "Crop yield assessment from remote sensing." Photogrammetric Engineering and Remote Sensing **69**(6): 665-674.

Dow, K. (1992). "Exploring Differences in Our Common Future(S) - the Meaning of Vulnerability to Global Environmental-Change." Geoforum **23**(3): 417-436.

Downing, T. E., R. Butterfield, S. Cohen, S. Huq, R. Moss, A. Rahman, Y. Sokona and L. Stephen (2001). Climate Change Vulnerability: Linking Impacts and Adaptation. Press, Oxford, Oxford University.

Dupigny-Giroux, L. A. (2001). "Towards characterizing and planning for drought in Vermont - Part I: A climatological perspective." Journal of the American Water Resources Association **37**(3): 505-525.

Eakin, H. and J. Conley (2002). "Climate variability and the vulnerability of ranching in southeastern Arizona: a pilot study." Climate Research **21**(3): 271-281.

Edwards, D. C. and T. B. McKee. (1997). Development of a surface water supply index for the western United States. Climatology Report. F. Collins. Colorado, Colorado State University.

Ferencz, C., P. Bognar, J. Lichtenberger, D. Hamar, G. Tarscai, G. Timar, G. Molnar, S. Pasztor, P. Steinbach, B. Szekely, O. E. Ferencz and I. Ferencz-Arkos (2004). "Crop yield estimation by satellite remote sensing." International Journal of Remote Sensing **25**(20): 4113-4149.

Gallopin, G. C. (2006). "Linkages between vulnerability, resilience, and adaptive capacity." Global Environmental Change-Human and Policy Dimensions **16**(3): 293-303.

Gemitzi, A., C. Petalas, V. A. Tsihrintzis and V. Pisinaras (2006). "Assessment of groundwater vulnerability to pollution: a combination of GIS, fuzzy logic and decision making techniques." Environmental Geology **49**(5): 653-673.

Gogu, R. C. and A. Dassargues (2000). "Current trends and future challenges in groundwater vulnerability assessment using overlay and index methods." Environmental Geology **39**(6): 549-559.

Gove, P. B., Ed. (1981). Webster's third new international dictionary.

Guttman, N. B. (1998). "Comparing the Palmer Drought Index and the standardized precipitation index." Journal of the American Water Resources Association **34**(1): 113-121.

Guttman, N. B. (1999). "Accepting the standardized precipitation index: A calculation algorithm." Journal of the American Water Resources Association **35**(2): 311-322.

Hatfield, J. L. (1983). "Remote-Sensing Estimators of Potential and Actual Crop Yield." Remote Sensing of Environment **13**(4): 301-311.

Hayes, M. J. (2005). Drought Indices, National Drought Mitigation Center. http://www.drought.unl.edu/whatis/indices.htm

Hayes, M. J., M. D. Svoboda, D. A. Wilhite and O. V. Vanyarkho (1999). "Monitoring the 1996 drought using the standardized precipitation index." Bulletin of the American Meteorological Society **80**(3): 429-438.

Hochheim, K. P. and D. G. Barber (1998). "Spring wheat yield estimation for Western Canada using NOAA NDVI data." Canadian journal of remote sensing **24**(0703-8992): 17-27.

Hoffmann, C. M. and M. Blomberg (2004). "Estimation of leaf area index of Beta-vulgaris L. based on optical remote sensing data." Journal of Agronomy and Crop Science **190**(3): 197-204.

Humphreys, M. W., R. S. Yadav, A. J. Cairns, L. B. Turner, J. Humphreys and L. Skot (2006). "A changing climate for grassland research." New Phytologist **169**(1): 9-26.

Idso, S. B., R. D. Jackson and R. J. Reginato (1977). "Remote-Sensing for Agricultural Water Management and Crop Yield Prediction." Agricultural Water Management **1**(4): 299-310.

IFPRI (2002). Reaching Sustainable Food Security for All by 2020: Get the Priorities and Responsibilities Right. Washington, DC, International Food Policy Research Institute**:** 44.

IPCC (2001). Impacts, adaptation, and vulnerability climate change 2001. <u>Third Assessment Report of the IPCC</u>. Cambridge, UK., University Press.

Jensen, J. R. (2005). <u>Introductory Digital Image Processing: A Remote Sensing Perspective.</u> London, Eng., Pearson.

Johnston, T. and Q. Chiotti (2000). "Climate change and the adaptability of agriculture: A review." <u>Journal of the Air & Waste Management Association</u> **50**(4): 563-569.

Jones, P. D., M. Hulme, K. R. Briffa, C. G. Jones, J. F. B. Mitchell and J. M. Murphy (1996). "Summer moisture availability over Europe in the Hadley Centre general circulation model based on the Palmer Drought Severity Index." <u>International Journal of Climatology</u> **16**(2): 155-172.

Kates, R. W. (1985). <u>The interaction of climate and society</u>. New York, Wiley.

Kellman, M., Y. Shachmurove and T. Saadawi (1996). "Import vulnerability of defense-related industries: An empirical model." <u>Journal of Policy Modeling</u> **18**(1): 87-107.

Labus, M. P., G. A. Nielsen, R. L. Lawrence, R. Engel and D. S. Long (2002). "Wheat yield estimates using multi-temporal NDVI satellite imagery." <u>International Journal of Remote Sensing</u> **23**(20): 4169-4180.

Lobell, D. B. and G. P. Asner (2003). "Comparison of Earth Observing-1 ALI and Landsat ETM+ for crop identification and yield prediction in Mexico." <u>Ieee Transactions on Geoscience and Remote Sensing</u> **41**(6): 1277-1282.

Lobell, D. B., G. P. Asner, J. I. Ortiz-Monasterio and T. L. Benning (2003). "Remote sensing of regional crop production in the Yaqui Valley, Mexico: estimates and uncertainties." <u>Agriculture Ecosystems & Environment</u> **94**(2): 205-220.

Lobell, D. B., J. I. Ortiz-Monasterio, G. P. Asner, R. L. Naylor and W. P. Falcon (2005). "Combining field surveys, remote sensing, and regression trees to understand yield variations in an irrigated wheat landscape." <u>Agronomy Journal</u> **97**(1): 241-249.

Lohani, V. K. and G. V. Loganathan (1997). "An early warning system for drought management using the Palmer drought index." <u>Journal of the American Water Resources Association</u> **33**(6): 1375-1386.

Lowry, J. H., H. J. Miller and G. F. Hepner (1995). "A GIS-Based Sensitivity Analysis of Community Vulnerability to Hazardous Contaminants on the Mexico/Us Border." <u>Photogrammetric Engineering and Remote Sensing</u> **61**(11): 1347-1359.

Luers, A. L., D. B. Lobell, L. S. Sklar, C. L. Addams and P. A. Matson (2003). "A method for quantifying vulnerability, applied to the agricultural system of the

Yaqui Valley, Mexico." Global Environmental Change-Human and Policy Dimensions **13**(4): 255-267.

McKee, T. B., N. J. Doeskin and J. Kleist (1993). The Relationshio of Drought Frequency and Drought Duration to Time Scales. 8th Conf. on Applied Climatology

McKee, T. B., N. J. Doeskin and J. Kleist (1995). Drought monitoring with Multiple Time Scales. American Meteorological Society. Boston, Massachusetts.

Mika, J., S. Horvath, L. Makra and Z. Dunkel (2005). "The Palmer Drought Severity Index (PDSI) as an indicator of soil moisture." Physics and Chemistry of the Earth **30**(1-3): 223-230.

Moore, P. D. (1998). "Climate change and the global harvest: Potential impacts of the greenhouse effect on agriculture." Nature **393**(6680): 33-34.

Moulin, S., A. Bondeau and R. Delecolle (1998). "Combining agricultural crop models and satellite observations: from field to regional scales." International Journal of Remote Sensing **19**(6): 1021-1036.

Muldavin, E. H., P. Neville and G. Harper (2001). "Indices of grassland biodiversity in the Chihuahuan Desert ecoregion derived from remote sensing." Conservation Biology **15**(4): 844-855.

Murray, C. (2003). "Risk factors, protective factors, vulnerability, and resilience - A framework for understanding and supporting the adult transitions of youth with high-incidence disabilities." Remedial and Special Education **24**(1): 16-26.

NDMC (2005). SPI program files, National Drought Mitigation Center http://www.drought.unl.edu/monitor/spi/program/spi_program.htm.

Plant, R. E., D. S. Munk, B. R. Roberts, R. L. Vargas, D. W. Rains, R. L. Travis and R. B. Hutmacher (2000). "Relationships between remotely sensed reflectance data and cotton growth and yield." Transactions of the ASAE **43**(3): 535-546.

Prasad, A. K., L. Chai, R. P. Singh and M. Kafatos (2006). "Crop yield estimation model for Iowa using remote sensing and surface parameters." International Journal of Applied Earth Observation and Geoinformation **8**(1): 26-33.

Ray, S. S., S. S. Pokharna and Ajai (1999). "Cotton yield estimation using agrometeorological model and satellite-derived spectral profile." International Journal of Remote Sensing **20**(14): 2693-2702.

Reilly, J. M. and D. Schimmelpfennig (1999). "Agricultural impact assessment, vulnerability, and the scope for adaptation." Climatic Change **43**(4): 745-788.

Richards, J. A. (1999). Remote Sensing Digital Image Analysis. Berlin, Springer-Verlag.

Sanchez-Arcilla, A., J. A. Jimenez and H. I. Valdemoro (1998). "The Ebro delta: Morphodynamics and vulnerability." Journal of Coastal Research **14**(3): 754-772.

Seaquist, J. W., L. Olsson and J. Ardo (2003). "A remote sensing-based primary production model for grassland biomes." Ecological Modelling **169**(1): 131-155.

Serrano, L., I. Filella and J. Penuelas (2000). "Remote sensing of biomass and yield of winter wheat under different nitrogen supplies." Crop Science **40**(3): 723-731.

Shao, Y., X. T. Fan, H. Liu, J. H. Xiao, S. Ross, B. Brisco, R. Brown and G. Staples (2001). "Rice monitoring and production estimation using multitemporal RADARSAT." Remote Sensing of Environment **76**(3): 310-325.

Smit, B. and J. Wandel (2006). "Adaptation, adaptive capacity and vulnerability." Global Environmental Change-Human and Policy Dimensions **16**(3): 282-292.

Smith, A. M., D. J. Major, M. J. Hill, W. D. Willms, B. Brisco, C. W. Lindwall and R. J. Brown (1994). "Airborne Synthetic-Aperture Radar Analysis of Range-Land Revegetation of a Mixed Prairie." Journal of Range Management **47**(5): 385-391.

Smith, A. M., D. J. Major, R. L. McNeil, W. D. Willms, B. Brisco and R. J. Brown (1995). "Complementarity of Radar and Visible-Infrared Sensors in Assessing Rangeland Condition." Remote Sensing of Environment **52**(3): 173-180.

Sonmez, F. K., A. U. Komuscu, A. Erkan and E. Turgu (2005). "An analysis of spatial and temporal dimension of drought vulnerability in Turkey using the standardized precipitation index." Natural Hazards **35**(2): 243-264.

Steinemann, A. (2003). "Drought indicators and triggers: A stochastic approach to evaluation." Journal of the American Water Resources Association **39**(5): 1217-1233.

Tao, F. L., Y. Hayashi and E. D. Lin (2002). "Soil vulnerability and sensitivity to acid deposition in China." Water Air and Soil Pollution **140**(1-4): 247-260.

Thomson, A. M., R. A. Brown, N. J. Rosenberg, R. C. Izaurralde and V. Benson (2005a). "Climate change impacts for the conterminous USA: An integrated assessment - Part 3. Dryland production of grain and forage crops." Climatic Change **69**(1): 43-65.

Thomson, A. M., N. J. Rosenberg, R. C. Izaurralde and R. A. Brown (2005b). "Climate change impacts for the conterminous USA: An integrated assessment - Part 5. Irrigated agriculture and national grain crop production." Climatic Change **69**(1): 89-105.

Turner, B. L., R. E. Kasperson, P. A. Matson, J. J. McCarthy, R. W. Corell, L. Christensen, N. Eckley, J. X. Kasperson, A. Luers, M. L. Martello, C. Polsky, A. Pulsipher and A. Schiller (2003a). "A framework for vulnerability analysis in

sustainability science." <u>Proceedings of the National Academy of Sciences of the United States of America</u> **100**(14): 8074-8079.

Turner, B. L., P. A. Matson, J. J. McCarthy, R. W. Corell, L. Christensen, N. Eckley, G. K. Hovelsrud-Broda, J. X. Kasperson, R. E. Kasperson, A. Luers, M. L. Martello, S. Mathiesen, R. Naylor, C. Polsky, A. Pulsipher, A. Schiller, H. Selin and N. Tyler (2003b). "Illustrating the coupled human-environment system for vulnerability analysis: Three case studies." <u>Proceedings of the National Academy of Sciences of the United States of America</u> **100**(14): 8080-8085.

Vicente-Serrano, S. M., J. M. Cuadrat-Prats and A. Romo (2006). "Early prediction of crop production using drought indices at different time-scales and remote sensing data: application in the Ebro valley (North-East Spain)." <u>International Journal of Remote Sensing</u> **27**(3): 511-518.

Vicente-Serrano, S. M. and J. I. Lopez-Moreno (2005). "Hydrological response to different time scales of climatological drought: an evaluation of the Standardized Precipitation Index in a mountainous Mediterranean basin." <u>Hydrology and Earth System Sciences</u> **9**(5): 523-533.

Villa, F. and H. McLeod (2002). "Environmental vulnerability indicators for environmental planning and decision-making: Guidelines and applications." <u>Environmental Management</u> **29**(3): 335-348.

Weber, M. and G. Hauer (2003). "A regional analysis of climate change impacts on Canadian agriculture." <u>Canadian Public Policy-Analyse De Politiques</u> **29**(2): 163-180.

Wei, Y. M., Y. Fan, C. Lu and H. T. Tsai (2004). "The assessment of vulnerability to natural disasters in China by using the DEA method." <u>Environmental Impact Assessment Review</u> **24**(4): 427-439.

WID (2004) <u>Annual report: 2004</u>, http://www.wid.net/AnnualReports/2004AnnRpt.pdf

Wilhelmi, O. V. and D. A. Wilhite (2002). "Assessing vulnerability to agricultural drought: A Nebraska case study." <u>Natural Hazards</u> **25**(1): 37-58.

Wu, H. and D. A. Wilhite (2004). "An operational agricultural drought risk assessment model for Nebraska, USA." <u>Natural Hazards</u> **33**(1): 1-21.

Xu, W. and J. A. Mage (2001). "A review of concepts and criteria for assessing agroecosystem health, including a preliminary case study of southern Ontario" <u>Agriculture Ecosystems & Environment</u> **83** (3): 215-233.

Zarco-Tejada, P. J., A. Berjon, R. Lopez-Lozano, J. R. Miller, P. Martin, V. Cachorro, M. R. Gonzalez and A. de Frutos (2005). "Assessing vineyard condition with hyperspectral indices: Leaf and canopy reflectance simulation in a row-structured discontinuous canopy." <u>Remote Sensing of Environment</u> **99**(3): 271-287.

Zhang, R. H. (1984). "An Improved Model of Crop Yield Estimate by Remote-Sensing." <u>Kexue Tongbao</u> **29**(2): 284-284.